ISOLATION, STRUCTURAL ELUCIDATION AND ANTIBACTERIAL ACTIVITY OF THE CHEMICAL CONSTITUENTS OF *SCAEVOLA SPINESCENS*

Michele Mejin, BSc in Biohealth Science (Hons)

A thesis submitted to the University of Adelaide in fulfillment of
the requirement for the degree of Master of Science

Department of Chemistry
School of Chemistry and Physics
Faculty of Sciences,
The University of Adelaide
Adelaide, South Australia, 5005

(February, 2009)

TABLE OF CONTENTS

TABLE OF CONTENTS…… i
LIST OF FIGURES…… iii
LIST OF TABLES…… vi
LIST OF ABBREVIATIONS…… vii
ABSTRACT…… viii
STATEMENT…… xi
ACKNOWLEDGEMENTS…… xii

CHAPTER 1 INTRODUCTION…… 1
1.1 GENERAL INTRODUCTION…… 2
1.2 GOODENIACEAE…… 4
1.3 *SCAEVOLA* SPECIES…… 4
1.3.1 *Distribution*…… 4
1.3.2 *Morphology*…… 5
1.3.3 *Uses*…… 6
1.4 CHEMICAL CONSTITUENTS…… 7
1.4.1 *Coumarins*…… 7
1.4.2 *Terpenoids*…… 9
1.4.3 *Iridoids*…… 13
1.4.4 *Alkaloids*…… 16
1.4.5 *Flavonoids*…… 18
1.5 BIOLOGICAL ACTIVITIES…… 20
1.5.1 *Antiviral*…… 20
1.5.2 *Anti-tumor and cytotoxicity*…… 20
1.5.3 *Antibacterial*…… 21
1.6 AIMS…… 24

CHAPTER 2 ISOLATION / STRUCTURE ELUCIDATION…… 25
2.1 GENERAL INTRODUCTION…… 26
2.2 PLANT COLLECTION…… 27

2.3 PLANT PREPARATION…… 29
2.4 EXTRACTION…… 29
2.4.1 *Hexane extract*…….. 31
2.4.2 *Ethyl acetate extract*…….. 60
2.4.3 *Methanol extract*…… 75
2.4.4 *Aqueous extract*…… 93

CHAPTER 3 ANTIBACTERIAL ASSAY…… 101
3.1 INTRODUCTION…… 102
3.2 HEXANE EXTRACT……104
3.3 ETHYL ACETATE EXTRACT……105
3.4 METHANOL EXTRACT……..109
3.5 AQUEOUS EXTRACT……112
3.6 DISCUSSION……118

CHAPTER 4 EXPERIMENTAL……... 120
4.1 GENERAL EXPERIMENTAL PROCEDURES……... 121
4.2 PLANT MATERIAL……122
4.3 EXTRACTION AND ISOLATION……..122
4.3.1 *Hexane extract*……123
4.3.2 *Ethyl acetate extract*…….. 127
4.3.3 *Methanol extract*…… 130
4.3.4 *Aqueous extract*…… 134
4.4 BACTERIA AND GROWTH CONDITIONS…… 138
4.5 BROTH MICRO-DILUTION ASSAY FOR MINIMUM INHIBITORY AND BACTERICIDAL CONCENTRATION (MIC AND MBC)…… 138

CHAPTER 5 CONCLUSION AND FUTURE WORK……142

REFERENCES……147

APPENDICES……152
APPENDIX A *Lorentzian / Gaussian resolution enhancement using SpinWorks 3*…152

LIST OF FIGURES

Figure 1.1: Distribution of *Scaevola spinescens*[10]…… 4

Figure 1.2: Morphology feature of *Scaevola spinescens*[10]…….... 5

Figure 1.3: Basic ring structure of flavonoid…….... 18

Figure 2.1: Picture of collection site (Photo: Michele Mejin, 2007)…… 28

Figure 2.2: Picture of the aerial parts of the plant taken at the collection site (Photo: Michele mejin, 2007)……...……..... 28

Figure 2.3: Picture of the aerial parts of the plant sent for herbarium identification (Photo: Michele Mejin, 2007)…….29

Figure 2.4: Flow chart of sample extraction…… 30

Figure 2.5: Fractionation from 8 g of hexane extract……... 32

Figure 2.6: Purification of H1007, H1008, H1103, H101003 and H1205……33

Figure 2.7: Fragment to build the 1st ring for [49] based on HMBC correlations…….....35

Figure 2.8: Closure of the 1st ring for [49] based on COSY and HMBC correlations……. 36

Figure 2.9: Closure of the 2nd ring for [49] based on COSY and HMBC correlations…….37

Figure 2.10: Closure of the 3rd ring for [49] based on HMBC correlations……. 38

Figure 2.11: Closure of the 4th ring for [49] based on HMBC correlations……. 39

Figure 2.12: Closure of the 5th ring for [49] based on COSY and HMBC correlations….. 40

Figure 2.13: Stereochemical assignments of the methyl hydrogens for [40] based on ROESY correlations…… 41

Figure 2.14: Stereochemical assignments of the hydrogens at δ_H 3.19 and δ_H 0.78 for [49] based on ROESY correlations……. 42

Figure 2.15: Stereochemical assignments of the hydrogens at δ_H 0.91, δ_H 0.96 and δ_H 1.41 for [49] based on ROESY correlations…… 43

Figure 2.16: Stereochemical assignments of the methyl hydrogens at δ_H 0.95 and δ_H 0.91 for [49] based on ROESY correlations…… 43

Figure 2.17: Comparison of stereochemistry between [49], [26] and [29]…….. 45

Figure 2.18: Fragment to build the 1st ring for [50] based on HMBC correlations……..48

Figure 2.19: Closure of the 1st ring for [50] based on COSY and HMBC correlations….. 50

Figure 2.20: Closure of the 2nd ring for [50] based on COSY and HMBC correlations….. 51

Figure 2.21: Closure of the 3rd ring for [50] based on HMBC correlations……. 52

Figure 2.22: Closure of the 4th ring for [50] based on HMBC correlations……. 53

Figure 2.23: Closure of the 5th ring for [50] based on COSY and HMBC correlations….. 54
Figure 2.24: Stereochemical assignments of the methyl hydrogens for [50] based on ROESY correlations……. 56
Figure 2.25: Stereochemical assignments of the hydrogens at δ_H 3.16 and δ_H 0.77 for [50] based on ROESY correlations……. 56
Figure 2.26: Stereochemical assignments of hydrogens at δ_H 0.77, δ_H 0.961 and δ_H 1.42 for for [50] based on ROESY correlations…… 57
Figure 2.27: Stereochemical assignments of methyl hydrogens at δ_H 0.89 and δ_H 0.964 for [50] based on ROESY correlations……. 57
Figure 2.28: Fractionation from 15 g of ethyl acetate extract…….. 61
Figure 2.29: Fractionation from 690 mg of fraction EA10…….. 62
Figure 2.30: Fractionation from 416 mg of fraction EA11……..……62
Figure 2.31: Fragment to build the 1st ring for [51] based on HMBC correlations……..64
Figure 2.32: Closure of the 1st ring for [51] based on COSY and HMBC correlations….. 65
Figure 2.33: Closure of the 2nd ring for [51] based on COSY and HMBC correlations….. 66
Figure 2.34: Closure of the 3rd ring for [51] based on COSY and HMBC correlations….. 67
Figure 2.35: Closure of the 4th ring for [51] based on COSY and HMBC correlations……67
Figure 2.36: Closure of the 5th ring for [51] based on COSY and HMBC correlations….. 69
Figure 2.37: Stereochemical assignments of the methyl hydrogens for [51] based on ROESY correlations…… 71
Figure 2.38: Stereochemical assignments of the hydrogens at δ_H 3.14 and δ_H 0.74 for [51] based on ROESY correlations……. 71
Figure 2.39: Stereochemical assignments of the hydrogens at δ_H 0.87, δ_H 1.11, δ_H 1.36 and δ_H 1.56 for [51] based on ROESY correlations……..... 72
Figure 2.40: Stereochemical assignments of the hydrogens at δ_H 0.87 and δ_H 0.95 and δ_H 2.19 for [51] based on ROESY correlations……... 72
Figure 2.41: Fractionation from 71 g of methanol extract……77
Figure 2.42: Closure of 1st ring for [56] based on COSY and HMBC correlations……. 80
Figure 2.43: Closure of 2nd ring for [56] based on COSY and HMBC correlations…… 80
Figure 2.44: Closure of 3rd ring for [56] based on HMBC correlations……... 81
Figure 2.45: ROESY correlations for [56] to show relative stereochemistry.……. 82
Figure 2.46: Closure of the 1st ring for [57] based on COSY and HMBC correlations……85
Figure 2.47: Closure of the 2nd ring for [57] based on HMBC correlations……86

Figure 2.48: Closure of the 3rd ring for [57] based on COSY and HMBC correlations….. 87
Figure 2.49: Fusing of the 3rd ring to the 2nd ring for [57] based on HMBC correlation…. 87
Figure 2.50: Closure of a sugar unit ring for [57] based on COSY coupling…….. 88
Figure 2.51: Stereochemical assignments for [57] based on ROESY correlations……. 89
Figure 2.52: Connection between the 4th and the 1st ring for [57] based on ROESY and HMBC correlations……. 90
Figure 2.53: Fractionation from 46 g of decoction aqueous extract…… 94
Figure 2.54: Fractionation from 71 g of soxhlet aqueous extract…… 96
Figure 2.55: Closure of a ring for [60] based on COSY coupling……98
Figure 2.56: Assignment of relative stereochemistry for [60] based on COSY coupling… 99
Figure 2.57: Different representations indicating the stereochemistry for [60]..... 99
Figure 3.1: Antibacterial testing on the crude extract of hexane as well as its sub-fractions (MIC value) (MBC value)…… 104
Figure 3.2: Antibacterial testing on the crude extract of ethyl acetate as well as its sub-fractions (MIC value) (MBC value)……106
Figure 3.3: Antibacterial testing on the crude extract of methanol as well as its sub-fractions (MIC value) (MBC value)……... 111
Figure 3.4: Antibacterial testing on the extracts from liquid-liquid partitioning of the aqueous decoction as well as its sub-fractions (MIC)..... 114
Figure 3.5: Antibacterial testing on the extracts from liquid-liquid partitioning of the aqueous soxhlet as well as its sub-fractions (MIC)……... 117
Figure 4.1: Template for broth micro-dilution assay[57] (adapted from Cos *et al*)…… 140
Figure 4.2: Template for duplicate plate (not treated with resazurin) to be tested for MBC[63] (adapted from Ndi *et al*)…… 141

LIST OF TABLES

Table 1.1: Summary of coumarins found in *Scaevola* species……. 9
Table 1.2: Classification of terpenoids……. 9
Table 1.3: Summary of terpenoids found in *Scaevola* species……. 13
Table 1.4: Summary of iridoids found in *Scaevola* species……. 16
Table 1.5: Presence of alkaloids in *Scaevola* species……... 17
Table 1.6: Flavonoids found in *Scaevola* species[39]……. 19
Table 1.7: List of microorganisms commonly used…… 22
Table 1.8: Pure compounds isolated from the crude fractions that may contribute to antibacterial activity[7]…….. 23
Table 2.1: Spectral data for [49] …….. 40
Table 2.2: ROESY correlations for [49]……... 44
Table 2.3: Comparison of the ^{13}C chemical shift between [49], and taraxerol [26]..... 45
Table 2.4: Spectral data for [50] …….. 54
Table 2.5: ROESY correlations for [50] ……..…… 58
Table 2.6: Comparison of the ^{13}C chemical shifts between [50] and myricadiol [24]…… 59
Table 2.7: Spectral data for [51] …….. 70
Table 2.8: ROESY correlations for [51]…..…… 73
Table 2.9: Comparison of the ^{13}C chemical shifts between [51] and ursolic acid [15]…… 74
Table 2.10: ROESY correlations for [56]…… 81
Table 2.11: Spectral data for [56]…… 82
Table 2.12: ^{1}H chemical shift values between [56] and [58]…… 83
Table 2.13: ^{13}C chemical shift values between [56] and [58]…….. 83
Table 2.14: Spectral data for [57]…… 91
Table 2.15: ROESY correlations for [57]…… 91
Table 2.16: ^{13}C chemical shift values between [57] and [44]…….. 92
Table 2.17: Spectral data for [60]…… 99
Table 3.1: Antibacterial testing on the crude extracts of *Scaevola spinescens*……..... 103

LIST OF ABBREVIATIONS

°C	degrees Celsius
v/v	volume per volume
ppm	parts per million
Hz	hertz
RNA	ribonucleic acid
CFU	colony forming units
TLC	Thin layer chromatography
UV	Ultraviolet
MP	melting point
FTIR	Fourier Transform InfraRed
NMR	Nuclear magnetic resonance
1D	one-dimensional
2D	two-dimensional
DEPT	Distortionless Enhancement by Polarization Transfer
COSY	Correlation Spectroscopy
HSQC	Heteronuclear Single Quantum Coherence
HMBC	Heteronuclear Multiple Bond Correlation
ROESY	Rotational nuclear Overhauser Effect Spectroscopy
m	multiplet
s	singlet
d	doublet
t	triplet
q	quadruplet
δ_C	chemical shift for ^{13}C
δ_H	chemical shift for ^{1}H
ATCC	American Type Culture Collection
IC_{50}	50% inhibitory concentrations

ABSTRACT

Scaevola spinescens, an Australian indigenous plant has been used by Australian Aboriginal people in their traditional medicines for treating colds, stomach ache, urinary problems and pain in the alimentary tract, skin rashes, boils and sores. An infusion of leaves and twigs of *Scaevola spinescens* and *Codonocarpus cotinifolius* has been reputed to cure cancer. Therefore, this plant has been deemed desirable for investigation to identify possible active compounds that contribute to these medicinal therapies used by the Aboriginal people.

Previous work has shown that coumarins, terpenoids, iridoids and flavonoids are the classes of compounds isolated from *Scaevola spinescens*. So far, chemical constituents of *Scaevola spinescens* have only been isolated from hexane and methanol fractions. One of the aims of this research was to isolate more of the chemical constituents of *Scaevola spinescens*. Therefore in this research, the ethyl acetate and aqueous fractions were also included to broaden the range of compounds being isolated.

In this research, eleven compounds have been isolated from *Scaevola spinescens*. Five of the isolated compounds are known – myricadiol, 20-*epi*-ursolic acid, decursinol, luteolin-7-*O*-glucoside, and 2-*deoxy*-D-chiro-inositol. A novel compound identified as 18-*epi*-taraxerol has been isolated from *Scaevola spinescens* in this study. The structures of these compounds were determined using 1D and 2D NMR, UV-Visible spectroscopy, FTIR and high-resolution mass spectrometry. The structures of the five remaining compounds are yet to be determined.

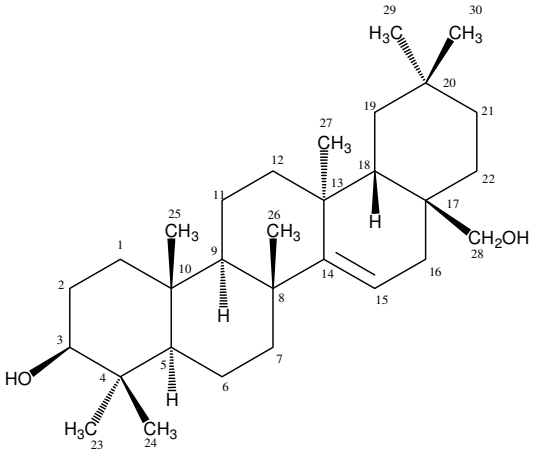

Myricadiol

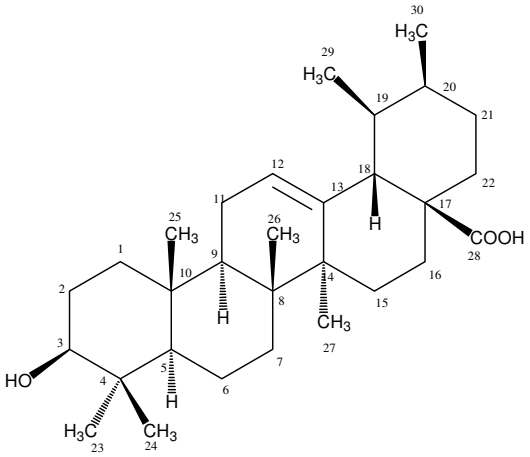

20-*epi*-ursolic acid

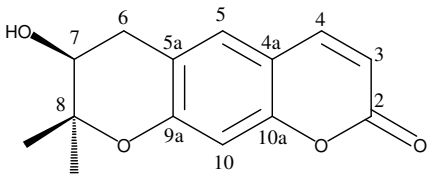

Decursinol

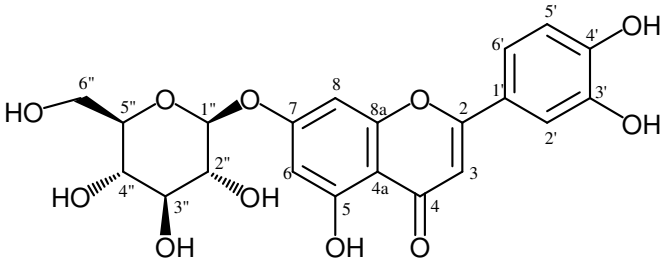

Luteolin-7-*O*-glucoside

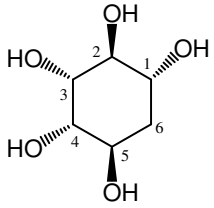

2-*deoxy*-D-chiro-inositol

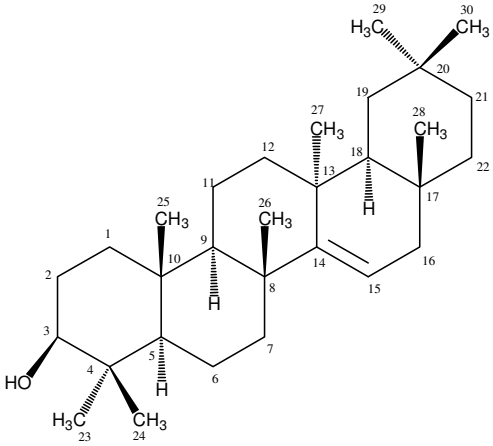

18-*epi*-taraxerol

The antiviral, antitumor and antibacterial activity of *Scaevola spinescens* extracts has been previously investigated. Previous work has shown that *Scaevola spinescens* was active against human cytomegalovirus (HCMV). However, previous work done on the antitumor activity of *Scaevola spinescens* was inconclusive. Previous work done on the antibacterial activity showed that some of the methanol fractions from *Scaevola spinescens* might contain antibacterial agents. However, these active compounds that contribute to the antibacterial activity were yet to be identified.

In this work, the organic (hexane, ethyl acetate and methanol) and aqueous crude extracts of *Scaevola spinescens* were screened for antibacterial activity against Gram-positive (*Staphylococcus aureus* ATCC 25923 and *Streptococcus pyogenes* ATCC 10389) and Gram-negative (*Pseudomonas aeruginosa* ATCC 27853 and *Escherichia coli* ATCC 25922) bacteria using a broth micro-dilution assay to determine minimum inhibitory concentration (MIC) and minimum bactericidal concentration (MBC).

The hexane, ethyl acetate and methanol crude extracts were found to have antibacterial activity against Gram-positive bacteria specifically *Streptococcus pyogenes* while the aqueous fractions showed significant antibacterial activity against *Staphylococcus aureus*. No antibacterial activity was observed against Gram-negative bacteria.

A promising antibacterial activity was observed on one of the isolated compounds, 20-*epi*-ursolic acid. This compound showed good antibacterial activity against *Streptococcus pyogenes* and *Staphylococcus aureus* with MIC in the range 1.87 to 7.5 µg/ml.

The research presented within this thesis shows that 20-*epi*-ursolic acid isolated from *Scaevola spinescens* might be a potential candidate as an antibacterial agent. This is supported by the results obtained from preliminary antibacterial screening on the organic and aqueous crude extracts.

STATEMENT

This work contains no material which has been accepted for the award of any other degree or diploma in any university or other tertiary institution and, to the best of my knowledge and belief, contains no material previously published or written by another person, except where due reference has been made in the text.

I give consent to this copy of my thesis, when deposited in the University Library, being available for loan and photocopying, subject to the provisions of the Copyright Act 1968.

Michele Mejin

February, 2009

ACKNOWLEDGEMENTS

I would like to express my sincere thanks to the people that have given me support from the beginning of my research, along the way and up till the completion of my thesis. Their assistance and support has been the key to my successful thesis.

First and foremost, I would like to express my sincere gratitude to my supervisor, Dr. Simon Pyke for his invaluable help and guidance during the course of my research, especially in the area of NMR. It is a completely new area of study for me and I'm grateful for his patience in teaching me the basic skill of NMR as well as data interpretation for structural elucidation. His optimism has been a great encouragement for me to face any obstacle along the way.

I would also like to express my sincere gratitude to Dr. Susan Semple, who has been supervising me in my anti-microbial work. Her constant guidance and advice in microbiology aspects has been a great help.

I would like to express my appreciation to Mr. Philip Clements for his assistance in running my 2D NMR experiments as well as his patience in processing my NMR data. Appreciation is also expressed to Mr. Marshall Hughes and Mr. Edwin Lowe for their assistance in obtaining my mass spectrometry data.

In here, I would also like to express my utmost gratitude to the Sarawak Government and my employer, Sarawak Biodiversity Centre for their sponsorship as well as their encouragement for further studies. Without them, this would have been impossible. I thank them with sincere heart.

In addition to all of the above people, I would also like to thank my family, especially my mum and dad, not forgetting my two lovely siblings, Rachel and Malcolm for their unconditional love and encouragement from a far. I would also like to thank Andrew and his parents for their unconditional love and understanding throughout the period of accomplishing this thesis.

Last but not least, I would like to thanks all my friends that have been supportive in giving their encouragement, advice and critics that help in accomplishing my thesis. Special thanks to Sally Nobbs, for her help in my NMR work. Also Belinda Ng and Hii Mei Mei for being here all along. Not forgetting my lovely labmates, Rhiannon Jones, Jessica Smith, Melissa Perrotta and Justin Nash. It has been fun working with them. For those that I've met throughout my 2 years of research work, especially new friends that I've made in the chemistry department as well as in my integrated bridging programme (IBP). I thank you all for putting spice into my research life.

Above all, I would like to thank GOD for making all this possible for me. He had this all planned out for me.

CHAPTER 1

Introduction

1.1 General Introduction

The Chinese pharmacopeia was the earliest record of medicinal usage of plants, being published in approximately 3000BC.[1] Herbal medicine might have started long before 3000BC and been verbally passed down from older generation to younger generation in any tribal group or race.

The tribal Aboriginal people in central and north Australia still practice traditional medicine and this knowledge is now recorded.[1] With the knowledge contributed by the Aboriginal communities of the Northern Territory, an Aboriginal pharmacopeia was published in 1988.[1] Traditional medicine is usually associated with various remedies using different parts of a plant. Different tribes of Aboriginal people have different ways of preparing their remedies. Hence, the same plant is often used medicinally in completely different ways by different Aboriginal people.[1]

Plants used in traditional medicine are more likely to have pharmacologically active compounds compared to random selections of plant material. Therefore, ethnomedicine plays a role in drug discovery. Relatively little research has been done on the plants used by the Aboriginal people. The ethnomedicine information gathered from these people can be used to drive research towards drug development. Various drugs used in today's medicines are derived from plants (eg. morphine, salicin, rotundine and codeine).[2]

One of the native Australian plants of interest is *Scaevola spinescens*. This small woody bush with its spiny fan flowers has been used by the Aboriginal people in their traditional medicine. Based on the ethnomedicine information, *Scaevola spinescens* has been deemed desirable for further studies.

The plant is thought to have antiviral properties. Therefore, studies on the antiviral activity of the plant have been done to verify this statement.[3,4] This statement is based on the cure used by the Aboriginal people in treating the common cold.

Besides antiviral properties, the plant is also thought to have antibacterial and antifungal properties. This is because most of the cures used by the Aboriginal people are related to bacterial and fungal infections. These activities have been investigated by Kerr *et al*[5] and Nobbs[6]. Nevertheless, further investigation on these activities can be done to identify active compounds that contribute to the antibacterial and/or antifungal activities.

Another interesting study done on the biological activity of the plant is the anti-tumor activity. This started with the remedy used by the Aboriginal medicine men, which is an infusion of this plant together with the Desert Poplar, *Codonocarpus cotinifolius*. To verify this activity in the plant, the Chemistry Centre of Western Australia (CCWA) has conducted research on this plant, which was funded by the Australian Government.[7] The funding was terminated in 1991 when CCWA was unable to prove scientifically that the plant extract had anti-cancer properties. Nevertheless, this has not restrained researchers from further investigating the anti-tumor activity in the plant. This form of activity was also studied by Kerr *et al*[5] and Nobbs[6] using different approaches. Kerr *et al* investigated the anti-tumor activity of the plant using the Crown Gall Tumor Assay[5] whereas Nobbs used the cytotoxicity approach, testing on different types of cancer cell lines[6]. Although there are promising results from their studies, further investigations need to be done to verify these results.

Generally, there has been a wide range of studies done on this plant from antiviral activity to antibacterial and anti-tumor activity. So far, the antibacterial activity of the aqueous extract has not been studied. There is a possibility that the aqueous extract of the plant might have antibacterial activity. This is said based on the cures claimed by the Aboriginal people, using aqueous decoctions of the plant as their remedy.

Until 1996 when Kerr and colleagues managed to isolate myricadiol and other taraxerenes in methanol extracts of *Scaevola spinescens*, there had been little work on profiling the chemical constituents of the plant.[5] There is a possibility that these compounds can be used as potential anti-cancer drugs or as a starting point for development of synthesized anti-cancer drugs. This is based on the observation made by Kerr in 1999[8]. So far, the chemical constituents in methanol extract have been studied by both Kerr[8] and Nobbs[6]. No chemical profile on an aqueous extract has been done yet. Therefore, there may still be more compounds in the plant that are yet to be identified.

1.2 Goodeniaceae

Goodeniaceae is a family of 11 genera comprise of about 400 species.[9] The 11 genera are *Scaevola*, *Anthotium, Lechenaultia, Dampiera, Coopernookia, Diaspasis, Goodenia, Selliera, Velleia, Pentaptilon* and *Verreauxia*. Most of these genera are confined to the southern hemisphere, mainly found in Australia and New Guinea.[9] The plants from Goodeniaceae family are usually herbs and shrubs.[9]

1.3 *Scaevola species*

1.3.1 Distribution

There are 96 *Scaevola* species occurring in Australia and tropical areas of the Indo-Pacific region.[9] Out of 71 species found in Australia, 70 species are endemic.[9]

NOTE:
This figure is included on page 4 of the print copy of the thesis held in the University of Adelaide Library.

Figure 1.1: Distribution of *Scaevola spinescens*[9]

Figure 1.1 shows the distribution of *Scaevola spinescens* in Australia. *Scaevola spinescens* is mostly found on sandy loams and hills in inland regions of Central and Western Australia as well as New South Wales.[4]

1.3.2 Morphology

Scaevola plants are usually perennial herbs, scramblers, shrubs or small trees of about 3 m height. These small, herbaceous plants can be distinguished by their spiny fan-shaped flower. The leaves are usually alternate and petiolate with axillary hair tufts.[9]

Scaevola spinescens is a rigid shrub of about 1-2 m tall, covered with scurfy hairs. It has short, spiny branchlets. The leaves, about 10-25 mm long, are often clustered on branchlets. It has flowers with 5 fan-shaped petals. The flowers are white to yellowish in colour and occasionally with purple veins. The 5-8 mm long fruit is usually ovoid, glabrous and black or dark purplish in colour.[3,4,9-11]

Figure 1.2: Morphology feature of *Scaevola* species[9]

Scaevola. **A–D**, *S. myrtifolia*. **A**, indusium; **B**, anther; **C**, corolla; **D**, habit (**A–D**, D.Whibley 1983, SYD). **E**, *S. spinescens*, habit (J.West 4008, SYD). **F–H**, *S. pulchella*. **F**, anther; **G**, indusium; **H**, corolla (**F–H**, J.Beard 2980, PERTH). **I**, *S. browniana* subsp. *browniana*. habit (G.Carr 47511, SYD). **J**, *S. revoluta* subsp. *revoluta*, habit (R.Carolin 9244, SYD). Scale bars: **A**, **G** = 2 mm; **B**, **D**, **F** = 1.5 mm; **C** = 5 mm; **E**, **I**, **J** = 30 mm; **H** = 6 mm. Drawn by D.Mackay.[9]

1.3.3 Uses

Scaevola species have been used in various traditional medicines. They are usually prepared in decoction form. However, some are used as an application on the surface. Different parts of the plant are used to treat various illnesses, diseases or wounds.

The study on the uses of each *Scaevola* species gives a general idea of their medicinal value. *Scaevola* species that have similar medicinal value might possess similar biological activities. These can later be linked to the chemical constituents that are responsible for any of these biological activities.

The crushed fruit of *Scaevola taccada* (Synonym: *Scaevola frutescens* and *Scaevola sericea*) has been used by early settlers to treat tinea.[3] It is said that the leaves were taken when having indigestion.[12] They were also used in a poultice to cure headache.[12] In addition, there are also reports indicating the use of leaf decoction and the flesh of the seeds as a contraceptive.[13] The juice from ripe fruit has been used to treat sores and infected eyes whereas a combination of juices from ripe fruit and stem has been used as a remedy for bites and stings.[14] This plant has also been used as a dermatological aid in Hawaii. A mixture of pounded root bark with salt is used for cut and skin diseases.[15] In Indonesia, the root is used as an antidote when poisonous fish and crabs are consumed.[12]

Scaevola montana is used as an agent promoting menstrual flow in New Caledonia.[13]

The root decoction of *Scaevola spinescens* has been used to treat stomach ache, urinary problems and pain in the alimentary tract.[4,16] As for the stem decoction, it is said to cure boils, skin rashes and sores.[4]

1.4 Chemical constituents

The chemical constituents in plants vary from one species to another. Plants of similar genus usually have similar major chemical constituents and additional compounds to distinguish each species. Therefore, information on the chemical constituents of other *Scaevola* species can give a general overview of chemical constituents in *Scaevola* plants. In addition, any novel compounds found in *Scaevola* species as well as *Scaevola spinescens* can be easily identified.

Secondary metabolites found found in plants are organic compounds that are not directly involved in the normal growth, development or reproduction of the plant. These compounds may be part of a defence mechanism of the plant or in facilitating reproductive processes.

The chemistry of known organic compounds such as coumarin, terpenoids, iridoids, alkaloids and flavonoids are interrelated with biological activities. Findings on the biological activities related to any of the chemical constituents found in *Scaevola* species can be used as a guideline to the possible biological activities in *Scaevola spinescens* that possess similar chemical constituents.

1.4.1 Coumarins

Coumarins [1] are phenolic substances made of fused benzene and α-pyrone rings. They are derived from the metabolism of phenylalanine via cinnamic acid.

Xanthyletin [2], a coumarin isolated from citrus, was found to inhibit the growth of *Phytophthora citrophthora*.[17] However, the anti-fungal activity degrades over time resulting from oxidation of xanthyletin in aqueous solution. There is a possibility that the antifungal activity can be improved by modifying the xanthyletin structure. Xanthyletin has also been found in *Scaevola spinescens*.[5]

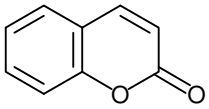

[1]

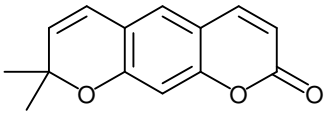

[2]

Studies on the structure-activity relationship (SAR) of the coumarins with antibacterial activity have been done. The presence of an aromatic dimethoxy arrangement in simple coumarins has the ability to inhibit the growth of microorganism that requires special growth factors such as beta-hemolytic *Streptococcus, Streptococcus pneumoniae* and *Haemophillus influenzae*.[18] In addition, a combination of two methoxy functions and at least one additional phenolic group gave promising results as a broad-spectrum antibacterial.[18]

Besides xanthyletin [2], nodakenetin / marmesin [3][5] and emmarin [4][6] were also found in *Scaevola spinescens*. The presence of coumarins in other *Scaevola* species has also been reported. Imperatorin [5] and (R)-(-)-nodakenetin [6] are two fluorescent coumarin compounds identified in *Scaevola frutescens*.[19]

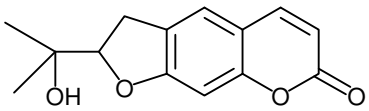

[3]

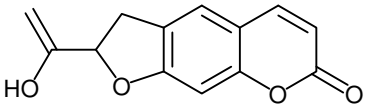

[4]

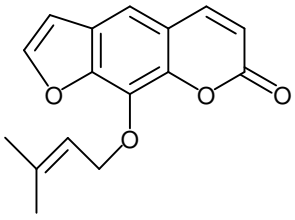

[5]

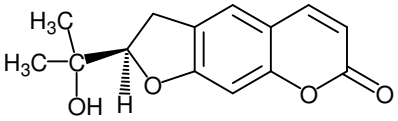

[6]

Table 1.1: Summary of coumarins found in *Scaevola* species

Compounds	*Scaevola spinescens*	Other *Scaevola* species
Xanthyletin [2]	5	
Emmarin [4]	6	
Nodakenetin [3]	5	
(R)-(-)-nodakenetin [6]		19
Imperatorin [5]		19

The references of the compounds found are as indicated in the table above

Found Not found

1.4.2. Terpenoids

Terpenoids are organic compounds derived from five-carbon isoprene [7] units assembled and modified in different ways. The classifications of terpenoids are summarized in the ***Table 1.2***.

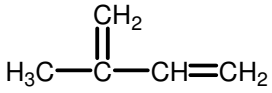

[7]

Table 1.2: Classification of terpenoids

Terpenes	Isoprene units	Carbon atoms
Monoterpenes	2	10
Sesquiterpenes	3	15
Diterpenes	4	20
Sesterterpenes	5	25
Triterpenes	6	30
Carotenoids	8	40

Sterols, which have the characteristics of a steroid skeleton, are produced from terpenoid precursors. These compounds are related to cholesterol. Sterols from plants are known as phytosterols. Examples of phytosterols are β-sitosterol [8], stigmasterol [9], ergosterol [10], (3β,22E)-stigmasta-5,22-dien-3-ol [11] and (3β,24S)-stigmast-5en-3-ol [12] .

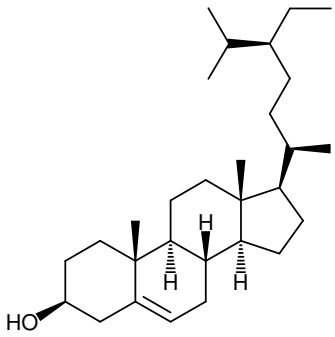

[8]

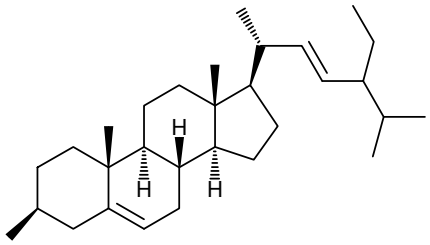

[9]

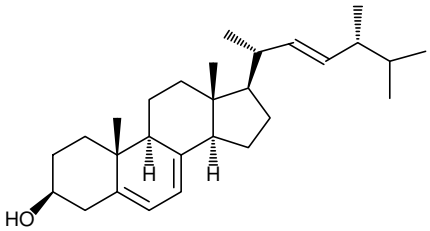

[10]

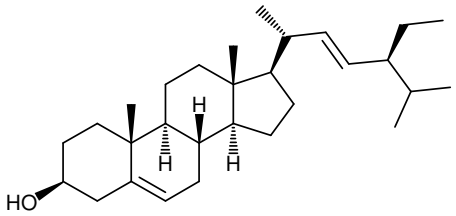

[11]

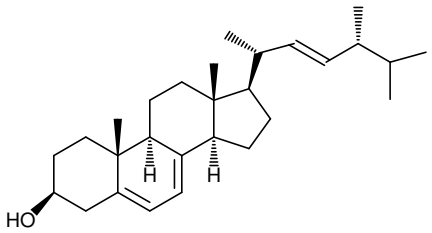

[12]

Terpenoids are variously said to have antiseptic activity, irritant properties and sedative properties.[20] Besides that, various studies show that they are active against bacteria, fungi, viruses and protozoa.[21] There is a wide range of pharmacological activities studied in natural triterpenoids. Based on these studies, betulinic acid [13], a pentacyclic triterpene, has been found to have significant anti-tumor, antiviral, antibacterial, anti-inflammatory, bronchovasodilator, analgesic and antiplasmodium activity.[22,23]

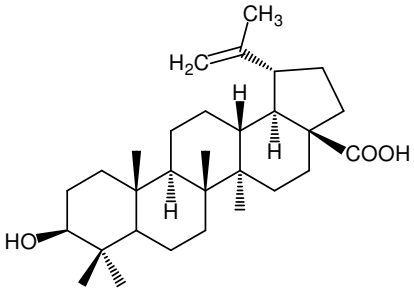

[13]

The pharmacological activity of lupeol [14] and ursolic acid [15] have also been studied. These compounds were found to possess anti-cancer effects, anti-inflammatory effects as well as hepato and cardio protective effects.[22,23] Analgesic properties was also reported for ursolic acid.[22] Ursolic acid [15] has been found in the methanol fraction isolated from *Scaevola spinescens*.[6] Therefore, there is a possibility that *Scaevola spinescens* might have those

biological activities. In addition, lupeol derivatives [16] have moderate antibacterial activity.[23] Lupenone [17] has been found in the hexane fraction isolated from *Scaevola spinescens*.[5]

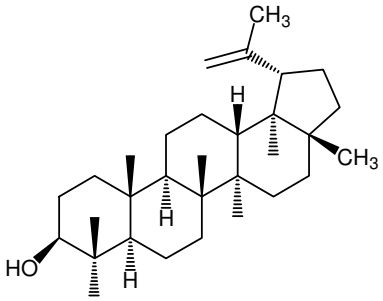

[14]

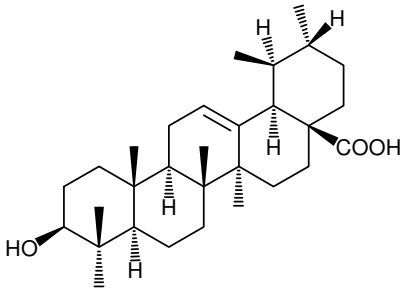

[15]

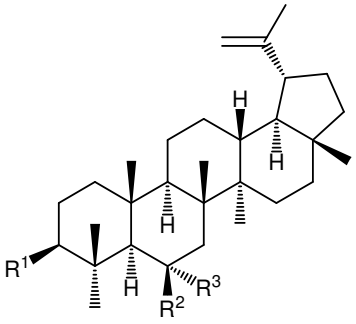

	R_1	R_2	R_3
(I)	OH	OH	H
(II)	$COC_{17}H_{35}$	H	OH

[16]

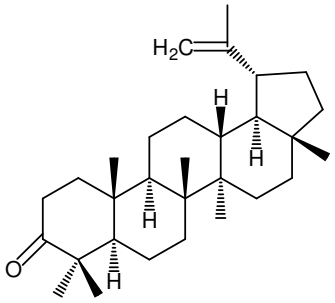

[17]

Terpenoids are commonly found in *Scaevola* species. A mixture of six novel γ-amyrin fatty esters with C_{20} – C_{30} acid moieties [18] have been isolated from the bark of *Scaevola florinbunda*.[24] Other triterpenes such as γ-amyrin [19], γ-amyrin acetate [20], ursolic acid acetate [21], betulinic acid [13] and betulin [22] have also been found in *Scaevola floribunda*.[24] β-Amyrin [23] has been found in the methanol fraction isolated from *Scaevola spinescens*.[6] Myricadiol (pentacylic triterpenoid, 14-taraxerene-3,28-diol) [24] and other taraxerenes [25-29] were isolated from *Scaevola spinescens*.[5,6] These terpenoids, found in *Scaevola spinescens* are summarized in **Table 1.3**, indicating their presence in which fractions.[5]

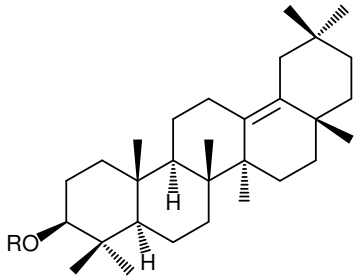

(I) R = $COC_{19}H_{39}$

(II) R = $COC_{21}H_{43}$

(III) R = $COC_{23}H_{47}$

(IV) R = $COC_{25}H_{51}$

(V) R = $COC_{27}H_{55}$

(VI) R = $COC_{29}H_{59}$

[18]

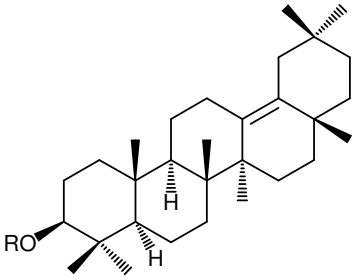

[19] **R = H**

[20] **R = $COCH_3$**

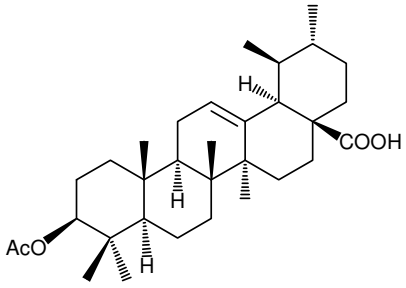

[21]

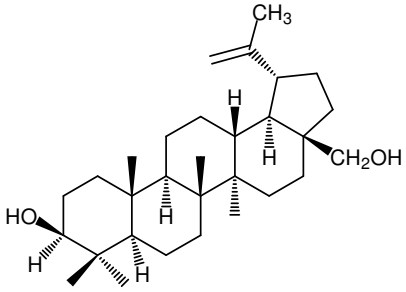

[22]

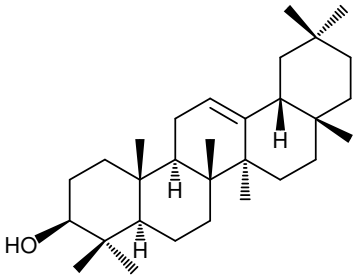

[23]

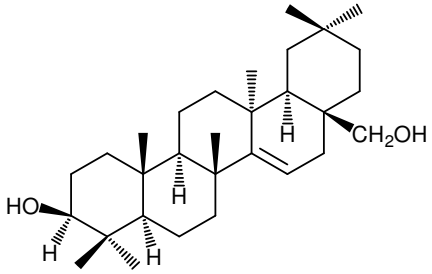

[24]

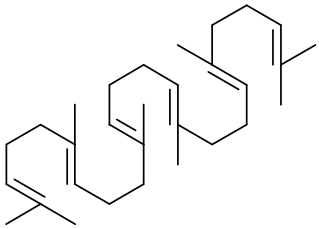

[25]

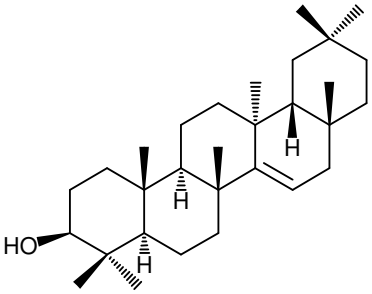

[26]

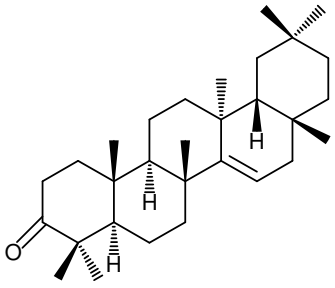

[27]

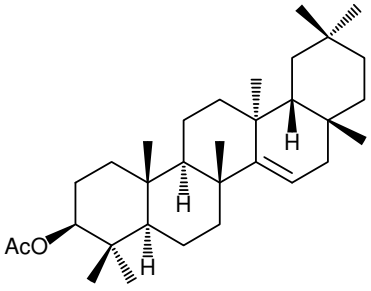

[28]

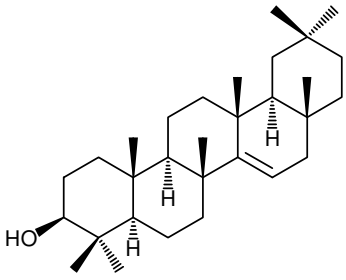

[29]

Table 1.3: Summary of terpenoids found in *Scaevola* species

Compounds	*Scaevola spinescens*		Other *Scaevola* species
	Methanol fraction	Hexane fraction	
β-sitosterol [8]	[5]		
(3β,22E)-stigmasta-5,22-dien-3-ol [11]		[5]	
(3β,24S)-stigmast-5en-3-ol [12]		[5]	
Betulinic acid [13]			[24]
Ursolic acid [15]	[6]		
Lupenone [17]		[5]	
Mixture of six novel γ-amyrin fatty esters with C_{20}-C_{30} [18]			[24]
γ-amyrin [19]			[24]
γ-amyrin acetate [20]			[24]
Ursolic acid acetate [21]			[24]
Betulin [22]			[24]
β-amyrin [23]		[5]	
Myricadiol [24]	[5]		
Squalene [25]	[5]		
Taraxerol [26]	[5,6]	[5]	
Taraxerone [27]		[5]	
Taraxerol acetate [28]	[6]	[5]	
13-*epi*,18-*epi*-taraxerol [29]	[6]		

The references for the compounds found are as indicated in the table above

Found Not found

1.4.3 Iridoids

Iridoids are monoterpenes that are derived biosynthetically from geranylpyrophosphate (C_{10}) and are typically bicyclic hemiacetals or lactones.[25] They are characterized by a cyclopenta-[c]-pyranoid skeleton and are often intermediates in the biosynthesis of alkaloids.[20]

Cantleyoside dimethyl acetal [30] and loganin [31] isolated from *Pterocephalus perennis* were found to have significant antibacterial and antifungal activity.[26] These compounds have also been found in some *Scaevola* species.

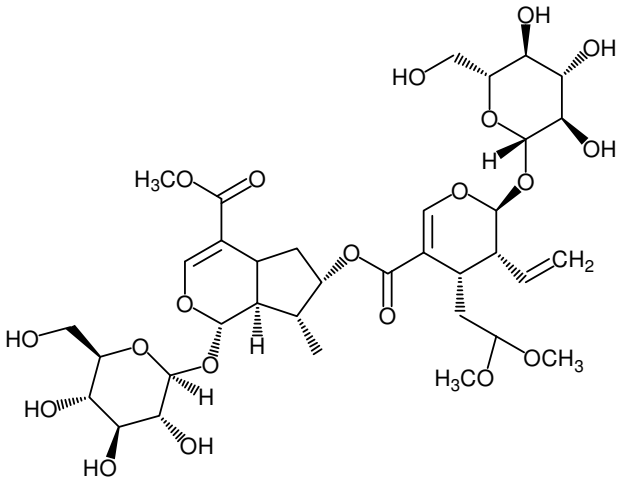

[30]

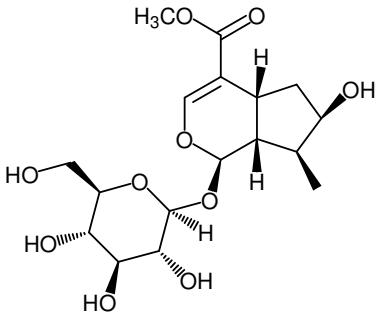

[31]

Based on literature reports, iridoids are largely found in *Scaevola* species. Five iridoids namely loganin [31], cantleyoside dimethyl acetal [30], cantleyoside [32], sylvestroside III [33] and scaevoloside [34] were identified in *Scaevola montana*.[13]

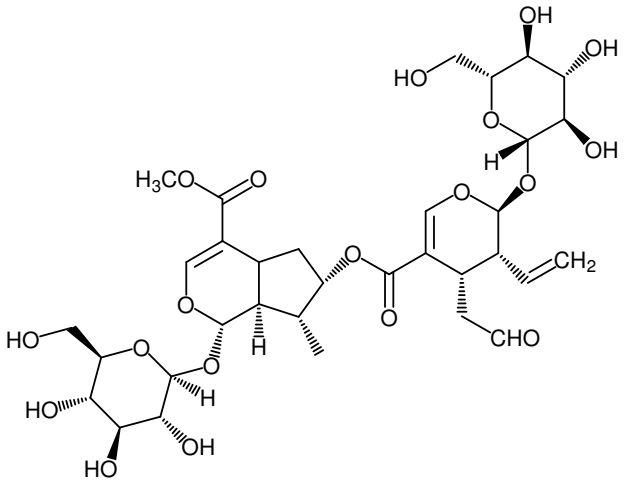

[32]

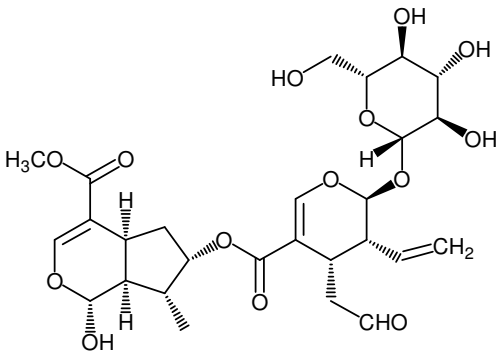

[33]

Five iridoids were also reported in *Scaevola racemigera*.[27] They were loganin [31], loganic acid [35], sylvestroside III [33], cantleyoside [32] and scaevoloside [34]. Loganin [31] and scaevoloside [34] were also found in *Scaevola spinescens*.[6]

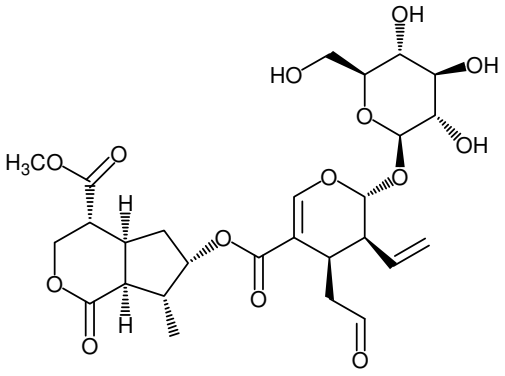

[34]

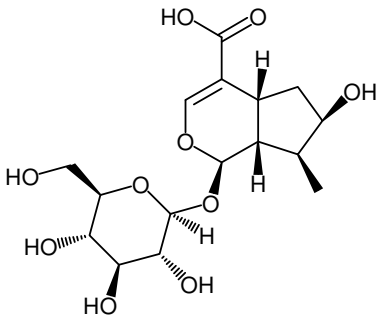

[35]

Floribundal [36], a nonglycosidic bisiridoid and loganin [31] have been isolated from the heartwood of *Scaevola floribunda*.[24] The presence of loganin [31] in these four *Scaevola* species shows that this compound might be a chemical precursor for other iridoids in other *Scaevola* species. There are possibilities that these *Scaevola* species might have antibacterial and antifungal activity.

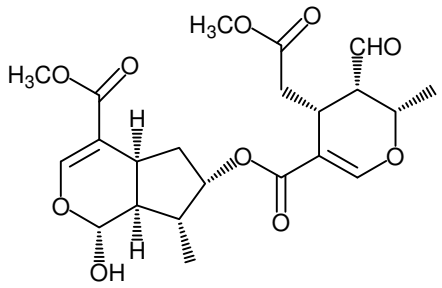

[36]

Two other iridoids, scaevoloside dimethyl acetal [37] and katecateroside [38] were newly found in *Scaevola spinescens*.[6] The presence of scaevoloside dimethyl acetal and loganin in *Scaevola spinescens* shows that there is a possibility that this plant might have antibacterial and antifungal activity. Therefore, the study of antibacterial activity on this plant is deemed desirable for investigation.

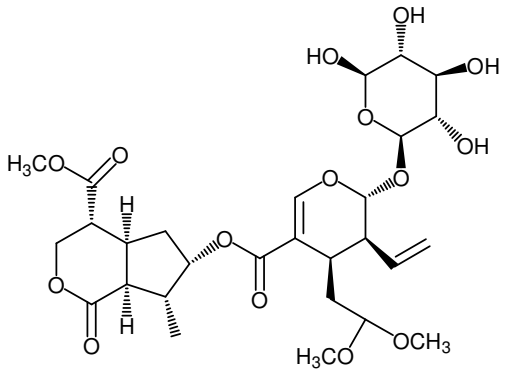

[37]

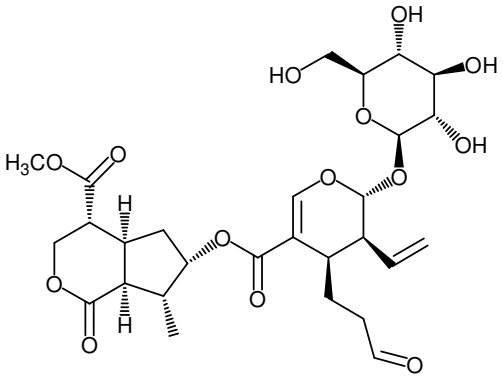

[38]

Table 1.4: Summary of iridoids found in *Scaevola* species

Compounds	*Scaevola spinescens*	Other *Scaevola* species
Cantleyoside dimethyl acetal [30]		13,26
Loganin [31]	6	24,26,27
Cantleyoside [32]		13,27
Sylvestroside III [33]		13,27
Scaevoloside [34]	6	13,27
Loganic acid [35]		27
Floribundal [36]		24
Scaevoloside dimethyl acetal [37]	6	
Katecateroside [38]	6	

The references for the compounds found are as indicated in the table above

Found Not found

1.4.4 Alkaloids

Alkaloids have a complex structure, usually defined as nitrogen-containing, basic substances of natural origin and of limited distribution. Their nitrogen atom is part of a heterocyclic system.

The presence of alkaloid compounds in *Scaevola* species has been studied. Four new dimeric monoterpene alkaloids have been isolated from the aerial parts of *Scaevola racemigera*.[28] They are Scaevodimerine A [39], Scaevodimerine B [40], Scaevodimerine C [41] and Scaevodimerine D [42].

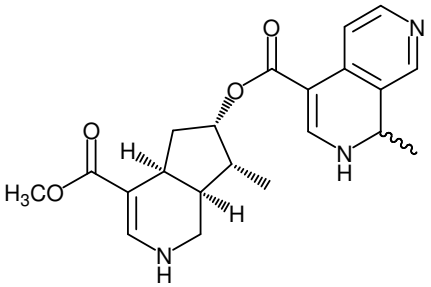

[39]

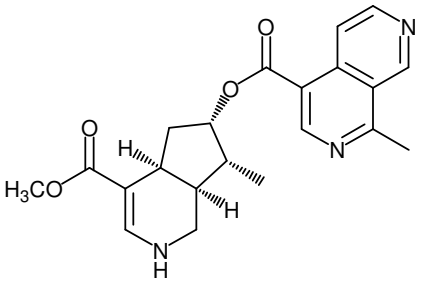

[40]

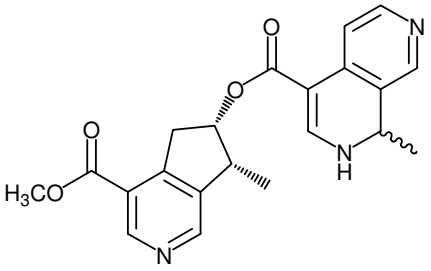

[41]

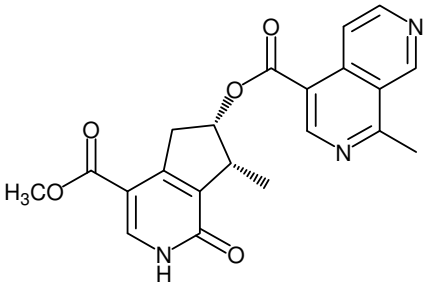

[42]

Out of the 11 *Scaevola* species previously tested, only *Scaevola densevestitia* tested positive to Mayer's reagent and silicotungstic acid.[29] Most alkaloids are precipitated from neutral or slightly acidic solution by Mayer's reagent (potassiomercuric iodide solution) to give a cream coloured precipitate. All the crude fractions from the methanol extract of *Scaevola spinescens* tested negative against Mayers's reagent.[6] The presence of alkaloids in all of the *Scaevola* species tested to date is shown in ***Table 1.***5.

Table 1.5: Presence of alkaloids in *Scaevola* species

Scaevola **species**	**Presence of alkaloid**
Scaevola aemula	Negative[29]
Scaevola albida	Negative[29]
Scaevola angustata	Negative[29]
Scaevola crassifolia	Negative[29]
Scaevola densevestitia	Positive[29]
Scaevola hispida	Negative[29]
Scaevola microcarpa	Negative[29]
Scaevola oppositifolia	Negative[29]
Scaevola ovalifolia	Negative[29]
Scaevola parviflora	Negative[29]
Scaevola racemigera	Four new dimeric monoterpene alkaloid found [38 -41][28]
Scaevola sericea	Negative[29]
Scaevola spinescens	Negative[6]

The references are as indicated in the table above

1.4.5 Flavonoids

Flavonoids are polyphenolic compounds that have a C_6-C_3-C_6 carbon framework, or more specifically a phenylbenzopyran functionality.

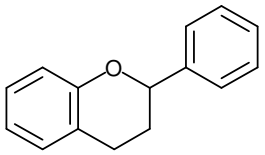

Figure 1.3: Basic ring structure of flavonoid

There are different types of flavonoids such as chalcones, dihydrochalcones, aurones, flavanones, flavones, flavonols, flavanols, flavanonols, flavans, leucoanthocyanins, anthocyanidins, anthocyanins, isoflavones and isoflavanones. Each of these have different characteristics with different biological effects.

The presence of polyphenols contributes to the free radical scavenging activities which is related to the antioxidant activity.[30] Some flavonoids such as quercetin [43] have been found to possess antioxidant and anti-inflammatory activity.[31] For example, in the study done by Bouaziz *et al*, the flavonoids which are the secondary metabolites found in olive tree showed significant antioxidant activity.[32] Luteolin-7-*O*-glucoside [44], one of the flavonoids compounds found in olive trees has also been found in *Scaevola spinescens*.[6] Besides possessing antioxidant activity, luteolin-7-*O*-glucoside was found to have antibacterial and antifungal activity.[33]

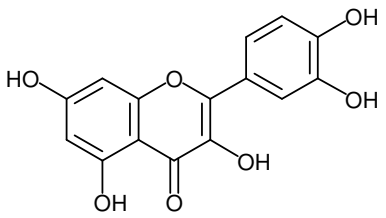

[43]

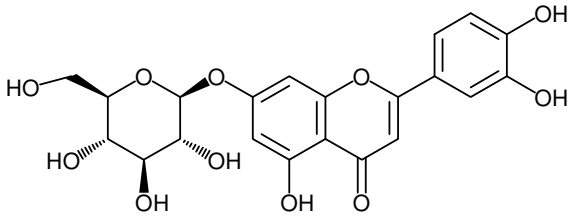

[44]

Flavonoids were also reported to have the ability to protect against peroxynitrite toxicity[34], which is associated with airway disease[35] and cardiovascular disease.[36]

Besides luteolin-7-*O*-glucoside, luteolin-7-*O*-glucuronide methyl ester [45] has also been isolated from *Scaevola spinescens*.[6] This indicated that *Scaevola spinescens* might possess

antioxidant activity as well as antibacterial and antifungal activity based on the findings found by Cho *et al*[31] and Bouaziz *et al*[32].

It is not uncommon for flavonoids to have conjugation with various sugars. The conjugation of flavonoids affects the mechanism by which the compound is absorbed by altering the basic physicochemical properties.[37] This will give the ability of the compounds to enter cells, to interact with transporters and to interact with cellular (lipo) proteins.[37]

Seven flavonoids have been isolated from Hawaiian *Scaevola* species (*Scaevola chamissoniana, Scaevola coriacea, Scaevola gaudichaudiana, Scaevola gaudichaudii, Scaevola kilaueae, Scaevola mollis, Scaevola procera*) as well as the hybrid (*Scaevola cerasifera*).[38] The seven flavonoids consist of apigenin [46] and quercetin [43] with various sugar conjugations. Flavonoid profiles for the seven species plus the hybrid are summarized in the ***Table 1.6***.

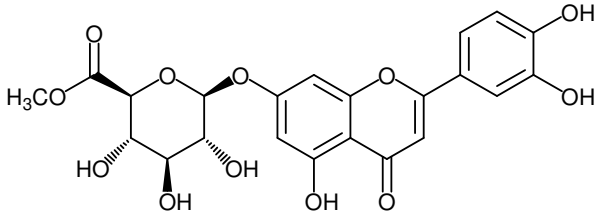

[45]

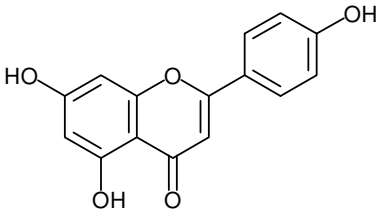

[46]

Table 1.6: Flavonoids found in *Scaevola* species[38]

1.5 Biological activities

1.5.1 Antiviral

The ethanol extract of *Scaevola spinescens* has previously been tested for antiviral activity against human cytomegalovirus strain AD 169 (HCMV, *Herpesviridae*), Ross River Virus strain T48 (RRV, *Togaviridae*) and poliovirus type 1 (*Picornaviridae*).[39] Human cytomegalovirus strain AD 169 is a DNA virus, whereas Ross River virus strain T48 and poliovirus type 1 are RNA viruses. Based on the study, the ethanol extract of *Scaevola spinescens* was found to be most active against human cytomegalovirus (HCMV).[39]

Six purified compounds from the methanol extract of *Scaevola spinescens* were submitted for antiviral testing against Herpes simplex type 1 (HSV1, *Herpesviridae*), Ross River virus strain T48 (RRV, *Togaviridae*) and Poliovirus type 2 (*Picornaviridae*).[6] The compounds tested were taraxerol [26], ursolic asid [15], emmarin [4], scaevoloside [34] and loganin [31]. However, these compounds did not show any antiviral activity.

1.5.2 Anti-tumor and cytotoxicity

The compounds isolated from *Scaevola spinescens* by Kerr *et al*[5] as well as the aqueous extract of *Scaevola spinescens* obtained from CCWA[7] were found to have significant anti-tumor activity based on the crown gall tumor assay.[8] The crown gall tumor assay (CGTA), used for investigating anti-tumor activity, is based on the inhibition of crown galls induced in wounded potato tissue by *Agrobacterium tumefaciens*.

The crude fractions of *Scaevola spinescens* have also been tested on different cancer cell lines for cytotoxicity activity.[6] However, the results obtained were inconclusive as some of the fractions showed massive stimulatory effects at higher concentration instead of inhibiting the growth of these cancer cell lines.

The anti-tumor and cytotoxicity activity of *Scaevola spinescens* are inconclusive at this stage. An infusion of leaves and twigs of *Scaevola spinescens* and *Codonocarpus cotinifolius* has been reputed to cure cancer. Therefore, there is a possibility that the anti-tumor and cytotoxcity activity is only exerted when in the presence of active compounds from both plants.

Scaevola aemula, Scaevola albida, Scaevola angustata, Scaevola hispida, Scaevola oppositifolia and *Scaevola sericea* have also been tested for anti-tumor activity but no significant activity was observed.[29]

1.5.3 Antibacterial

Disk diffusion assay, also referred to as the Kirby-Bauer disk diffusion procedure, is a method commonly used to screen antibacterial activity by measuring the diameter of zone inhibition. By measuring the size of the zone, one can determine which drugs or extracts the microbe is sensitive to and which it is resistant to. The resistance and sensitivity of the organism to the drug is determined by comparing the zone sizes with the known values for each drug. This is because the rate of diffusion depends on the molecular weight of a drug. Larger molecular weight molecules diffuse slowly compared to lower molecular weight. This method is not used to determine whether a chemical compound tested is bactericidal (kills bacteria) or bacteriostatic (inhibits bacterial growth). Instead, these characteristics can be measured using a tube dilution assay. The tube dilution assay, unlike the disk diffusion assay, is quantitative in its measurement. By using this assay, the minimum inhibitory concentration (MIC) of a drug or extract can be determined.[40]

The microorganisms selected for the antibacterial tests usually range from Gram positive and negative bacteria to fungi as well as yeasts. The list of microorganisms commonly used is shown in **Table 1.7**.

Table 1.7: List of microorganisms commonly used

Classification	Microorganism
Gram positive	*Staphylococcus aureus* [8,26,41]
	Bacillus subtilis [8,41]
Gram negative	*Escherichia coli* [8,26,41]
	Pseudomonas aeruginosa [8,26,41]
	Klebsiella pneumoniae [8,26,41]
	Salmonella typhimurium [8,41]
	Proteus vulgaris [8,41]
Fungi	*Aspergillus fumigatum* [8]
	Aspergillus niger [8]
Yeast	*Candida albicans* [8,26]

The compounds isolated from *Scaevola spinescens* by Kerr *et al*,[5] as well as the aqueous extract of *Scaevola spinescens* obtained from CCWA,[7] were tested for their antibacterial activity using a disk diffusion assay.[8] However, the results for this bioactivity were inconclusive as some of the fractions have the ability to enhance the bacterial growth rather than inhibiting it.

Despite this, the antibacterial activity of *Scaevola spinescens* was also investigated by Nobbs in 2000 using a disk diffusion assay.[6] Based on the study, some of the crude fractions isolated from the methanol extract showed significant antibacterial activity.[6] Further isolation and purification of compounds were done on these crude fractions. However, these pure compounds were not further tested for antibacterial activity. There is the possibility that these compounds might contribute to the observed biological activity. **Table 1.8** shows the pure compounds isolated from these crude fractions.

Table 1.8: Pure compounds isolated from the crude fractions that may contribute to antibacterial activity[6]

NOTE:
This figure is included on page 23 of the print copy of the thesis held in the University of Adelaide Library.

1.6 Aims

Aim 1 : To isolate and identify chemical components in the hexane, ethyl acetate, methanol and aqueous extracts of *Scaevola spinescens*.

The objective of the first aim is to carry out chemical profiling of hexane, ethyl acetate and aqueous extracts as these extracts have not been thoroughly studied. As for the methanol extract, any new compounds discovered will be identified and added to the list of compounds found in this extract.

Aim 2: To identify which compounds have antibacterial activity.

The main objective of the second aim is to identify any possible antibacterial activity in the hexane, ethyl acetate, methanol and aqueous extracts. This will assist with the identification of chemical compounds that are responsible for antibacterial activity. Another objective of this aim is to verify the antibacterial activity in pure compounds isolated from the crude fractions that have significant antibacterial activity. This would extend the work of Nobbs.

CHAPTER 2

Isolation / Structure elucidation

2.1 General Introduction

In the isolation of chemical compounds from plant material, the general procedures are plant collection, preparation, extraction, fractionation / purification and lastly, structure elucidation.

Collection of voucher specimens is a legitimate and important part of scientific research. According to the Royal Botanic Garden Melbourne, voucher specimens provide a permanent record validating the occurrence of a plant species at a particular location and site of collection. Vouchers are also a verifiable and invaluable source of information to help in identification of plant species collected. For accurate identification, a good voucher should have well-collected specimens as well as labelling. The flower or fruits of a plant are usually critical for identification as they are a distinct feature of a plant species. Information about the habitat where the plant is collected is also crucial in the herbarium specimen documentation.

The plant material must first be preserved so that the active compounds will remain unchanged. The most common method for preserving plant material is drying. Drying also decreases the risk of external attack by moulds. In general, plant material should be dried at a temperature below 30°C to avoid decomposition of thermolabile compounds.[42] When air-dried, the plant material has to be spread out with good ventilation to facilitate drying.

Grinding improves efficiency of extraction by increasing the surface area of plant material.[42] This decreases the amount of solvent needed for extraction as it allows the plant material to pack more densely. Therefore, it is essential to grind samples into finer size for better extraction results.

Some of the commonly used extraction methods are maceration, Soxhlet extraction, liquid-liquid extraction and decoction. Maceration is a common method for extraction of small amount of plant material that can be carried out conveniently in Erlenmeyer flask.[42] This process is usually repeated with fresh solvent until the solvent is almost colourless. Soxhlet extraction is a convenient method for extraction of small to moderate volumes of plant material.[42] The amount of solvent needed for Soxhlet extraction is minimal because the extraction takes place in a system where the solvent is continually recycled. However, the heat needed to distill the solvent will likely cause thermolabile compounds to form artifacts or

decomposition products. Liquid-liquid extraction, also called solvent extraction, is a process that allows separation of two or more components due to the unequal solubility in the immiscible liquid phases. A decoction is made by boiling herb or plant material in water. This method may also cause thermolabile compounds to form artifacts or decomposition products due to the high temperature.

Fractionation / purification of compounds can be done using chromatographic techniques. The classical chromatographic techniques includes thin layer chromatography (TLC), preparative thin layer chromatography (PTLC), open column chromatography and flash column chromatography.[42] The modern chromatographic techniques are high performance thin layer chromatography (HPTLC), solid-phase extraction, radial chromatography, droplet countercurrent chromatography (DCCC) and high performance liquid chromatography (HPLC).[42]

The purity of the isolated compound can be determined using melting point. UV-visible spectroscopy, infrared spectroscopy (IR), mass spectrometry and nuclear magnetic resonance spectroscopy (NMR) are important techiques in structural elucidation and compound identification of the isolated compounds.

2.2 Plant collection

Scaevola spinescens is mostly found on sandy loams and hills in inland regions of Central and Western Australia as well as New South Wales. The plant had previously been collected from a site 10 km west of Morgan, on the Morgan-Eudunda Road.[6] Therefore, a day trip of plant collection at the Morgan-Eudanda road was organized on 9th April 2007. A picture of the collection site is shown in ***Figure 2.1***. About 1.6 kg of the aerial parts of the plant (leaves and branches) was collected. A picture of the aerial parts of the plant taken at the collection site is shown in ***Figure 2.2***. A voucher specimen was deposited at the State Herbarium of South Australia - Voucher Number AD99702040. A picture of the aerial parts of the plant sent for herbarium identification is shown in ***Figure 2.3***.

Figure 2.1: Picture of collection site (Photo: Michele Mejin, 2007)

Figure 2.2: Picture of the aerial parts of the plant taken at the collection site (Photo: Michele Mejin, 2007)

Figure 2.3: Picture of the aerial parts of the plant sent for herbarium identification (Photo: Michele Mejin, 2007)

2.3 Plant preparation

The plant sample was air dried before being processed into smaller pieces using a mortar and pestle. To provide fine material, a blender was then used. The total loss of moisture was about 160 g. The ground up samples were mixed then divided into two lots, one with about two-thirds of the total sample (Sample A) and the other with about one-third of the total sample (Sample B).

2.4 Extraction

The extraction of samples involved two methods - Soxhlet extraction and decoction. Soxhlet extraction is a common laboratory method. In comparison, decoction was also done as it would be useful to relate it to the traditional approach of the Aboriginal people.

Sample A was sequentially extracted using Soxhlet extraction based on increasing polarity of solvent, starting from hexane, then ethyl acetate, methanol and lastly water. The solvents for each extraction were removed using a rotary evaporator. **(*Figure 2.4*)**

Sample B was extracted using a decoction method. The sample was soaked in warm water for half an hour, heated to boiling, then simmered for about 45 minutes. The sample was then filtered using a Buchner funnel and the water from the filtrate was removed using a rotary evaporator. Sample B was re-extracted twice using the same procedure to increase the yield of extracted material. **(*Figure 2.4*)**

Figure 2.4: Flow chart of sample extraction

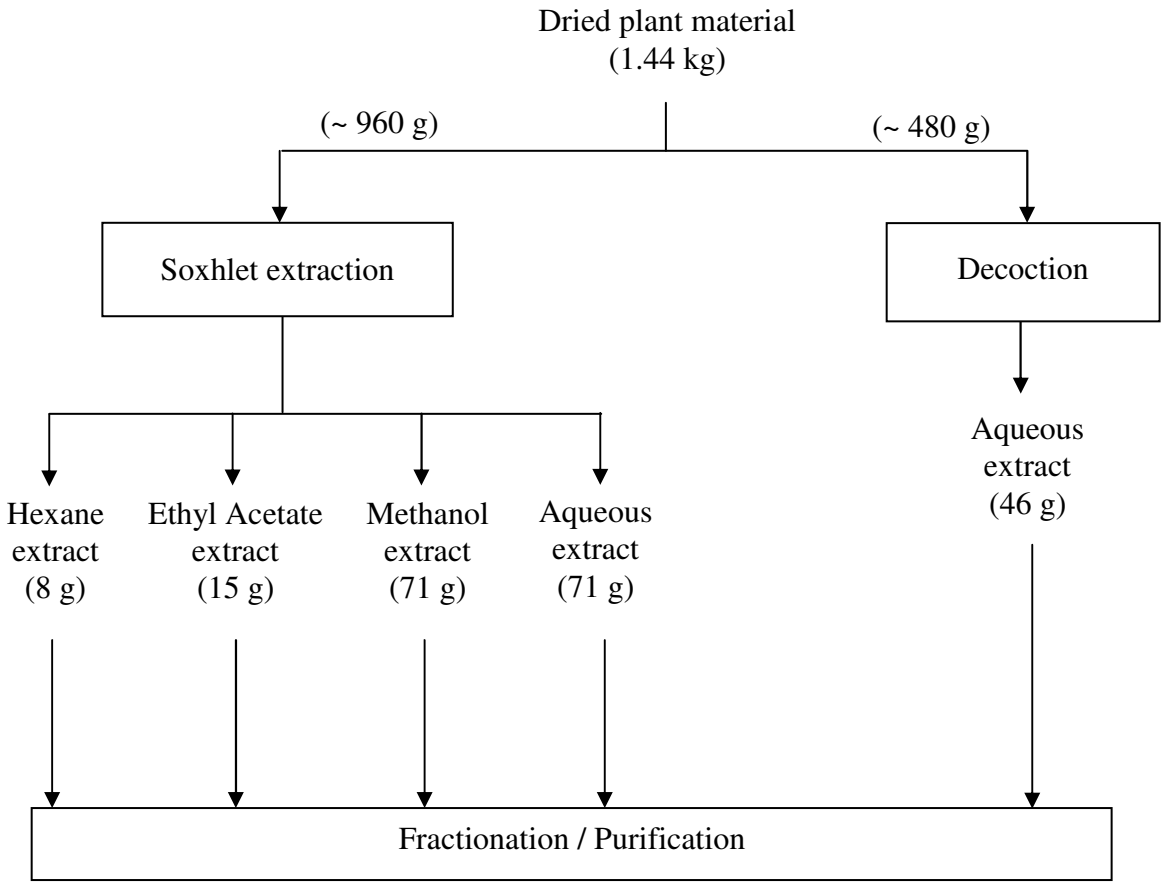

2.4.1 Hexane Extract

Fractionation and purification of compounds from the hexane extract

A total of 8 g of hexane extract was obtained from the Soxhlet extraction. The hexane extract was then subjected to fractionation and purification by flash column chromatography. The fractionation and purification of compounds from hexane extract are summarized in ***Figure 2.5***. Below are the details of the fractionation of compounds from the hexane extract.

- The hexane extract (8 g) was subjected to flash column chromatography (100 mm column diameter) using a series of increasing polarity solvents to yield 22 fractions, H01-H22 **(*Figure 2.5*)**.

- Fraction H10 (500 mg) was then subjected to further flash column chromatography (40 mm column diameter) using a series of increasing polarity solvents to yield 10 sub-fractions, H1001-H1010 **(*Figure 2.5*)**.

- Sub-fraction H1010 (150 mg) was subjected to further purification by flash column chromatography (20 mm column diameter) using 5% hexane / 95% dichloromethane as the eluting solvent to yield 5 sub-fractions, H101001-H101005 **(*Figure 2.5*)**.

- Fraction H11 (980 mg) was subjected to flash column chromatography (50 mm column diameter) using a series of increasing polarity solvents to yield 14 sub-fractions, H1101-H1114 **(*Figure 2.5*)**.

- Fraction H12 (900 mg) was subjected to flash column chromatography (50 mm column diameter) using a series of increasing polarity solvents to yield 14 sub-fractions, H1201-H1214 **(*Figure 2.5*)**.

- Fraction H14 (580 mg) was subjected to flash column chromatography (40 mm column diameter) using a series of increasing polarity solvents to yield 16 sub-fractions, H1401-H1416 **(*Figure 2.5*)**.

Figure 2.5: Fractionation from 8 g of hexane extract

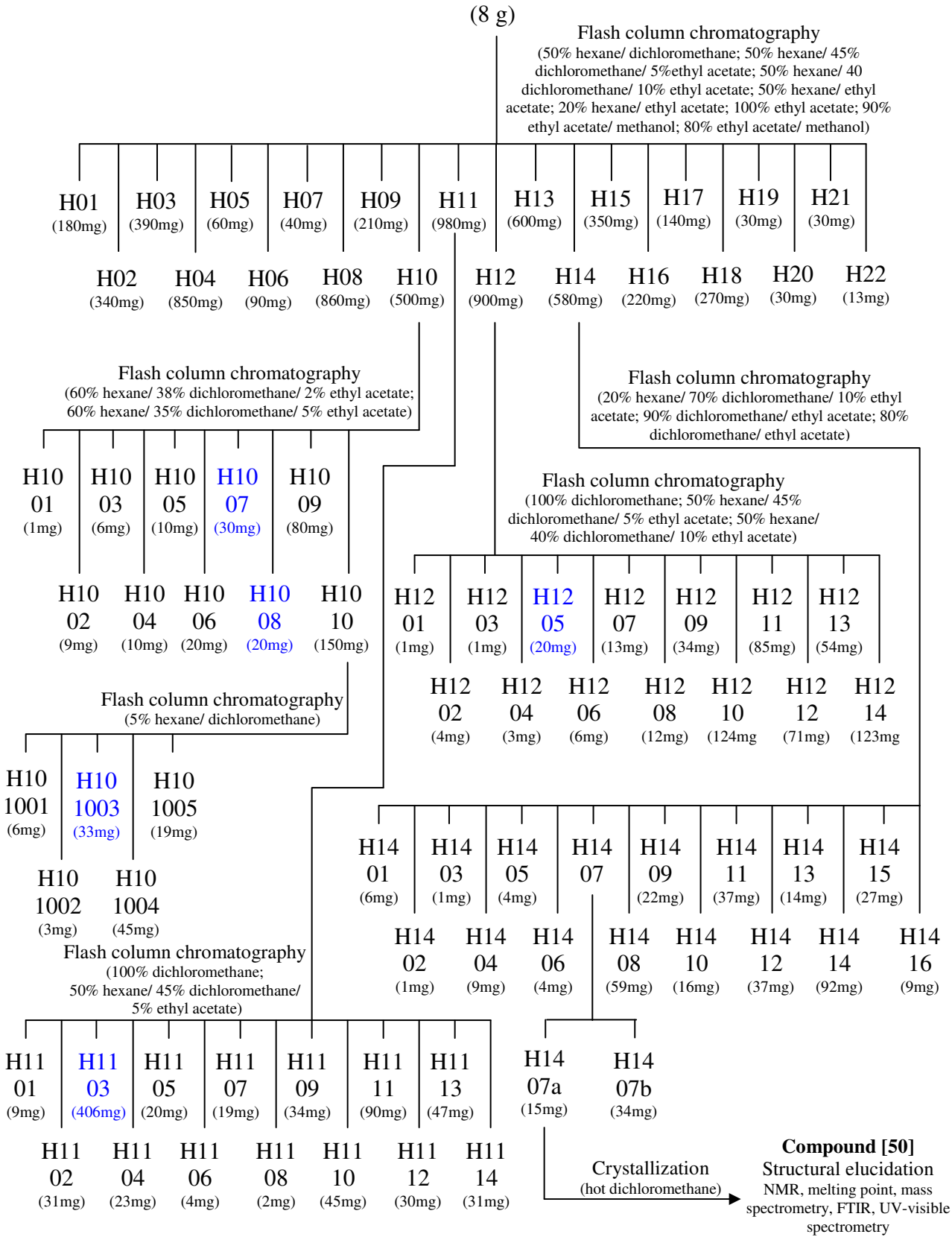

Sub-fractions with similar ^{1}H NMR profiles were combined and subjected to further purification by crystallization (***Figure 2.6***). Below are the details of the purication of compounds that have similar ^{1}H NMR profiles.

- Fractions H1007, H1008 and H1103 were found to have similar ^{1}H NMR profiles (***Figure 2.5 and 2.6***). These fractions were combined and crystallized from hot dichloromethane. The white solids (56 mg) that crystallized out of solution were then re-crystallized again from hot dichloromethane to give fine, white crystals (31 mg).

- Fractions H101003 and H1205 were also found to have similar ^{1}H NMR profiles (***Figure 2.5 and 2.6***). These fractions were combined and crystallized from hot dichloromethane to afford fine, white crystals (7 mg). The ^{1}H NMR profile of these crystals was found to be similar to the compound isolated from fraction H1007, H1008 and H1103 (***Figure 2.5 and 2.6***). These compounds were combined [49] and further characterized using 2D NMR, melting point, mass spectrometry, FTIR and UV-visible spectroscopy.

Figure 2.6: Purification of H1007, H1008, H1103, H101003 and H1205

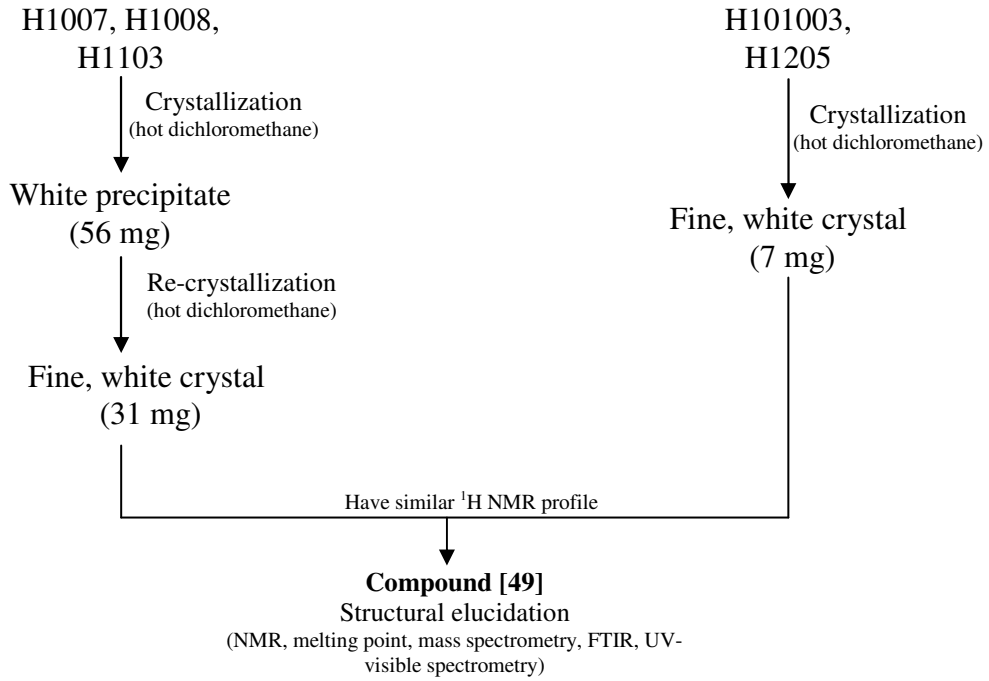

When a solution of sub-fraction H1407 was left standing, white solid (15 mg) crystallized out of solution (***Figure 2.5***). The white solid was re-crystallized from hot dichloromethane to give a white amorphous solid (11 mg) [50]. The ^{1}H NMR profile of compound [50] showed that it was different from the compound [49]. Therefore, compound [50] was further characterized using 2D NMR, melting point, mass spectrometry, FTIR and UV-visible spectroscopy.

Compounds found in hexane extract

Compound [49]

Compound [49] (38 mg) were isolated as fine, white crystals with a melting point of 282 - 283°C. Using high-resolution EI mass spectrometry (HREIMS), the molecular formula was determined to be $C_{30}H_{50}O$ from the molecular ion peak at *m/z* 426.3858 (Calculated 426.3861). This indicated that the compound had six degrees of unsaturation. The IR spectrum indicated the presence of hydroxyl group(s) as there was an absorption at 3480 cm^{-1}. There was also an absorption at 1641 cm^{-1} in the IR spectrum, which indicated the presence of double bond group (s).

Some difficulties were encountered in assigning the hydrogens and carbons of this structure. The COSY spectrum did not give much information as most of the hydrogens are overlapping in the chemical shift region of 1.2 – 1.6 ppm. So it was impossible to unambiguously assign the signals for each hydrogen by this method. Therefore, most of the NMR assignments were based on HMBC and ROESY correlations. Only unambiguously assigned signals were taken into consideration when determining this structure.

The ^{13}C and DEPT NMR spectra indicated a total of 30 unique carbons, eight methyls (δ_C 15.44, 15.41, 21.3, 25.9, 27.9, 29.8, 29.9, 33.3), ten sp^3 methylenes (δ_C 17.4, 18.7, 27.1, 33.0, 33.6, 35.1, 36.6, 37.74, 37.71, 41.3), four sp^3 methines (δ_C 48.7, 49.2, 55.5, 79.0), one sp^2 methine (δ_C 116.8), six quaternary sp^3 carbons (δ_C 28.7, 35.7, 37.5, 38.0, 38.7, 38.9) and one quaternary sp^2 carbon (δ_C 158.0). All these resonances accounted for a partial molecular formula $C_{30}H_{49}$. The remaining hydrogen atom and oxygen atom suggested the presence of a hydroxyl group, which is supported by the infrared spectra. The two sp^2 carbons (δ_C 116.8 and

158.0) indicate one double-bond functionality, which accounts for one degree of unsaturation. This suggested that the compound contained 5 rings.

All the methyl, methylene and methine carbons identified in the DEPT NMR were then assigned to their directly attached protons using the HSQC experiment.

The structural determination of compound [49] was mainly based on the HMBC correlations and COSY coupling (where available). The relative stereochemistry of the structure was then investigated using the ROESY correlations. These correlations are shown in ***Table 2.1 and 2.2***.

In the HMBC spectrum, the methyl hydrogens at δ_H 0.95 (δ_C 33.3 as shown in HSQC spectrum) showed correlations with the methyl carbon at δ_C 29.9, methylene carbons at δ_C 33.0 and δ_C 36.6 as well as the quaternary carbon at δ_C 28.7. The methyl carbon at δ_C 29.9 had a ^{1}H chemical shift at δ_H 0.91 which was indistinguishable with the ^{1}H chemical shift for the methyl carbon at δ_C 21.3. However, in the HMBC spectrum, the methyl hydrogens at δ_H 0.91 did show correlations with methylene carbons at δ_C 33.0 and δ_C 36.6 as well as the quaternary carbon at δ_C 28.7. This indicated that the two methyl groups are likely to be attached to the quaternary carbon at δ_C 28.7. **(*Figure 2.7*)**

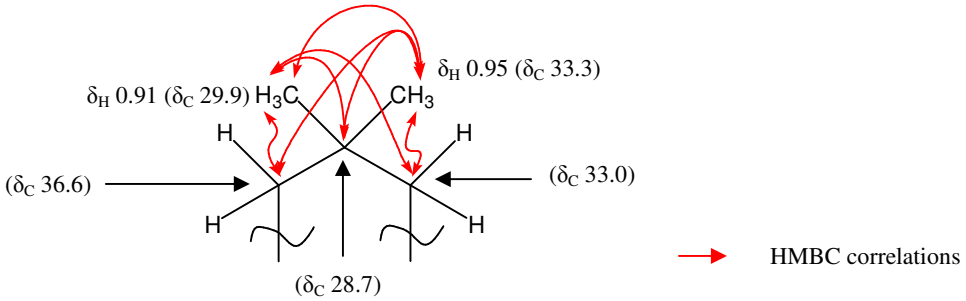

Figure 2.7: Fragment to build the 1st ring for [49] based on HMBC correlations

In the COSY spectrum, the methylene hydrogen at δ_H 1.24 showed correlations with the methylene hydrogen at δ_H 1.01. In the HSQC spectrum, the signal at δ_H 1.24 is attached to δ_C 33.0 and δ_H 1.01 to δ_C 35.1. HMBC correlations were observed between the signal at δ_H 1.24 (δ_C 33.0) with the methyl carbon at δ_C 33.3 and the quaternary carbon at δ_C 35.7. The methyl hydrogens at δ_H 0.82 (δ_C 29.8) had HMBC correlations with the methine carbon at δ_C 48.7, the methylene carbon at δ_C 35.1 and the quaternary carbon at δ_C 35.7. This indicated that the

methyl hydrogens at δ_H 0.82 (δ_C 29.8) are likely to be attached to the quaternary carbon at δ_C 35.7. The methylene hydrogen at δ_H 1.31 (δ_C 36.6) showed HMBC correlations with the methine carbon at δ_C 48.7 and the quaternary carbon at δ_C 35.7. The HMBC correlations, as well as the COSY correlations, supported the closure of a ring, thus accounting for one additional degree of unsaturation. Therefore, this accounted for the second degree of unsaturation (1st ring). ***(Figure 2.8)***

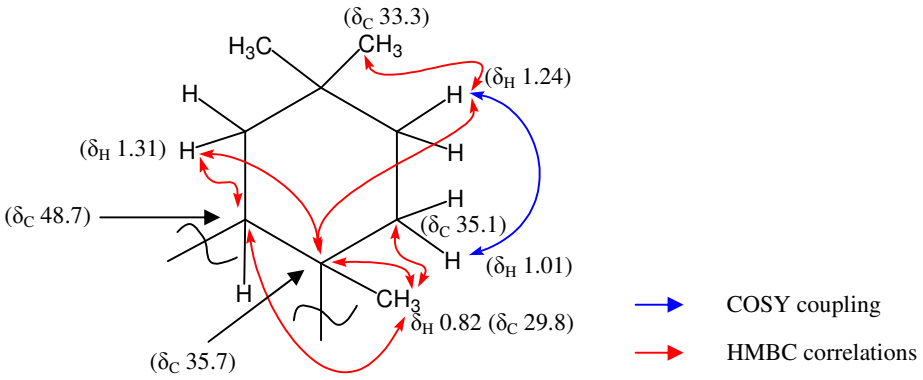

Figure 2.8: Closure of the 1st ring for [49] based on COSY and HMBC correlations

The chemical shift of the quaternary sp^2 carbon at δ_C 158.0 and sp^2 methine carbon at δ_C 116.8 indicated that they must be attached together as there were no other sp^2 carbons. In the HSQC spectrum, the sp^2 methine carbon at δ_C 116.8 is attached to the methine hydrogen at δ_H 5.53. The sp^2 methine hydrogen at δ_H 5.53 (δ_C 116.8) showed COSY coupling with the methylene hydrogen at δ_H 1.91. In the ^{1}H NMR spectrum, the methine hydrogen at δ_H 5.53 showed a multiplicity of double of doublet with a coupling constant (*J*) of 3.0 Hz and 7.4 Hz. The coupling constant (*J*) of 3.0 Hz matches the coupling constant for the methylene hydrogen at δ_H 1.91. The small coupling constant (*J*) indicated that the methine hydrogen at δ_H 5.53 had a bigger dihedral angle with the methylene hydrogen at δ_H 1.91 than the methylene hydrogen at δ_H 1.63. This suggested that the methylene hydrogen at δ_H 1.91 is a pseudoaxial. Therefore, the other methylene hydrogen at δ_H 1.63 had to be pseudoequatorial. This is supported by the coupling constant (*J*) of 7.4 Hz for the methine hydrogen at δ_H 5.53, which indicated a small dihedral angle between two coupling hydrogens. In the HSQC spectrum, the signal at δ_H 1.91 is attached to the carbon at δ_H 37.74. HMBC correlations were observed between the hydrogen at δ_H 5.53 with the quaternary carbons at δ_C 35.7, δ_C 37.5 and δ_C 38.9. The HMBC correlation with the quaternary carbon at δ_C 35.7 indicated that this fragment is linked to the 1st ring. This

is also supported by the HMBC correlations observed between the hydrogen at δ_H 1.91 with the methine carbon at δ_C 48.7 and the quaternary carbon at δ_C 35.7.

The methine carbon at δ_C 48.7 also showed a HMBC correlation with methyl hydrogens at δ_H 0.91 (δ_C 21.3). HMBC correlations were also observed between the methyl hydrogens at δ_H 0.91 (δ_C 21.3) with the methylene carbon at δ_C 33.6 and the quaternary carbon at δ_C 37.5. This indicated that the methyl hydrogens at δ_H 0.91 (δ_C 21.3) are likely to be attached to the quaternary carbon at δ_C 37.5. The HMBC correlations and COSY coupling supported the closure of a ring that fused to the 1st ring, thus accounting for one additional degree of unsaturation. Therefore, this accounted for the third degree of unsaturation (2nd ring). (***Figure 2.9***)

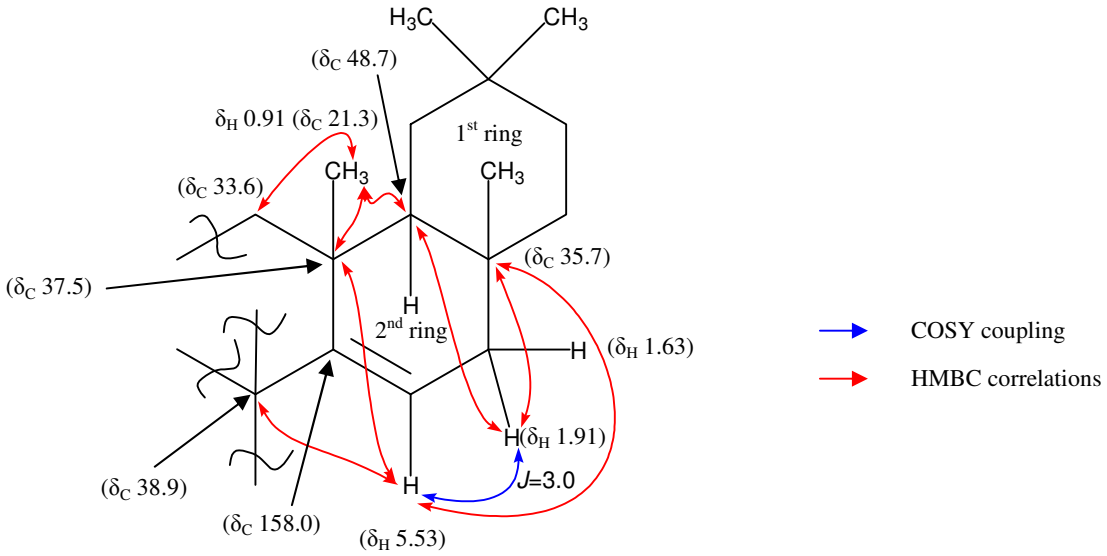

Figure 2.9: Closure of the 2nd ring for [49] based on COSY and HMBC correlations

The methyl hydrogens at δ_H 1.09 (δ_C 25.9) showed HMBC correlations with the methine carbon at δ_C 49.2, the methylene carbon at δ_C 41.3, and quaternary carbons at δ_C 38.9 and δ_C 158.0. The signal at δ_H 1.41 (δ_C 49.2) showed HMBC correlations with the methylene carbon at δ_C 17.4 and the quaternary carbon at δ_C 38.9. HMBC correlations were observed between the methylene hydrogen at δ_H 1.55 (δ_C 33.6) with the methyl carbon at δ_C 21.3, the methine carbon at δ_C 48.7, the methylene carbon at δ_C 17.4 and quaternary carbons at δ_C 37.5 and δ_C 158.0. The HMBC correlations observed supported the closure of the 3rd ring that fused to the 2nd ring, thus accounting for one additional degree of unsaturation. Therefore, this accounted for the fourth degree of unsaturation (3rd ring). (***Figure 2.10***)

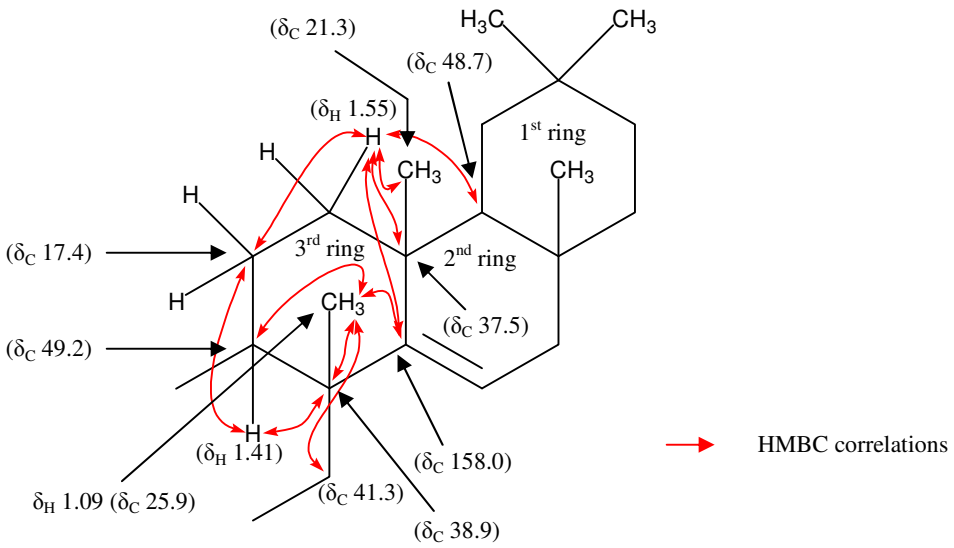

Figure 2.10: Closure of the 3rd ring for [49] based on HMBC correlations

The methyl hydrogens at δ_H 0.98, which are attached to δ_C 27.9 showed HMBC correlations with the methyl carbon at δ_C 15.44, methine carbons at δ_C 55.5 and δ_C 79.0 as well as the quaternary carbon at δ_C 38.7. HMBC correlations were observed between the methyl hydrogens at δ_H 0.80 (δ_C 15.44) with the methyl carbon at δ_H 27.9, methine carbons at δ_C 55.5 and δ_C 79.0 as well as the quaternary carbon at δ_C 38.7. The HMBC correlations observed for both methyl hydrogens indicated that they are likely to be attached to the quaternary carbon at δ_C 38.7.

The chemical shift of the methine carbon at δ_C 79.0 indicated that an oxygen group is likely to be attached to this methine carbon. Therefore, this accounted for one hydroxyl group.

In the HMBC spectrum, the methine hydrogen at δ_H 0.78 (δ_C 55.5) showed correlations with the methyl carbons at δ_C 27.9, δ_C 15.41 and δ_C 15.44, the methine carbon at δ_C 49.2, the methylene carbon at δ_C 18.7 as well as the quaternary carbon at δ_C 38.7. HMBC correlations were also observed between the methylene carbon at δ_C 18.7 with the hydrogens at δ_H 1.34 and δ_H 2.03. In the HSQC spectrum, both hydrogens are attached to a methylene carbon at δ_C 41.3. The methyl hydrgens at δ_H 0.92 (δ_C 15.41) showed HMBC correlations with the methine carbons at δ_H 49.2 and δ_H 55.5 as well as the quaternary carbon at δ_C 38.0. This indicated that

the methyl hydrogens at δ_H 0.92 are likely to be attached to the quaternary carbon at δ_C 38.0. The HMBC correlations observed supported the closure of the 4th ring that is fused to the 3rd ring, thus accounting for one additional degree of unsaturation. Therefore, this accounted for the fifth degree of unsaturation (4th ring). **(*Figure 2.11*)**

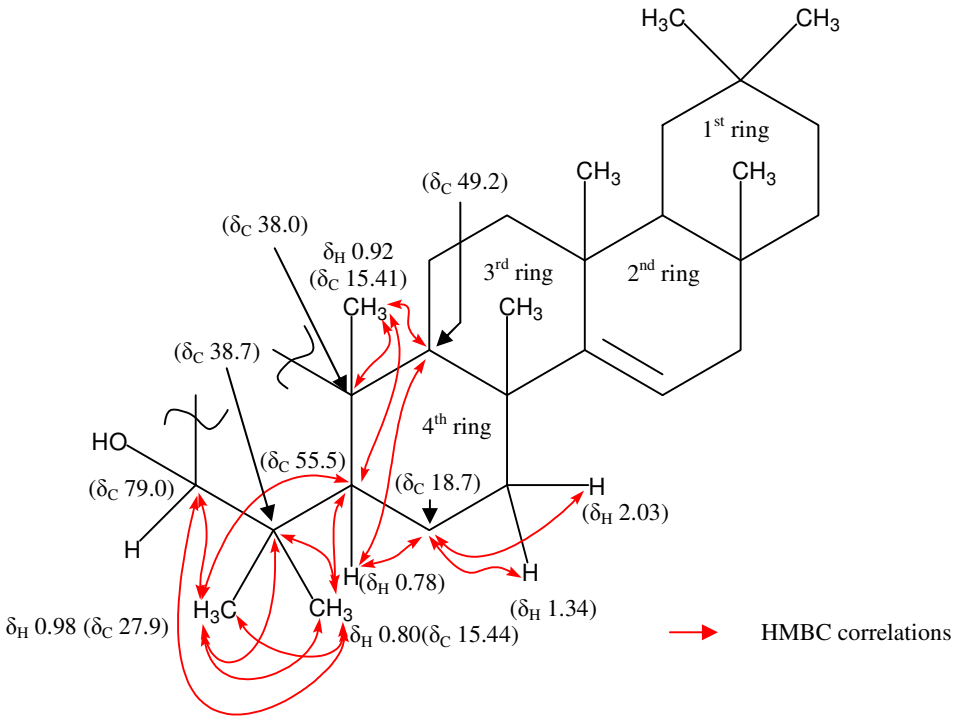

Figure 2.11: Closure of the 4th ring for [49] based on HMBC correlations

The methine hydrogen at δ_H 3.19 (δ_C 79.0) showed COSY correlations with the methylene hydrogen at δ_H 1.57. HMBC correlations were observed between the hydrogen at δ_H 1.57 with the quaternary carbon at δ_C 38.0. The methyl hydrogen at δ_H 0.92 (δ_C 15.41) also showed HMBC correlations with the methylene carbon at δ_C 37.71. In the HSQC spectrum, δ_H 1.59 and δ_H 0.93 are attached to the methylene carbon at δ_C 37.71. HMBC correlations were observed between the methylene hydrogen at δ_H 1.59 with methine carbons at δ_C 79.0 and δ_C 49.2. The methylene hydrogen at δ_H 0.93 showed HMBC correlations with the methine carbon at δ_C 55.5. The HMBC correlations supported the closure of a ring, which accounted for the sixth degree of unsaturation (5th ring). **(*Figure 2.12*)**

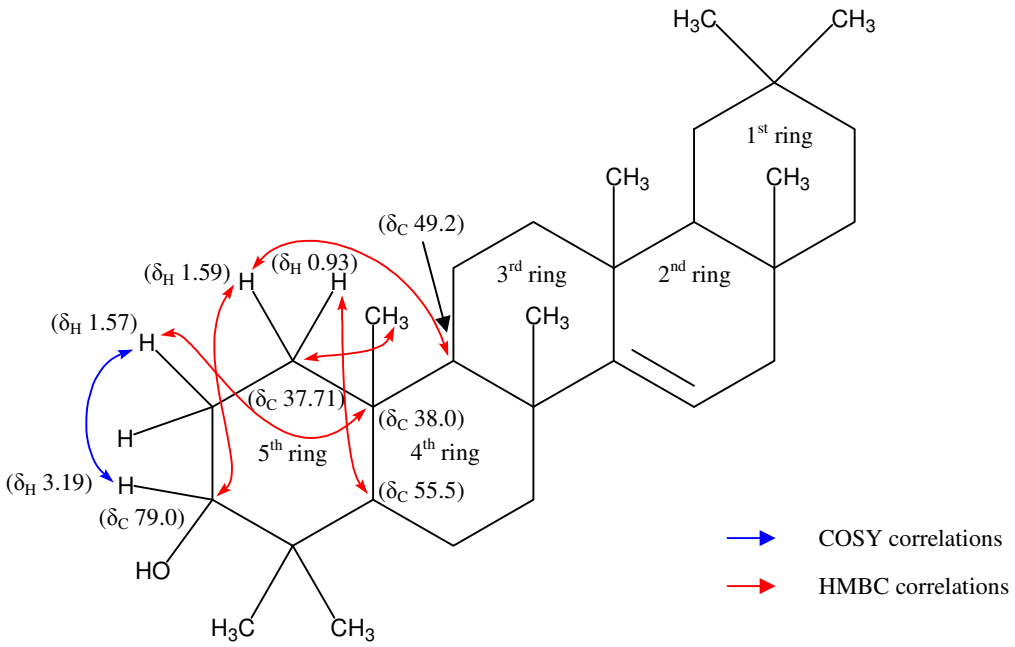

Figure 2.12: Closure of the 5th ring for [49] based on COSY and HMBC correlations

Table 2.1: Spectral data for [49]

C	δC	H	δ_H	I	M	*J*(Hz)	COSY	HMBC
C_{1*}	37.71	$H_{1\alpha}$ $H_{1\beta}$	1.59 0.93	1 1	m m			C_3, C_9 C_5
C_2	27.1	$H_{2\alpha}$ $H_{2\beta}$	1.60 1.57	1 1	m m		 $H_{3\alpha}$	 C_{10}
C_3	79.0	H_3	3.19	1	m		$H_{24\beta}$	C_{23}, $C_{29/30}$
C_4	38.7							H_5, Me_{23}, Me_{24}
C_5	55.5	H_5	0.78	1	dd	2.4, 12.0	$H_{28\beta}$	C_9, C_4, C_{23}, $C_{24/25}$
C_6	18.7	$H_{6\alpha}$ $H_{6\beta}$	1.61 1.47	1 1	m m			C_5, C_7
C_7	41.3	$H_{7\alpha}$ $H_{7\beta}$	2.03 1.34	1 1	dd m	6.6, 12.0		C_6 C_5, C_8, C_{26}, C_6
C_8	38.9							$H_{15\alpha}$, Me_{26}, Me_{23}
C_9	49.2	H_9	1.41	1	m			C_8, C_{11}, C_{25}
C_{10}	38.0							Me_{25}
C_{11}	17.4	$H_{11\alpha}$ $H_{11\beta}$	1.63 1.47	1 1	m m			C_9, C_{12}
C_{12}	33.6	$H_{12\alpha}$ $H_{12\beta}$	1.61 1.55	1 1	m m			 C_{14}, C_{18}, C_{13}, C_{27}, C_{11}
C_{13}	37.5							$H_{15\alpha}$, Me_{27}
C_{14}	158.0							$H_{7\beta}$, $H_{16\alpha}$, $H_{12\beta}$, Me_{26}, Me_{27}
C_{15}	116.8	H_2	5.53	1	dd	3.0, 7.4	$H_{11\alpha}$,	C_8, C_{13}, C_{17}
C_{16*}	37.74	$H_{16\alpha}$	1.91	1	dd	3.0, 15.0	$H_{11\alpha}$	C_{14}, C_{15}, C_{18}, C_{17}, C_{28}

C	δC	H	δ_H	I	M	*J*(Hz)	COSY	HMBC
		$H_{16\beta}$	1.63	1	m			
C_{17}	35.7							$H_{15\alpha}$, $H_{18\alpha}$, $H_{16\alpha}$, $H_{16\beta}$, $H_{19\alpha}$, $H_{19\beta}$, Me_{28}
C_{18}	48.7	H_{18}	0.96	1	m			C_{17}, C_{27}
C_{19}	36.6	$H_{19\alpha}$ $H_{19\beta}$	1.31 0.97	1 1	m m			C_{18}, C_{17}, C_{29}, C_{30}, C_{20} C_{17}, C_{20}
C_{20}	28.7							$H_{19\alpha}$, $H_{19\beta}$, Me_{29}, Me_{30}
C_{21}	33.0	$H_{21\alpha}$ $H_{21\beta}$	1.33 1.24	1 1	m m		 $H_{16\beta}$	 C_{17}, C_{29}
C_{22}	35.1	$H_{22\alpha}$ $H_{22\beta}$	1.36 1.01	1 1	m m		 $H_{19\beta}$	 C_{21}
C_{23}	27.9	Me_{23}	0.98	3	s			C_3, C_5, C_4, C_{24}
C_{24*}	15.44	Me_{24}	0.80	3	s			C_3, C_5, C_4, C_{23}
C_{25*}	15.41	Me_{25}	0.92	3	s			C_5, C_9, C_{10}
C_{26}	25.9	Me_{26}	1.09	3	d			C_{14}, C_9, C_7, C_8
C_{27}	21.3	Me_{27}	0.91	3	s			C_{18}, C_{13}, C_{19}, C_{12}, C_{21}, C_{20}
C_{28}	29.8	Me_{28}	0.82	3	s			C_{18}, C_{17}, C_{22}
C_{29}	33.3	Me_{29}	0.95	3	s		$H_{17\alpha}$	C_{19}, C_{21}, C_{30}, C_{20}
C_{30}	29.9	Me_{30}	0.91	3	s			C_{18}, C_{13}, C_{19}, C_{12}, C_{21}, C_{20}

* Interchangeable [49] 600MHz (^{1}H and ^{13}C): δ (ppm) from internal TMS in $CDCl_3$

I = Integration
M = Multiplicity

The ROESY experiment unambiguously assigned the methyl hydrogens at δ_H 0.80 (δ_C 15.44), δ_H 0.82 (δ_C 29.8), δ_H 0.92 (δ_C 15.41), δ_H 1.09 (δ_C 25.9) to be on the same side of the molecule as there were strong ROESY correlations between these methyl hydrogens. ROESY correlations are possible for the two methyl hydrogens at δ_H 1.09 (δ_C 25.9) and δ_H 0.82 (δ_C 29.8) if the rings they are attached to are twisted and in a boat shape. (***Figure 2.13***)

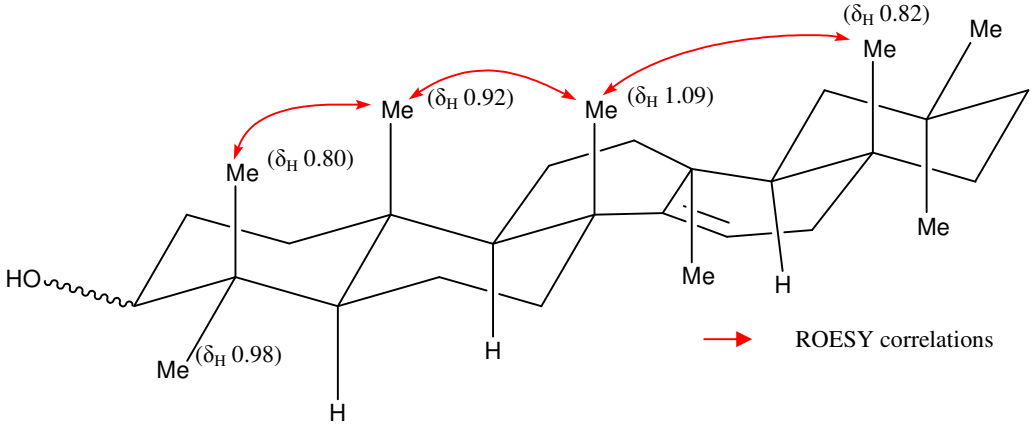

Figure 2.13: Stereochemical assignments of the methyl hydrogens for [49] based on ROESY correlations

The geminal methyl groups at δ_H 0.98 (δ_C 27.9) showed ROESY correlations with the methyl hydrogens at δ_H 0.80 (δ_C 15.44) as well as methine hydrogens at δ_H 0.78 (δ_C 55.5) and δ_H 3.19 (δ_C 79.0). Therefore, the hydrogens at δ_H 0.78, δ_H 0.98 and δ_H 3.19 were assigned to be on the same side of the molecule. This indicated that the hydroxyl group attached to methine carbon at δ_C 79.0 would be on the same side of the molecule with the methyl hydrogens at δ_H 0.80. **(*Figure 2.14*)**

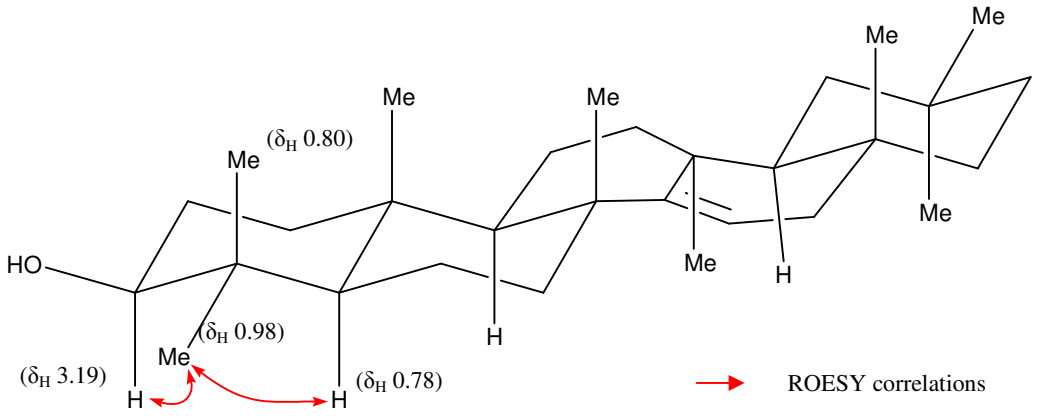

Figure 2.14: Stereochemical assignments of hydrogens at δ_H 3.19 and δ_H 0.78 for [49] based on ROESY correlations.

ROESY correlations were observed between both methine hydrogens at δ_H 0.78 (δ_C 55.5) and δ_H 01.41 (δ_C 49.2), followed by the methine hydrogen at δ_H 01.41 (δ_C 49.2) with the methyl hydrogens at δ_H 0.91 (δ_C 21.3). ROESY correlations between the methine hydrogen at δ_H 1.41 (δ_C 49.2) with the methyl hydrogens at δ_H 0.91 (δ_C 21.3) were possible because of the shape of the ring, which brings these hydrogens close into space. The methyl hydrogens at δ_H 0.91 (δ_C 21.3) had ROESY correlations with the methine hydrogen at δ_H 0.96 (δ_C 48.7). The ROESY correlations observed between these hydrogens showed that they were on the same side of the molecule as the methine hydrogen at δ_H 0.78. **(*Figure 2.15*)**

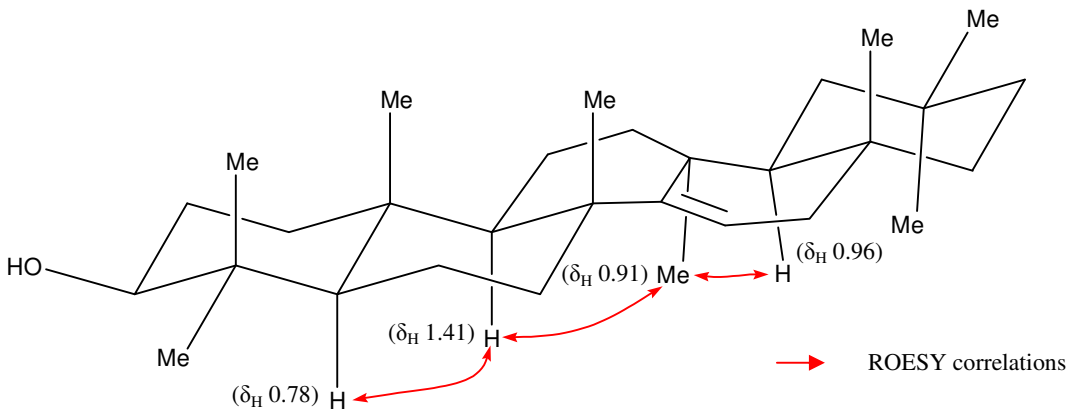

Figure 2.15: Stereochemical assignments of hydrogens at δ_H 0.91, δ_H 0.96 and δ_H 1.41 for [49] based on ROESY correlations

The last two methyl hydrogens at δ_H 0.95 (δ_C 33.3) and δ_H 0.91 (δ_C 29.9) were assigned based on the ROESY correlations with the adjacent methylene hydrogens. Neither one of these methyl hydrogens showed ROESY correlations with the methyl hydrogens at δ_H 0.82 (δ_C 29.8). This is likely due to the shape of the ring that positioned these two methyl groups in a distance. The methylene hydrogen at δ_H 1.33 (δ_C 33.0) showed ROESY correlations with the methyl hydrogens at δ_H 0.82 (δ_C 29.8) and δ_H 0.91(δ_C 29.9). This indicated that the methyl hydrogens at δ_H 0.91 (δ_C 29.9) is on the same side of the molecule with methyl hydrogens at δ_H 0.82 (δ_C 29.8). ROESY correlations were also observed between the methyl hydrogens at δ_H 0.95 (δ_C 33.3) with the methylene hydrogen at δ_H 1.24 (δ_C 33.0). This further supported the stereochemical assignments for both methyl hydrogens at δ_H 0.95 (δ_C 33.3) and δ_H 0.91 (δ_C 29.9). (***Figure 2.16***)

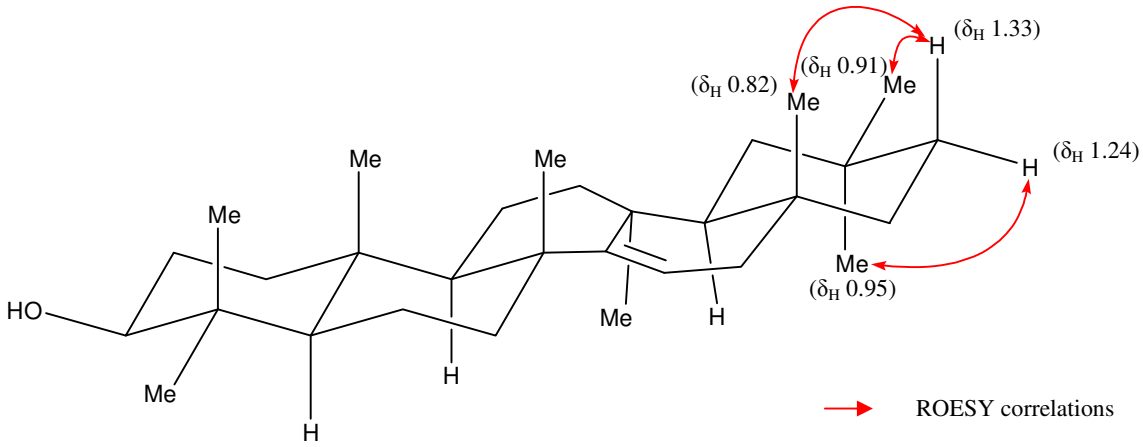

Figure 2.16: Stereochemical assignments of methyl hydrogens at δ_H 0.95 and δ_H 0.91 for [49] based on ROESY correlations

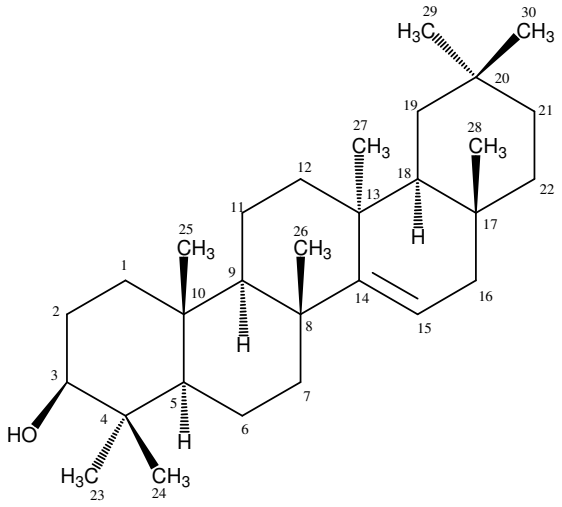

[49]

Table 2.2: ROESY correlations for [49]

Proton	ROESY	Proton	ROESY	Proton	ROESY
$H_{1\alpha}$		$H_{11\alpha}$	Me_{27}	$H_{21\beta}$	$H_{22\alpha}$, Me_{29}
$H_{1\beta}$	H_9	$H_{11\beta}$	Me_{26}, Me_{25}	$H_{22\alpha}$	$H_{16\alpha,}$ $H_{22\beta}$
$H_{2\alpha}$		$H_{12\alpha}$		$H_{22\beta}$	$H_{22\alpha}$, $H_{21\alpha}$, $H_{21\beta}$, Me_{28}
$H_{2\beta}$		$H_{12\beta}$	Me_{26}	Me_{23}	H_3, $H_{5\alpha}$, Me_{24}
H_3	H_5, Me_{23}	H_{15}	$H_{7\alpha}$, $H_{7\beta}$, $H_{16\alpha}$, $H_{16\beta}$	Me_{24}	Me_{23}, Me_{25}
H_5	H_9, $H_{7\beta}$, $H_{6\beta}$,Me_{23}	$H_{16\alpha}$	H_{15}, $H_{22\alpha}$, Me_{27}	Me_{25}	Me_{26}, Me_{24}
$H_{6\alpha}$	H_7, Me_{25}	$H_{16\beta}$		Me_{26}	H_7, $H_{12\beta}$, $H_{6\alpha}$, $H_{11\beta}$, $Me_{28,}Me_{25}$
$H_{6\beta}$	H_7	H_{18}	Me_{27}	Me_{27}	H_9, H_{18}, $H_{16\alpha}$, $H_{11\alpha}$
$H_{7\alpha}$	H_{15}, $H_{7\beta}$, $H_{6\alpha}$, $H_{6\beta,}$ Me_{26}	$H_{19\alpha}$	Me_{30}, Me_{28}	Me_{28}	$H_{19\alpha}$, $H_{21\alpha,}$ Me_{26}
$H_{7\beta}$		$H_{19\beta}$		Me_{29}	$H_{21\beta}$
H_9	H_5, $H_{11\alpha}$,Me_{27}	$H_{21\alpha}$	$H_{22\beta}$, $Me_{30,}$ Me_{28}	Me_{30}	$H_{19\alpha}$, $H_{21\alpha}$

[49] 600MHz (^{1}H): δ (ppm) from internal TMS in $CDCl_3$

The NMR assignments suggested that [49] is 18-*epi*-taraxerol. As discussed, the methine hydrogen at δ_H 0.96 is positioned below the ring. In comparison, the stereochemistry of the equivalent methine hydrogen in taraxerol [26] is inverted (***Figure 2.17***). An isomer of taraxerol, 13-*epi*,18-*epi*-taraxerol [29], has previously been isolated from *Scaevola spinescens.*[6] (See ***Figure 2.17*** for comparison between 18-*epi*-taraxerol [49], taraxerol [26] and 13-*epi*,18-*epi*-taraxerol [29]) A comparison of the ^{13}C chemical shifts between [49], taraxerol [26] and 13-*epi*,18-*epi*-taraxerol [29] are shown in ***Table 2.3***. The ^{13}C chemical shifts for [49] are broadly consistent with the literature reports for [26][6,43] and [29][6] except for the ones highlighted in red.

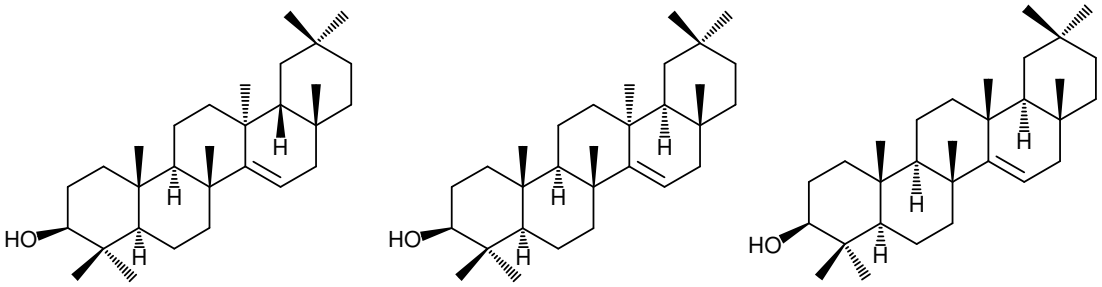

[26] [49] [29]

Figure 2.17: Comparison of stereochemistry between [49], [26] and [29]

Table 2.3: Comparison of the ^{13}C chemical shifts between [49], [26] and [29]

C	δ_C [49]	δ_C [26][6]	δ_C [26][43]	δ_C [29][6]
Solvent	$CDCl_3$	$CDCl_3$	$CDCl_3$	$CDCl_3$
C_1	37.71*	38.2	38.1	37.7
C_2	27.1	27.3	27.3	27.1
C_3	79.0	78.9	79.2	79.0
C_4	38.7	39.8	39.1	38.7
C_5	55.5	55.2	55.7	55.5
C_6	18.7	19.1	19.0	18.8
C_7	41.3	35.3	35.3	41.3
C_8	38.9	38.7	38.9	38.9
C_9	49.2	48.2	48.9	49.2
C_{10}	38.0	37.9	37.9	38.0
C_{11}	17.4	17.8	17.7	17.5
C_{12}	33.6	35.1	35.9	33.7
C_{13}	37.5	37.0	37.9	37.5
C_{14}	158.0	159.1	158.1	158.0
C_{15}	116.8	117.3	117.0	116.8
C_{16}	37.74*	36.4	36.9	37.7
C_{17}	35.7	38.6	38.1	35.7
C_{18}	48.7	50.3	49.4	48.7
C_{19}	36.6	41.7	41.4	36.6
C_{20}	28.7	29.5	29.0	28.8
C_{21}	33.0	33.9	33.9	33.3
C_{22}	35.1	32.8	33.2	35.1
C_{23}	27.9	27.2	28.1	28.0
C_{24}	15.44*	15.2	15.6	15.4
C_{25}	15.41*	15.2	15.6	15.4
C_{26}	25.9	29.5	30.1	25.9
C_{27}	21.3	25.0	26.0	29.9
C_{28}	24.8	29.7	30.1	29.7
C_{29}	33.3	33.4	33.5	33.1
C_{30}	29.9	21.7	21.5	21.3

* Assignments may be reversed

As indicated in ***Table 2.3***, the assignments for carbons 1 and 16 may be reversed as they have the same ^{13}C chemical shifts. The assignments for carbon 24 and 25 may also be reversed. Carbon 7, 17, 19, 22, 26, and 28 clearly shows that they are in the right position as discussed earlier based on the HMBC correlations and COSY correlations (where available). Carbon 27 and 30 which have the same ^{1}H chemical shifts were able to be assigned in this structure based on the HMBC correlations observed in carbon 30. There were HMBC correlations between carbon 30 with the methylene hydrogen (δ_H 1.31) at carbon 19 as well as the methyl hydrogens δ_H 0.95 at carbon 29.

As shown in ***Table 2.3***, there are more differences in the ^{13}C chemical shifts between [26] and [49] compared to the isomer [29] that has been previously isolated from *Scaevola spinescens*. The differences of the ^{13}C chemical shifts between [26] and [49] might be due to the change of stereochemistry in [49] at position 18. As for the isomer [29], the differences of the ^{13}C chemical shifts between [29] and [49] are only at carbon 27, 28 and 30. This might be due to the different stereochemistry in [29] at position 13, which possibly affect the ^{13}C chemical shifts of [49] at the region close to position 13.

From the literature reports, the melting point of taraxerol [26] has been reported to be 280 – 284°C[6] and 278 - 279°C[43]. As for 13-*epi*,18-*epi*-taraxerol [29], the melting point has been reported to be 191 - 193°C.[6] The melting point for [49] is in the region of taraxerol [26], which is 282 -283°C.

Literature research indicates that [49] had not previously been isolated from *Scaevola spinescens* or any other *Scaevola* species.

Compound [50]

Compound [50] (11 mg) was isolated as a white amorphous solid with a melting point of 265 – 270 °C. The low-resolution EI mass spectrum showed an ion peak at *m/z* 411. Using the high-resolution EI mass spectrum (HREIMS), the molecular formula was determined to be $C_{29}H_{47}O$ from the ion *m/z* 411.3633 (calculated 411.3626).

However, the ^{13}C and DEPT NMR spectra indicated a total of 30 unique carbons; seven methyls (δ_C 15.2, 15.3, 21.3, 25.8, 27.8, 29.6, 33.3), eleven sp^3 methylenes ((δ_C 17.1, 18.5, 26.9, 27.6, 30.4, 32.4, 33.2, 35.6, 37.5, 41.1, 64.8), four sp^3 methines (δ_C 44.6, 48.9, 55.3, 78.5), one sp^2 methine (δ_C 115.6), six quaternary sp^3 carbons (δ_C 28.3, 37.2, 37.7, 38.5, 38.8, 40.2) and one quaternary sp^2 carbon (δ_C 158.6). All these resonances accounted for a partial molecular formula $C_{30}H_{48}$.

Therefore, it was concluded that the molecular ion of this compound is not at *m/z* 411. There is an ion peak at *m/z* 442 at a low intensity. This indicated a potential loss of mass of *m/z* 31. The partial molecular formula $C_{30}H_{48}$ obtained from the ^{13}C and DEPT NMR spectra indicated that there is an additional CH which accounts for a mass of *m/z* 13. The remaining *m/z* 18 to obtain a molecular weight of *m/z* 442 accounted for two hydrogen atoms and an oxygen atom. The ion peak at *m/z* 411 that gives the molecular formula of $C_{29}H_{47}O$ corresponds to the lost of CH_2OH from the ion peak at *m/z* 442. Therefore, the molecular formula for compound [51] was determined to be $C_{30}H_{50}O_2$. This indicated that the compound had six degree of unsaturation. The IR spectum indicated the presence of hydroxyl group(s) as there was an absorption at 3340 cm^{-1}.

From the partial molecular formula $C_{30}H_{48}$, the remaining two hydrogen atoms and two oxygen atoms suggested the presence of two hydroxyl groups. This is supported by the infrared spectra. The two sp^2 carbons (δ_C 115.6 and 158.6) indicate one double-bond functionality, which accounts for one degree of unsaturation. This suggested that the compound contained 5 rings.

All the methyl, methylene and methine carbons identified in the DEPT NMR were assigned to their directly attached protons based on correlations from the HSQC experiment.

The structure of compound [50] was determined mainly based on the HMBC and ROESY correlations as well as and COSY coupling (where available). The COSY spectrum did not give much information as most of the hydrogens are overlapping in the chemical shift region of 1.2 – 1.6 ppm. Therefore, it was impossible to unambiguously assign all the signals for each hydrogen coupling by this method. Only unambiguously assigned signals were taken into consideration when determining this structure.

The assignments for the methylene carbons at δ_C 17.1 and δ_C 18.5 were based on HMBC correlations with the adjacent protons. In the HSQC experiment, the hydrogens attached to the methylene carbon at δ_C 17.1 and δ_C 18.5 were not observed. The relative stereochemistry of the structure was then investigated using the ROESY correlations. These correlations are shown in ***Table 2.4*** and ***2.5***.

In the HMBC spectrum, the methyl hydrogens at δ_H 0.964 showed correlations with the methyl carbon at δ_C 29.6, the methylene carbons at δ_C 32.4 and δ_C 35.6 as well as the quaternary carbon at δ_C 28.3. The methyl carbon at δ_C 33.3 had ^{1}H chemical shift at δ_H 0.964 which was indistinguishable with the ^{1}H chemical shift for the methyl carbon at δ_C 21.3 (δ_H 0.961 as shown in HSQC spectrum). However, this problem was resolved based on the HMBC correlations observed between the methylene hydrogens at δ_H 1.24 and δ_H 1.26 (δ_C 32.4) with the methyl carbon at δ_C 33.3 (δ_H 0.964). The HMBC correlations indicated that the two methyl carbons at δ_C 29.6 and δ_C 33.3 are likely to be attached to the quaternary carbon at δ_C 28.3. **(*Figure 2.18*)**

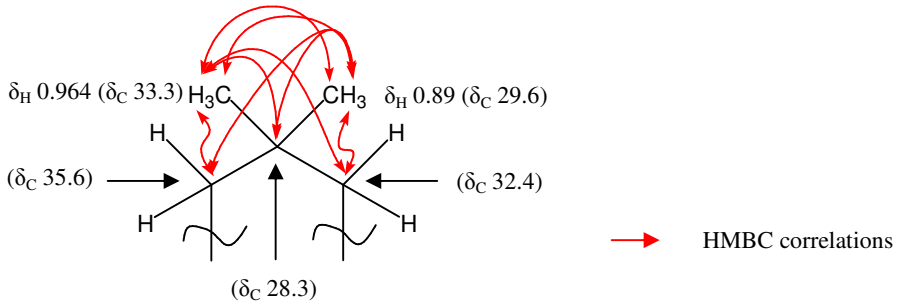

Figure 2.18: Fragment to build the 1st ring for [50] based on HMBC correlations

In the COSY spectrum, the methylene hydrogen at δ_H 1.00 (δ_C 35.6) showed correlations with the methine hydrogen at δ_H 0.57 (δ_C 44.6). In the ^{1}H NMR spectrum, the methine hydrogen δ_H 0.57 (δ_C 44.6) showed a multiplicity of doublet of doublet with coupling constant (*J*) of 3.6 Hz and 13.8 Hz. The ^{1}H NMR spectrum showed that both hydrogens at δ_H 0.57 and δ_H 1.00 had a coupling constant (*J*) of 3.6 Hz. The small coupling constants (*J*) indicated that the hydrogen at δ_H 0.57 had a bigger dihedral angle with the hydrogen at δ_H 1.00 than the hydrogen at δ_H 1.41. This suggested that the methylene hydrogen at δ_H 1.00 would be in equatorial position as the methine hydrogen at δ_H 0.57 had to be in axial position. Therefore, the other methylene hydrogen at δ_H 1.41 had to be in axial position. This is supported by the coupling constant (*J*) of 13.8 Hz for the hydrogen at δ_H 0.57. The multiplicity of hydrogen at δ_H 0.57 indicated that this hydrogen is likely to be split by the methylene hydrogens at δ_H 1.00 and δ_H 1.41. Therefore, the other neighbours of the hydrogen at δ_H 0.57 would be quaternary carbons.

In the COSY spectrum, the methylene hydrogens at δ_H 1.24 and δ_H 1.26 (δ_C 32.4) showed correlations with the methylene hydrogens at δ_H 1.47 and δ_H 1.50 (δ_C 27.6). HMBC correlations were also observed between the hydrogens at δ_H 1.47 and δ_H 1.50 (δ_C 27.6) with the methyl carbon at δ_C 33.3, the methylene carbon at δ_C 32.4 and the quaternary carbon at δ_C 37.2.

The methylene hydrogens at δ_H 1.24 and δ_H 1.26 (δ_C 32.4) showed HMBC correlations with methyl carbons at δ_C 29.6 and δ_C 33.3 as well as quaternary carbon at δ_C 40.2. HMBC correlations were also observed between the methylene hydrogens at δ_H 1.00 and δ_H 1.41 (δ_C 35.6) with methyl carbons at δ_C 29.6 and δ_C 33.3, the methine carbon at δ_C 44.6 as well as the quaternary carbons at δ_C 28.3 and δ_C 40.2. The HMBC and COSY correlations (where applicable) supported the closure of a ring, thus accounting for one additional degree of unsaturation. Therefore, this accounted for the second degree of unsaturation (1st ring). **(*Figure 2.19*)**

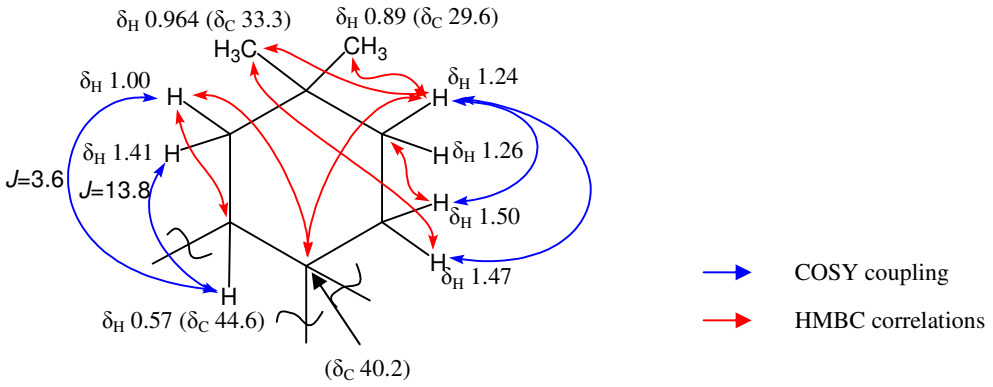

Figure 2.19: Closure of the 1st ring for [50] based on COSY and HMBC correlations

The chemical shift of the quaternary sp^2 carbon at δ_C 158.6 and sp^2 methine carbon at δ_C 115.6 indicated that they must be attached together as there were no other sp^2 carbons. In the HSQC spectrum, the sp^2 methine carbon at δ_C 115.6 is attached to the hydrogen at δ_H 5.51. The sp^2 methine hydrogen at δ_H 5.51 (δ_C 115.6) showed COSY coupling with the methylene hydrogens at δ_H 1.70 and δ_H 2.14. In the ^{1}H NMR spectrum, the hydrogen at δ_H 5.51 showed a multiplicity of double of doublet with coupling constant (*J*) of 3.0 Hz and 8.4 Hz. The coupling constant (*J*) of 3.0 Hz matches the coupling constant for the hydrogen at δ_H 1.70. The small coupling constant (*J*) indicated that the hydrogen at δ_H 5.51 had a bigger dihedral angle with the hydrogen at δ_H 1.70 than the hydrogen at δ_H 2.14. This suggested that the hydrogen at δ_H 1.70 is a pseudoaxial. Therefore, the other methylene hydrogen at δ_H 2.14 had to be pseudoequatorial. This is supported by the coupling constant (*J*) of 8.4 Hz. In the HSQC spectrum, the methylene hydrogens at δ_H 1.70 and δ_H 2.14 are attached to the carbon at δ_C 30.4. HMBC correlations were observed between the hydrogen at δ_H 5.51 with the quaternary carbons at δ_C 37.2, δ_C 38.8 and δ_C 40.2. The HMBC correlation with the quaternary carbon at δ_C 40.2 indicated that this fragment is linked to the 1st ring. This is also supported by the HMBC correlations observed between the hydrogen at δ_H 1.70 with methine carbons at δ_C 44.6 and δ_C 115.6, the methylene carbon at δ_C 27.6 and quaternary carbons at δ_C 40.2 and δ_C 158.6.

The methine hydrogen at δ_H 0.57 (δ_C 44.6) had HMBC correlations with the methyl carbon at δ_C 21.3, the methylene carbon at δ_C 64.8 as well as quaternary carbons at δ_C 37.2 and δ_C 40.2. HMBC correlations were observed between the methylene hydrogens at δ_H 3.10 and δ_H 3.24

with methylene carbons at δ_C 27.6 and δ_C 30.4 as well as the quaternary carbon at δ_C 40.2. The HMBC correlations showed that the methylene carbon at δ_C 64.8 is likely to be attached to the quaternary carbon at δ_C 40.2. The chemical shift of the methylene carbon at δ_C 64.8 indicated that an oxygen group is likely to be attached to this methylene carbon. Therefore, this accounted for one hydroxyl group (1st hydroxyl group). The HMBC correlations and COSY coupling supported the closure of a ring that fused to the 1st ring, thus accounting for one additional degree of unsaturation. Therefore, this accounted for the third degree of unsaturation (2nd ring). (***Figure 2.20***)

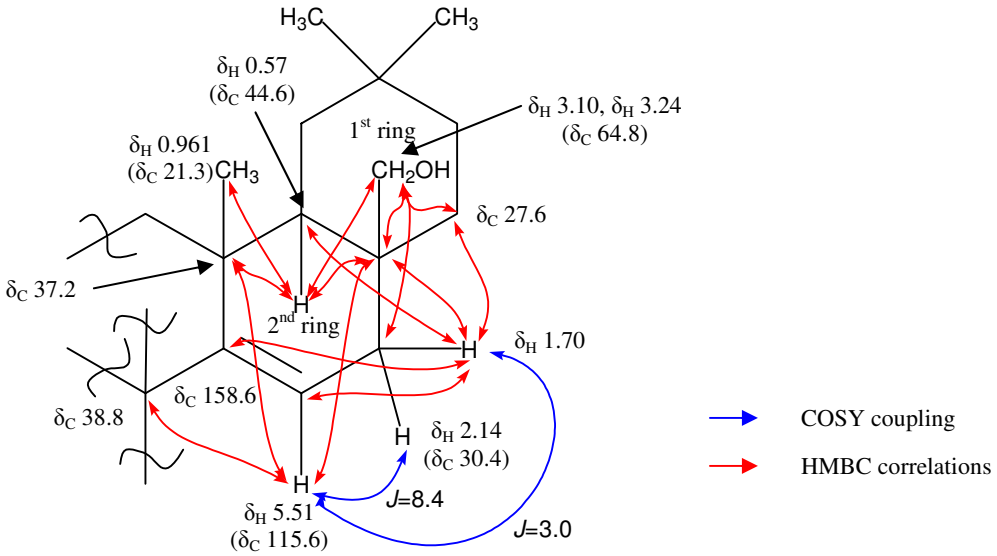

Figure 2.20: Closure of the 2nd ring for [50] based on COSY and HMBC correlations

The methyl hydrogens at δ_H 1.06 (δ_C 25.8) showed HMBC correlations with the methine carbon at δ_C 48.9, the methylene carbon at δ_C 41.1 and the quaternary carbon at δ_C 38.8. The HMBC correlations indicated that the methyl hydrogens at δ_H 1.06 are likely to be attached to the quaternary carbon at δ_C 38.8. HMBC correlations were observed between methine hydrogen at δ_H 0.57 (δ_C 44.6) with the methylene carbon at δ_C 33.2. The methylene hydrogen at δ_H 1.62 (δ_C 33.2) showed HMBC correlations with the methyl carbon at δ_C 21.3, the methine carbon at δ_C 48.9, the methylene carbon at δ_C 17.1 and quaternary carbons at δ_C 37.2 and δ_C 38.8. The HMBC correlations supported the closure of an additional ring that fused to the 2nd ring. Therefore, this ring closure accounted for the fourth degree of unsaturation (3rd ring). (***Figure 2.21***)

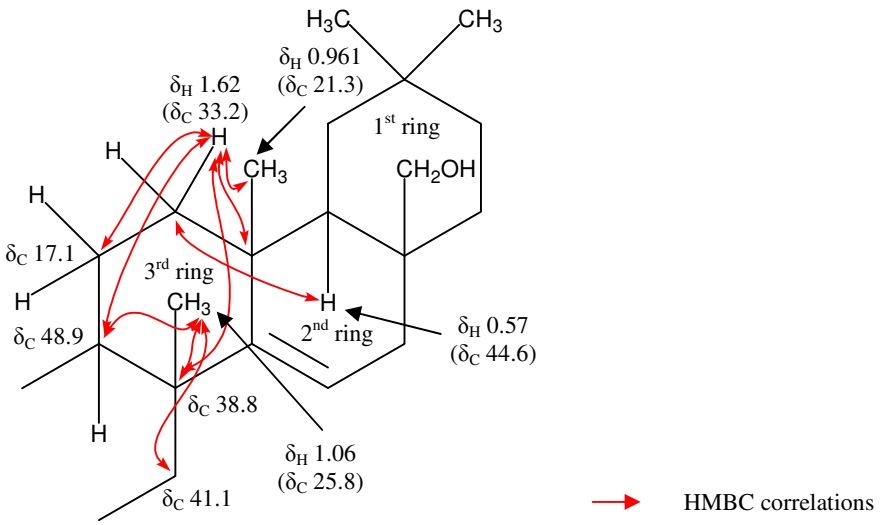

Figure 2.21: Closure of the 3rd ring for [50] based on HMBC correlations

The methyl hydrogens at δ_H 0.97, which are attached to δ_C 27.8 showed HMBC correlations with the methyl carbon at δ_C 15.3, methine carbon at δ_C 55.3 and the quaternary carbon at δ_C 38.5. HMBC correlations were observed between the methyl hydrogens at δ_H 0.79 (δ_C 15.3) with the methyl carbon at δ_C 27.8, methine carbons at δ_C 55.3 and δ_C 78.5 as well as the quaternary carbon at δ_C 38.5. The HMBC correlations observed for both methyl hydrogens indicated that they are likely to be attached to the quaternary carbon at δ_C 38.5.

The chemical shift of the methine carbon at δ_C 78.5 indicated that an oxygen group is likely to be attached to this methine carbon. Therefore, this is accounted for one additional hydroxyl group (2nd hydroxyl group).

In the HMBC spectrum, the methine hydrogen at δ_H 0.77 (δ_C 55.3) showed correlations with the methyl carbons at δ_C 15.3 and δ_C 27.8, the methine carbons at δ_C 48.9 and δ_C 78.5, the methylene carbons at δ_C 18.5 and δ_C 41.1 as well as the quaternary carbon at δ_C 38.5. HMBC correlations were observed between the methylene hydrogens at δ_H 1.33 and δ_H 2.01 with the methylene carbon at δ_C 18.5. HMBC correlations were also observed between the methine proton at δ_H 1.42 (δ_C 48.9) with the methyl carbons at δ_C 15.2 and δ_C 25.8. The methyl hydrogens at δ_H 0.91 (δ_C 15.2) showed HMBC correlations with the methine carbons at δ_C 48.9 and δ_C 55.3, the methylene carbon at δ_C 26.9 and the quaternary carbon at δ_C 37.7. Therefore, the methyl group at δ_H 0.91 (δ_C 15.2) is likely to be attached to the quaternary

carbon at δ_C 37.7. The HMBC correlations supported the closure of an additional ring that fused to the 3rd ring, thus accounted for the fifth degree of unsaturation (4th ring). (***Figure 2.22***)

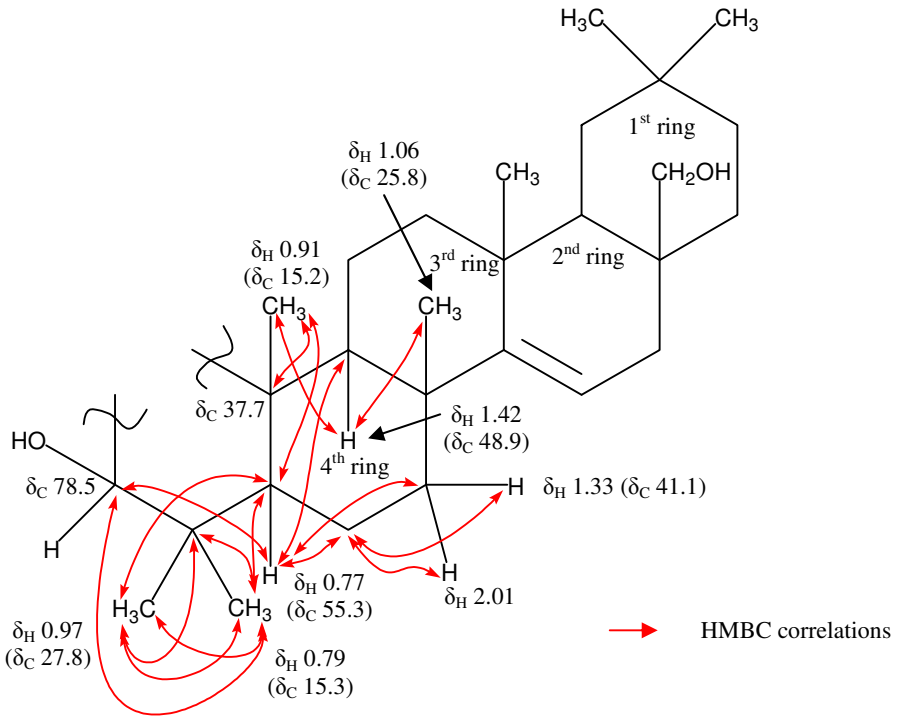

Figure 2.22: Closure of the 4th ring for [50] based on HMBC correlations

The methine hydrogen at δ_H 3.16 (δ_C 78.5) showed COSY coupling with the methylene hydrogens at δ_H 1.59 and δ_H 1.60. The ^{1}H NMR showed that the methine hydrogen at δ_H 3.16 had a coupling constant (*J*) of 4.8 Hz and 10.8 Hz. HMBC correlations were observed between the methylene hydrogens at δ_H 1.58 and δ_H 1.61 with the methine carbon at δ_C 78.5. As mentioned earlier, the methyl hydrogens at δ_H 0.91 showed HMBC correlation with the methylene carbon at δ_C 26.9. The HMBC correlations as well as the COSY coupling supported the closure of a ring that fused to the 4th ring, thus accounted for the sixth degree of unsaturation (5th ring). (***Figure 2.23***)

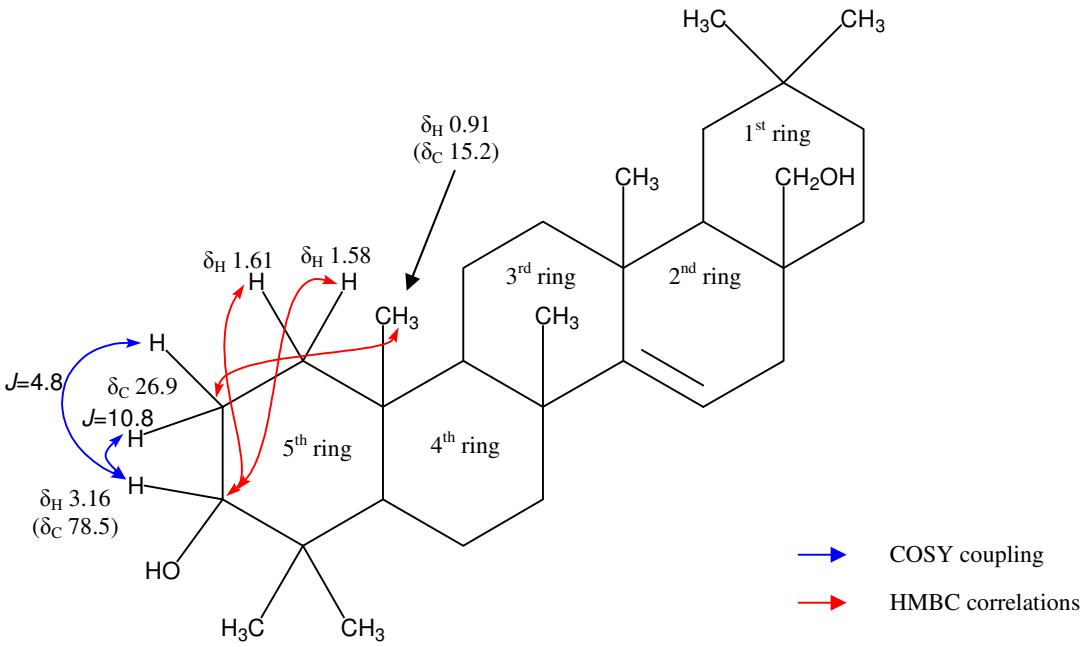

Figure 2.23: Closure of the 5th ring for [50] based on COSY and HMBC correlations

Table 2.4: Spectral data for [50]

C	δ_C	H	δ_H	I	M	J(Hz)	COSY	HMBC
C_1	37.5	$H_{1\alpha}$ $H_{1\beta}$	1.61 1.58	1 1	m m			C_3 C_3
C_2	26.9	$H_{2\alpha}$ $H_{2\beta}$	1.60 1.59	1 1	m m			C_{10} C_{10}
C_3	78.5	H_3	3.16	1	dd	4.8, 10.8	$H_{2\alpha}$, $H_{2\beta}$	C_{23}, C_{24}
C_4	38.5							H_5, Me_{23}, Me_{24}
C_5	55.3	H_5	0.77	1	dd	2.4, 12.6		C_4, C_3, C_6, C_7, C_9, C_{23}, C_{24}
C_6	18.5	$H_{6\alpha}$ $H_{6\beta}$						
C_7	41.1	$H_{7\alpha}$ $H_{7\beta}$	2.01 1.33	1 1	dt td	3.0, 12.6 3.0, 12.6		C_6, C_{12} C_6 ,C_{12}
C_8	38.8							$H_{7\alpha}$, $H_{7\beta}$, $H_{12\beta}$, H_{15}, Me_{26}
C_9	48.9	H_9	1.42	1	m			C_{25}, C_{26}
C_{10}	37.7							Me_{25}
C_{11}	17.1	$H_{11\alpha}$ $H_{11\beta}$						
C_{12}	33.2	$H_{12\alpha}$ $H_{12\beta}$	1.66 1.62	1 1	m m			C_9, C_{11}, C_{13}, C_{27} C_8, C_9, C_{11}, C_{13}, C_{27}
C_{13}	37.2							$H_{12\beta}$, H_{15}, H_{18}, $H_{22\alpha}$, $H_{22\beta}$, Me_{26},Me_{27}
C_{14}	158.6							$H_{16\alpha}$, Me_{26}, Me_{27}
C_{15}	115.6	H_{15}	5.51	1	dd	3.0, 8.4	$H_{16\alpha}$,$H_{16\beta}$	C_8, C_{13}, C_{16}, C_{17}

C	δ_C	H	δ_H	I	M	J(Hz)	COSY	HMBC
C_{16}	30.4	$H_{16\alpha}$	2.14	1	dd	8.4, 15.0	H_{15}, $H_{16\beta}$	C_{14}, C_{15}, C_{17}, C_{18}, C_{28}
		$H_{16\beta}$	1.70	1	dd	3.0, 15.0	H_{15}, $H_{16\alpha}$	C_{14}, C_{15}, C_{17}, C_{18}, C_{22}, C_{28}
C_{17}	40.2							$H_{16\alpha}$, $H_{16\beta}$, H_{18}, $H_{19\alpha}$, $H_{19\beta}$, $H_{21\alpha}$, $H_{21\beta}$
C_{18}	44.6	H_{18}	0.57	1	dd	3.6, 13.8	$H_{19\alpha}$, $H_{19\beta}$	C_{12}, C_{13}, C_{17},C_{19}, C_{20}, C_{27}, C_{28},C_{29},
C_{19}	35.6	$H_{19\alpha}$	1.41	1	m			C_{17}, C_{18}, C_{20}, C_{29}, C_{30},
		$H_{19\beta}$	1.00	1	dd	3.6, 13.2		C_{17}, C_{18}, C_{20}, C_{21}, C_{30}
C_{20}	28.3							H_{18}, $H_{19\alpha}$, $H_{19\beta}$, $H_{21\alpha}$, $H_{21\beta}$, Me_{29}, Me_{30}
C_{21}	32.4	$H_{21\alpha}$	1.26	1	m			C_{17}, C_{20}, C_{29}, C_{30}
		$H_{21\beta}$	1.24	1	m			C_{17}, C_{20}, C_{29}, C_{30}
C_{22}	27.6	$H_{22\alpha}$	1.50	1	m			C_{13}, C_{21}, C_{29}
		$H_{22\beta}$	1.47	1	m			C_{13}, C_{21}, C_{29}
C_{23}	27.8	Me_{23}	0.97	3	s			C_5, C_4, C_{24}
C_{24}	15.3	Me_{24}	0.79	3	s			C_3, C_4, C_5, C_{23}
C_{25}	15.2	Me_{25}	0.91	3	s			C_2, C_5, C_9, C_{10}
C_{26}	25.8	Me_{26}	1.06	3	s			C_7, C_8 C_9,
C_{27*}	21.3	Me_{27}	0.961	3	s			C_{13}, $C_{1,4}$, C_{18}
C_{28}	64.8	$H_{28\alpha}$	3.24	1	d	10.8	$H_{28\beta}$	C_{16}, C_{17}, C_{22}
		$H_{28\beta}$	3.10	1	d	10.8	$H_{28\alpha}$	C_7, C_8, C_{16}, C_{22}
C_{29*}	33.3	Me_{29}	0.964	3	s			C_{19}, C_{20}, C_{21}, C_{30}
C_{30}	29.6	Me_{30}	0.89	3	s			C_{19}, C_{20}, C_{21}, C_{29}

* Interchangeable [51] 600MHz (^{1}H and ^{13}C): δ (ppm) from internal TMS in $CDCl_3$

I = Integration
M = Multiplicity

The ROESY experiment unambiguously assigned the methyl hydrogens at δ_H 0.79 (δ_C 15.3), δ_H 0.91 (δ_C 15.2), δ_H 1.06 (δ_C 25.8) to be on the same side of the molecule as there were strong ROESY correlations between these methyl groups. **(*Figure 2.24*)**

The geminal methyl groups at δ_H 0.97 (δ_C 27.8) showed ROESY correlations with the methyl hydrogens at δ_H 0.79 (δ_C 15.3) as well as methine hydrogens at δ_H 0.77 (δ_C 55.3) and δ_H 3.16 (δ_C 78.5). Therefore, the hydrogens at δ_H 0.77, δ_H 0.97 and δ_H 3.16 were assigned to be on the same side of the molecule. This indicated that the hydroxyl group attached to methine carbon at δ_C 78.5 would be on the same side of the molecule with the methyl hydrogens at δ_H 0.79. **(*Figure 2.25*)**

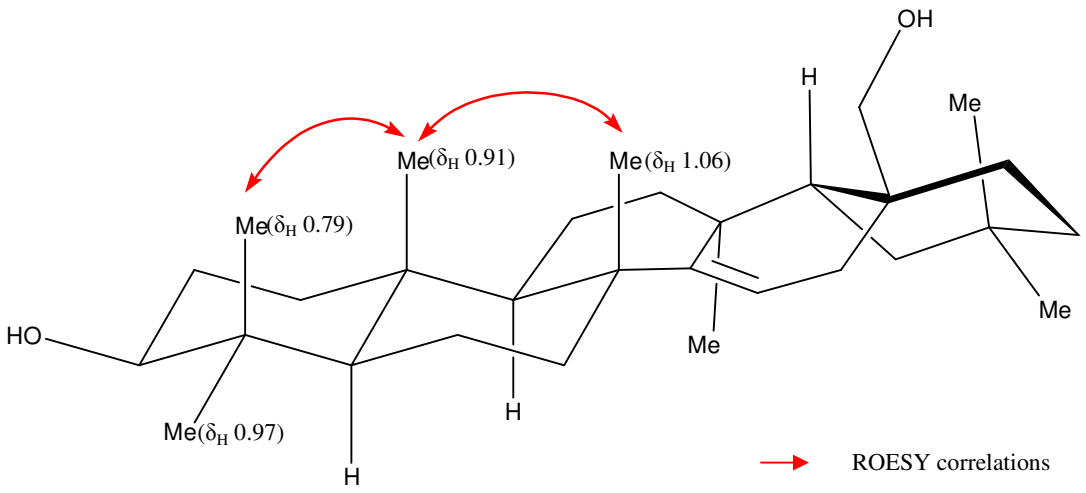

Figure 2.24: Stereochemical assignments of the methyl hydrogens for [50] based on ROESY correlations

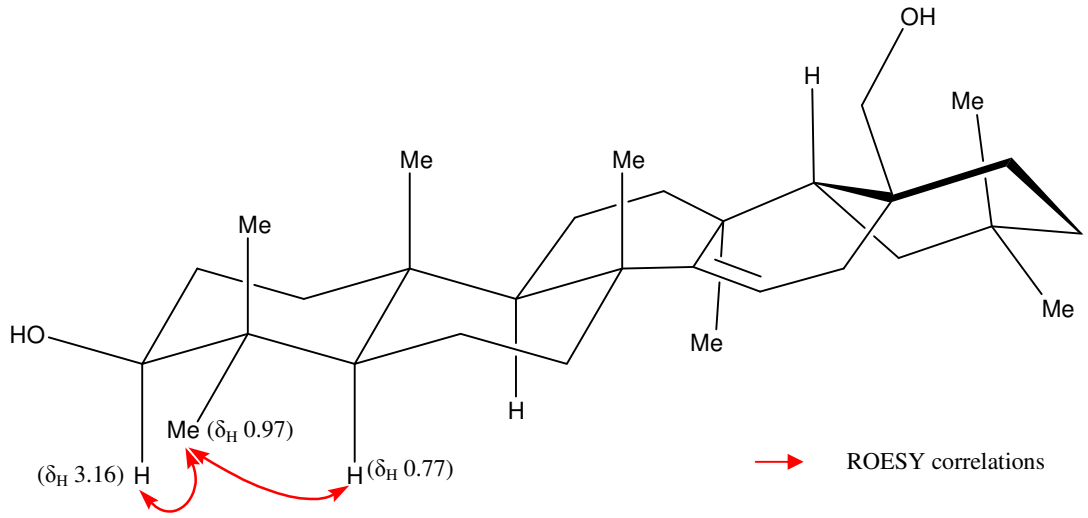

Figure 2.25: Stereochemical assignments of hydrogens at δ_H 3.16 and δ_H 0.77 for [50] based on ROESY correlations.

ROESY correlations were observed between both methine hydrogens at δ_H 0.77 (δ_C 55.3) and δ_H 1.42 (δ_C 48.9), followed by the methine hydrogen at δ_H 1.42 (δ_C 48.9) with the methyl hydrogens at δ_H 0.961 (δ_C 21.3). ROESY correlations between the methine hydrogen at δ_H 1.42 (δ_C 48.9) with the methyl hydrogens at at δ_H 0.961 (δ_C 21.3) are possible as the ring they are attached to are twisted and in a boat shape. **(*Figure 2.26*)**

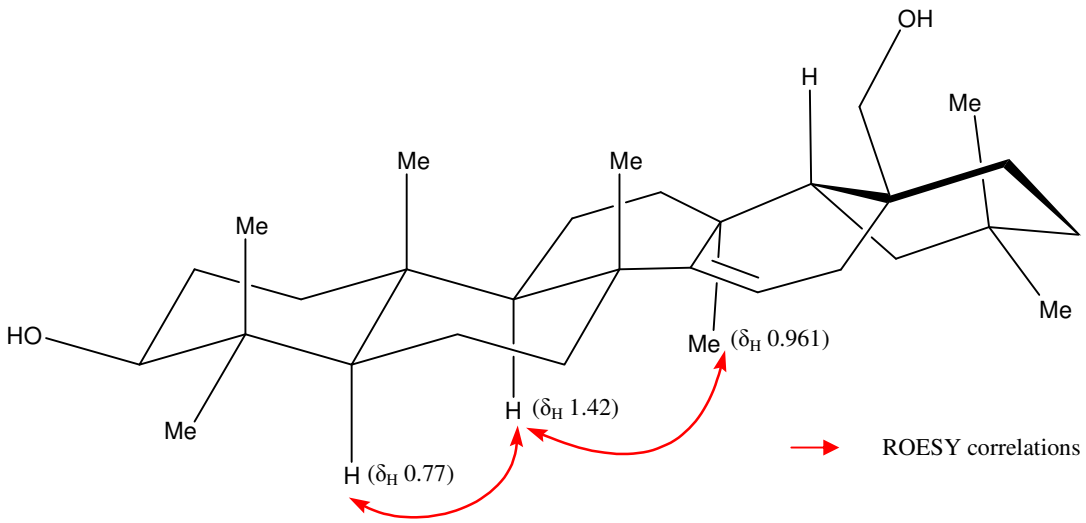

Figure 2.26: Stereochemical assignments of hydrogens at δ_H 0.77, δ_H 0.961 and δ_H 1.42 for [50] based on ROESY correlations

The methyl hydrogens at δ_H 1.06 (δ_C 25.8) showed ROESY correlations with the methylene hydrogen at δ_H 3.24 (δ_C 64.8). The methylene hydrogens at δ_H 3.24 and δ_H 3.10 (δ_C 64.8) had ROESY correlations with the methine hydrogen at δ_H 0.57 (δ_C 44.6). ROESY correlations were also observed between the methine hydrogen at δ_H 0.57 (δ_C 44.6) with the methyl hydrogens at δ_H 0.89 (δ_C 29.6). The ROESY correlations indicated that the hydrogens at δ_H 0.57 , δ_H 3.10 , δ_H 3.24 and δ_H 0.89 were on the same side of the molecule as the methyl hydrogens at δ_H 1.06 (δ_C 25.8). Therefore, methyl hydrogens at δ_H 0.964 (δ_C 33.3) had to be on the other side of the molecule. **(*Figure 2.27*)** The final structure is shown below.

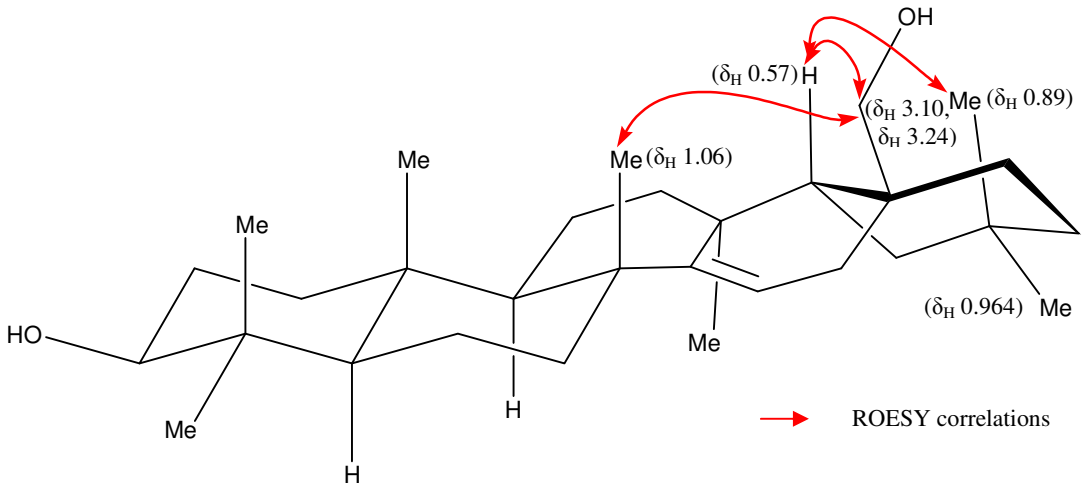

Figure 2.27: Stereochemical assignments of methyl hydrogens at δ_H 0.89 and δ_H 0.964 for [50] based on ROESY correlations

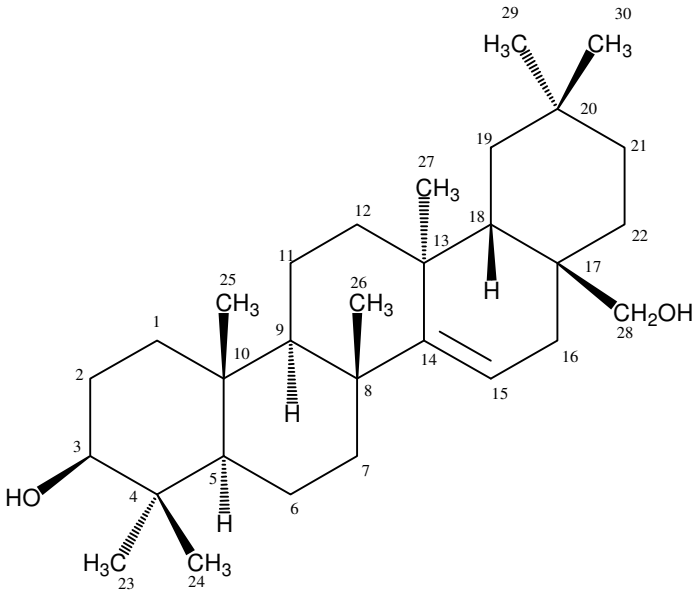

[50]

Table 2.5: ROESY correlations for [50]

Proton	ROESY	Proton	ROESY
$H_{1\alpha}$		$H_{16\beta}$	$H_{16\alpha}$, $Me_{29/27}$
$H_{1\beta}$		H_{18}	$H_{28\alpha}$, $H_{28\beta}$, $H_{19\alpha}$, $H_{19\beta}$, Me_{30}
$H_{2\alpha}$		$H_{19\alpha}$	H_{18}, Me_{27}
$H_{2\beta}$		$H_{19\beta}$	H_{18}, Me_{27}, Me_{30}
H_3	H_5,$H_{2\alpha}$, Me_{23}	$H_{21\alpha}$	
H_5	H_3 , $H_{8\beta}$, H_9, Me_{23}	$H_{21\beta}$	$H_{22\beta}$, Me_{29},Me_{30}
$H_{6\alpha}$		$H_{22\alpha}$	$H_{19\alpha}$, $H_{21\beta}$
$H_{6\beta}$		$H_{22\beta}$	
$H_{7\alpha}$	$H_{7\beta}$, Me_{26}	$H_{28\alpha}$	H_{18},Me_{26}
$H_{7\beta}$	H_5	$H_{28\beta}$	H_{18},$H_{21\alpha}$, Me_{30}
H_9	H_5	Me_{23}	H_3,H_5, Me_{24}
$H_{11\alpha}$		Me_{24}	$H_{2\beta}$,Me_{23}, Me_{25}
$H_{11\beta}$		Me_{25}	$H_{2\beta}$, Me_{26}, Me_{24}
$H_{12\alpha}$	H_{18}, $H_{19\alpha}$	Me_{26}	$H_{28\alpha}$, $H_{7\alpha}$
$H_{12\beta}$		Me_{27}	H_9, $H_{16\beta}$, $H_{19\alpha}$, $H_{19\beta}$
H_{15}	$H_{7\alpha}$, $H_{7\beta}$,$H_{16\alpha}$	Me_{29}	$H_{22\alpha}$
$H_{16\alpha}$	H_{15}, $H_{16\beta}$	Me_{30}	H_{18}, $H_{19\beta}$, $H_{21\beta}$

[50] 600MHz (^{1}H): δ (ppm) from internal TMS in $CDCl_3$

The NMR assignments suggested that [50] is myricadiol [24]. A comparison of the ^{13}C chemical shifts between [50] with other literature reports on myricadiol is shown in ***Table 2.6***.

Table 2.6: Comparison of the ^{13}C chemical shifts between [50] and myricadiol [24]

C	δ_C [50]	δ_C [24][43]	δ_C [24][44]	δ_C [24][45]
C_1	37.5	37.8	37.8	37.9
C_2	26.9	28.0	28.0	27.8
C_3	78.5	78.2	78.2	78.4
C_4	38.5	41.4	41.4	41.2
C_5	55.3	56.0	56.0	55.9
C_6	18.5	19.2	19.2	19.2
C_7	41.1	36.3	41.7	36.3
C_8	38.8	39.3	39.3	39.2
C_9	48.9	45.6	49.6	45.9
C_{10}	37.7	37.8	37.8	37.9
C_{11}	17.1	17.9	17.9	17.7
C_{12}	33.2	31.2	33.2	32.0
C_{13}	37.2	38.3	38.2	38.3
C_{14}	158.6	158.7	158.7	158.7
C_{15}	115.6	116.8	116.8	116.9
C_{16}	30.4	33.2	31.28	32.9
C_{17}	40.2	38.3	38.3	38.1
C_{18}	44.6	49.6	45.6	49.5
C_{19}	35.6	41.7	36.3	41.5
C_{20}	28.3	28.8	28.8	28.8
C_{21}	32.4	33.8	33.8	33.9
C_{22}	27.6	28.7	28.7	28.7
C_{23}	27.8	28.4	16.5	28.4
C_{24}	15.3	16.5	28.4	16.6
C_{25}	15.2	15.7	14.8	15.6
C_{26}	25.8	30.1	30.1	30.1
C_{27}	21.3	26.2	26.2	26.1
C_{28}	64.8	64.6	64.6	64.1
C_{29}	33.3	33.8	22.0	33.7
C_{30}	29.6	22.0	33.8	22.1

There are three literature reports for myricadiol [24].[43-45] However, there is inconsistency in the reported ^{13}C chemical shifts in these sources. The ^{13}C chemical shifts of myricadiol [24] were first reported by Sakurai *et al.*[43] The ^{13}C chemical shifts of myricadiol [24] were then later reassigned by Merfort *et al.*[44] The assignments of the ^{13}C chemical shifts for myricadiol [24] by Soo Lee *et al*[45] are based on the literature report by Sakurai *et al*[43]. Therefore, there are similarities between the ^{13}C chemical shifts reported by Sakurai *et al*[43] and Soo Lee *et al*[45]. The ^{13}C chemical shifts for [50] are broadly consistent with the literature reports for myricadiol [24] except for the ones highlighted in red. Among the three literature reports for

myricadiol [24], the ^{13}C chemical shifts for [50] are more consistent with the literature report by Merfort *et al*[44].

From the literature reports, the melting point for myricadiol [24] has been reported to be 269 - 271°C[45] and 278-279°C[43]. The melting point for [50] (265 - 270°C) is in the region of the literature reports for myricadiol [24][43,45]. This further supported that compound [50] was myricadiol.

Myricadiol [24] has previously been isolated from *Scaevola spinescens*[5].

2.4.2 Ethyl Acetate Extract

Fractionation and purification of compounds from ethyl acetate extract

A total of 15 g of ethyl acetate extract was obtained from the Soxhlet extraction. The ethyl acetate extract was then subjected to fractionation and purification by flash column chromatography. The fractionation and purification of compounds from the ethyl acetate extract are summarized in ***Figure 2.28***. Below are the details of the fractionation of compounds from the ethyl acetate extract.

- Two batches of the ethyl acetate extract (~ 7.5 g each time) were subjected to flash column chromatography (100 mm column diameter) using a series of increasing polarity solvents to yield 19 fractions, EA01/1-EA19/1 and 17 fractions, EA01/2-EA17/2 respectively. The fractions from these two batches that had similar TLC profiles were combined. The combined fractions are indicated by colour coding in red (***Figure 2.28***). This was to enable further purification of the material and to allow a reasonable amount of pure compound to be isolated. The fractions that had slightly different TLC profiles were assigned with different colours to distinguish between the two batches. Fractions from the first batch of extraction were color coded in dark green and the fractions from the second batch of extraction were colour coded in blue (***Figure 2.28***).

Figure 2.28: Fractionation from 15 g of ethyl acetate extract

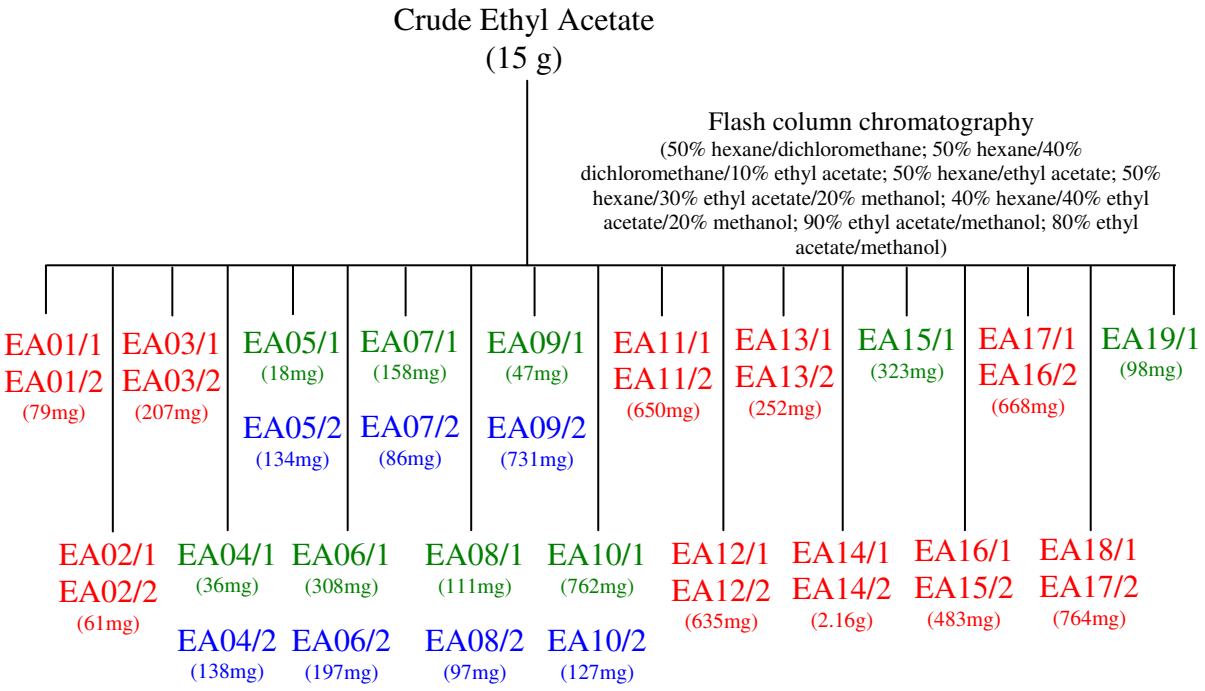

- Fraction EA10/1 (690 mg) was then subjected to further flash column chromatography (40 mm column diameter) using a series of increasing polarity solvents to yield 8 sub-fractions, EA1001-EA1008 (***Figure 2.29***).

- When solutions of Fractions EA1003 and EA1005 were left standing, white solids crystallized out of each solution. The white solids were labeled as EA1003a and EA1005a respectively (***Figure 2.29***). Both of these white solids were found to have similar ^{1}H NMR spectra. However, the amount of these white solids was insufficient for structural elucidation. Nevertheless, the filtrate from fraction EA1005 (EA1005b) was tested for purity by ^{1}H NMR spectrometer as this compound showed good antibacterial activity (See **Chapter 3: Antibacterial assay**) and was found to be reasonably pure, which should allow for further characterization. Therefore, EA1005b [51] was further characterized using 2D NMR, mass spectrometry, FTIR and UV-visible spectroscopy.

Figure 2.29: Fractionation from 690 mg of fraction EA10

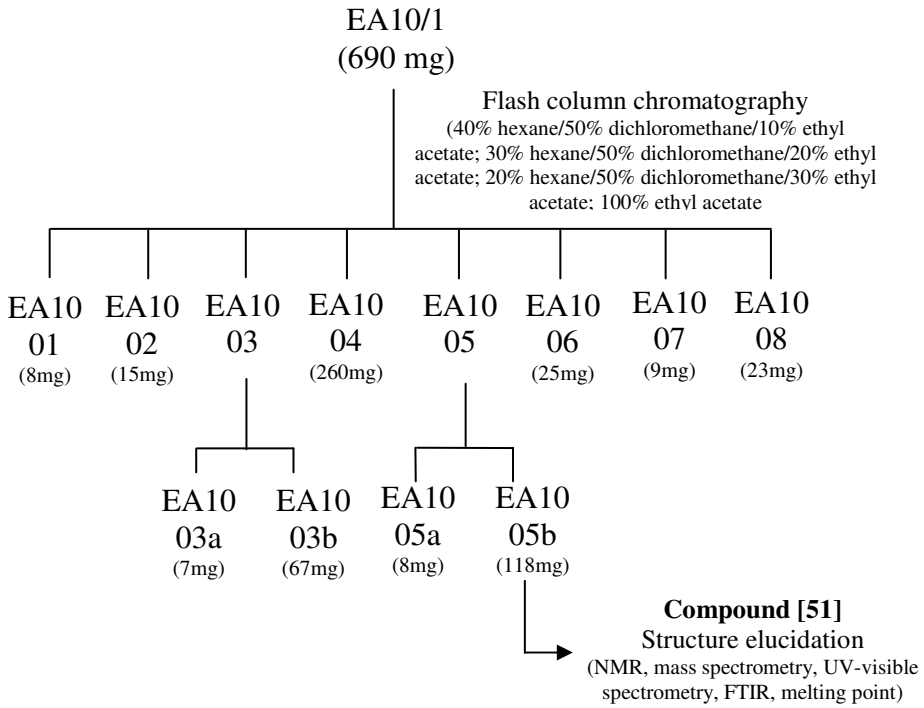

- Fraction EA11 (416 mg) was subjected to further flash column chromatography (40 mm column diameter) using a series of increasing polarity solvents to yield 10 sub-fractions, EA1101-EA1110 (***Figure 2.30***). Sub-fraction EA1106 [52] was then further characterized using 2D NMR, melting point, mass spectrometry, FTIR and UV-Visible spectroscopy (***Figure 2.30***).

Figure 2.30: Fractionation from 416 mg of fraction EA11

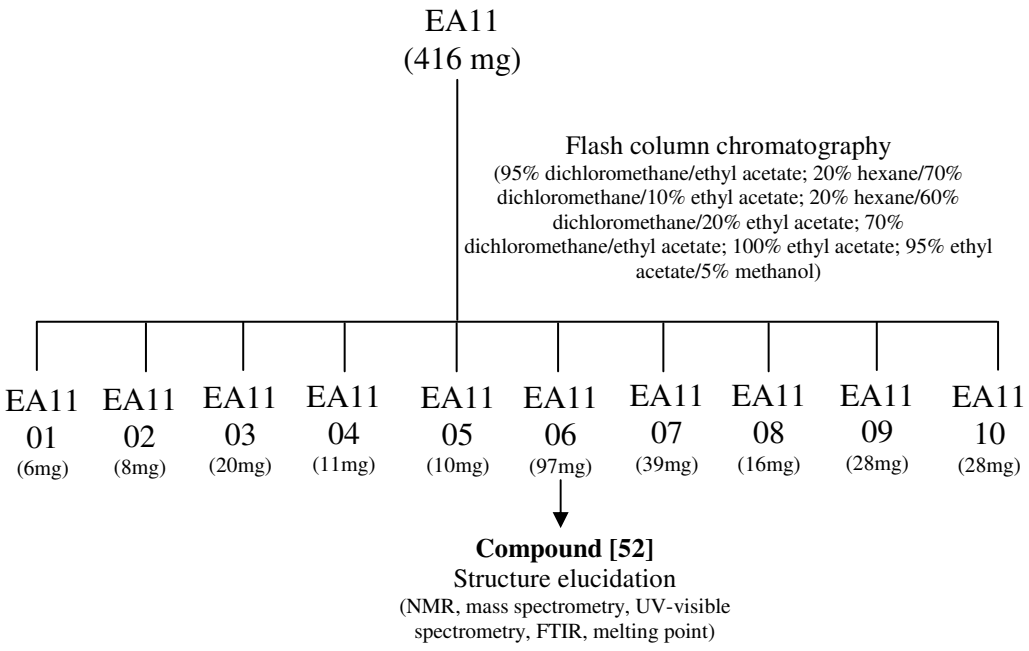

Compound [51]

Compound [51] (118 mg) was isolated as a white amorphous solid with a melting point of 238 – 240 °C. Using high-resolution EI mass spectrometry, the molecular formula was determined to be $C_{30}H_{48}O_3$ from the molecular ion peak at *m/z* 456.3599 (calculated 456.3603). This indicated that the compound had 7 degrees of unsaturation. The IR spectrum indicated the presence of hydroxyl group(s) as there were absorptions at 3416 cm^{-1} and 2850 cm^{-1}. There was also an absorption at 1686 cm^{-1} in the IR spectrum, which indicated the presence of a carbonyl group. The combination of the absorption at 2850 cm^{-1} and 1686 cm^{-1} are strongly suggestive of a carboxylic acid functionality.

Some difficulties were encountered in assigning the hydrogens and carbons of this structure. The COSY spectrum did not give much information as most of the hydrogens are overlapping in the chemical shift region of 1.2 – 1.7 ppm. So it was impossible to unambiguously assign all the signals for each hydrogen by this method. Therefore, most of the NMR assignments were based on HMBC and ROESY correlations. Only unambiguously assigned signals were taken into consideration when determining this structure. These correlations are shown in ***Table 2.7*** and ***Table 2.8***.

The ^{13}C and DEPT NMR spectra indicated a total of 30 unique carbons; seven methyls (δ_C 16.5, 16.8, 18.1, 18.3, 22.0, 24.6, 29.2), nine sp^3 methylenes ((δ_C 19.9, 24.8, 25.8, 28.4, 29.7, 32.2, 34.8, 38.6, 40.5), six sp^3 methines (δ_C 38.6, 40.9, 49.5, 54.8, 57.2, 80.2), one sp^2 methine (δ_C 127.4), five quaternary sp^3 carbons (δ_C 40.3, 40.9, 41.3, 43.7, 50.0) and two quaternary sp^2 carbon (δ_C 140.1, 182.0). All these resonances accounted for a partial molecular formula $C_{30}H_{46}$.

The three sp^2 carbons (δ_C 127.4, 140.1, 182.0) indicated a double bond functionality and carbonyl group, which accounts for two degrees of unsaturation. This suggested that the compound contained 5 rings. The carbonyl group accounted for an oxygen atom, which is supported by the infrared spectra. Therefore, the remaining two hydrogen atoms and two oxygen atoms accounted for two hydroxyl groups, which are also supported by the infrared spectra.

All the methyl, methylene and methine carbons identified in the DEPT NMR were assigned to their directly attached hydrogens using the HSQC experiment.

In the HMBC spectrum, the methyl hydrogens at δ_H 0.77 (δ_C 16.8 as shown in HSQC spectrum) showed correlations with the methyl carbon at δ_C 29.2, methine carbons at δ_C 57.2 and δ_C 80.2 as well as the quaternary carbon at δ_C 40.3. HMBC correlations were also observed between the methyl hydrogens at δ_H 0.97 (δ_C 29.2 as shown un HSQC spectrum) with the methyl carbon at δ_C 16.8, methine carbons at δ_C 57.2 and δ_C 80.2 as well as the quaternary carbon at δ_C 40.3. This indicated that the two methyl groups are likely to be attached to the quaternary carbon at δ_C 40.3. The chemical shift of the methine carbon at δ_C 80.2 indicated that an oxygen group is likely to be attached to this methine carbon. Therefore this accounted for one hydroxyl group. **(*Figure 2.31*)**

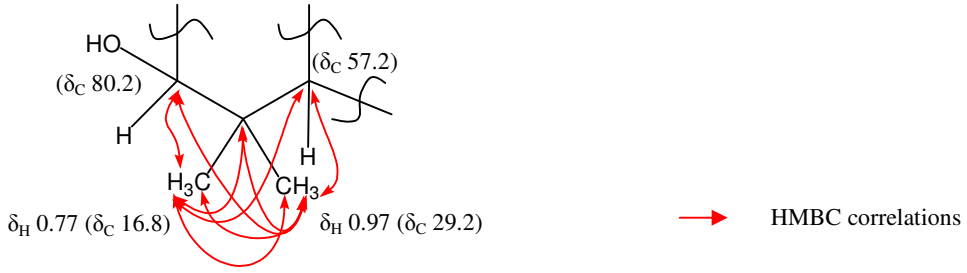

Figure 2.31: Fragment to build the 1st ring for [51] based on HMBC correlations

In the COSY spectrum, the methine hydrogen at δ_H 3.14 (δ_C 80.2) showed correlations with the methylene hydrogens at δ_H 1.57 and δ_H 1.62 (δ_C 28.4). In the ^{1}H NMR spectrum, the hydrogen at δ_H 3.14 showed multiplicity of doublet of doublet with coupling constant (*J*) of 4.2 Hz ad 11.4 Hz. The methylene hydrogen at δ_H 1.62 also showed COSY correlations with the methylene hydrogen at δ_H 1.68 (δ_C 38.6). HMBC correlations were also observed between the methylene hydrogen at δ_H 1.57 with the methylene carbon at δ_C 38.6 as well as quaternary carbons at δ_C 40.9 and δ_C 40.3. The methine hydrogen at δ_H 0.74 (δ_C 57.2) had HMBC correlations with the methylene carbon at δ_C 38.6. The HMBC and COSY correlations supported the closure of a ring, thus accounting for one additional degree of unsaturation. Therefore, this accounted for the third degree of unsaturation (1st ring). **(*Figure 2.32*)**

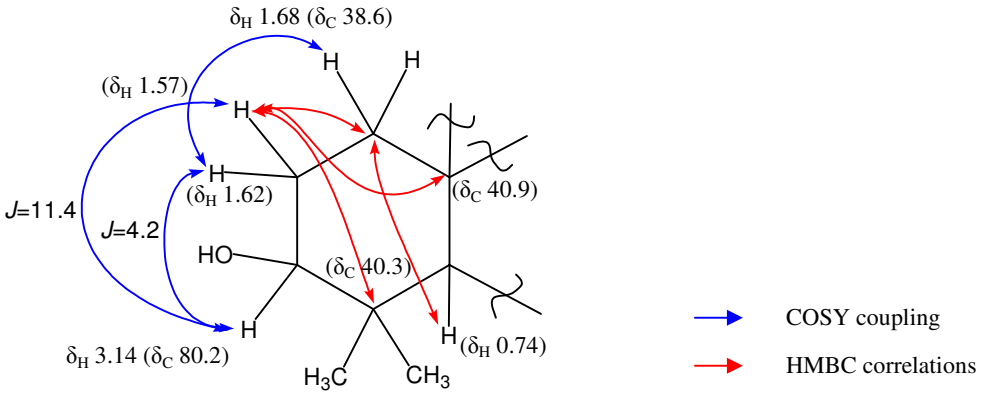

Figure 2.32: Closure of the 1st ring for [51] based on COSY and HMBC correlations

In the COSY spectrum, the methine hydrogen at δ_H 0.74 (δ_C 57.2) showed correlations with the methylene hydrogen at δ_H 1.39 (δ_C 19.9). HMBC correlations were also observed between the methine hydrogen at δ_H 0.74 with the methine carbon at δ_C 49.5, the methylene carbons at δ_C 19.9 and δ_C 34.8 as well as the methyl carbon at δ_C 16.5. The methine hydrogen at δ_H 1.56 (δ_C 49.5) had HMBC correlations with the methine carbon at δ_C 57.2, the methylene carbons at δ_C 24.8 and δ_C 38.6, the methyl carbons at δ_C 16.5 and δ_C 18.3 as well as the quaternary carbons at δ_C 41.3 and δ_C 43.7. In the COSY spectrum, the methine at δ_H 1.56 (δ_C 49.5) showed correlations with the methylene hydrogens at δ_H 1.92. The two methylene hydrogens at δ_H 1.92 were indistinguishable as they have the same chemical shifts. The methyl hydrogens at δ_H 0.84 (δ_C 18.3) showed HMBC correlations with the methine carbon at δ_C 49.5, methylene carbon at δ_C 34.8 as well as quaternary carbons at δ_C 40.9, δ_C 41.3 and δ_C 43.7. HMBC correlations were also observed between the quaternary carbon at δ_C 41.3 with the methylene hydrogen at δ_H 1.92 (δ_C 24.8) as well as the methyls hydrogens at δ_H 0.84 (δ_C 18.3) and δ_H 1.11 (δ_C 24.6). The quaternary carbon at δ_C 43.7 had HMBC correlations with the methine hydrogens at δ_H 5.22 (δ_C 127.4) and δ_H 2.19 (δ_C 54.8). Therefore, the methyl group at δ_H 0.84 (δ_C 18.3) is likely to be attached to the quaternary carbon at δ_C 41.3. The HMBC and COSY correlations (where applicable) supported the closure of a ring that fused to the 1st ring, thus accounting for one additional degree of unsaturation, which accounted for the fourth degree of unsaturation (2nd ring). (***Figure 2.33***)

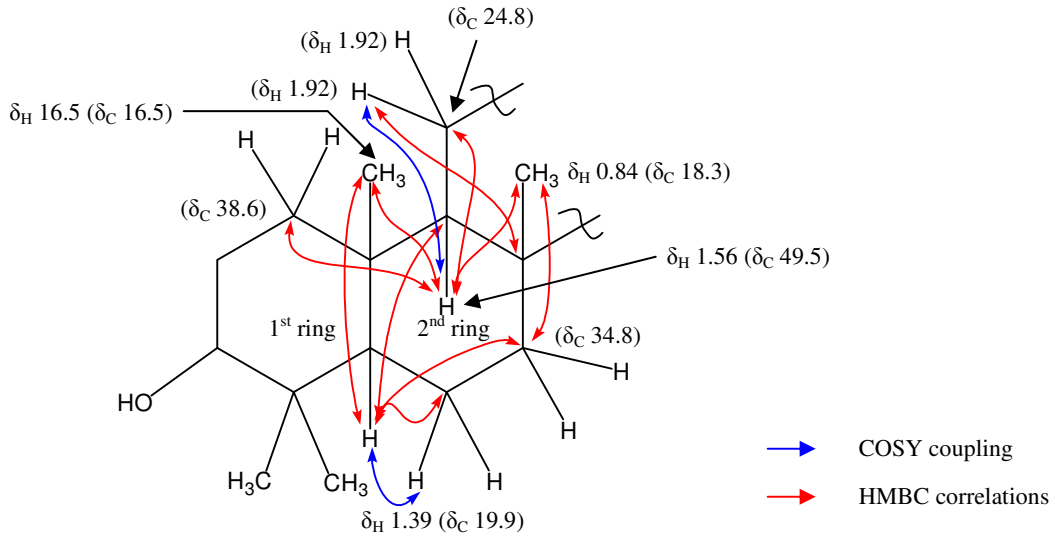

Figure 2.33: Closure of the 2nd ring for [51] based on COSY and HMBC correlations

In the COSY spectrum, the methylene hydrogens at δ_H 1.92 (δ_C 24.8) showed correlations with the methine hydrogen at δ_H 5.22 (δ_C 127.4). In the ^{1}H NMR spectrum, the methine hydrogen at δ_H 5.22 (δ_C 127.4) showed multiplicity of triplet with a coupling constant (*J*) of 3.6 Hz. The chemical shift of the methine carbon at δ_C 127.4 indicated that it must be attached to the sp^2 quaternary carbon at δ_C 140.1. HMBC correlations were observed between the methine hydrogen at δ_H 5.22 (δ_C 127.4) with the methine carbons at δ_C 49.5 and 54.8, the methylene carbon at δ_C 24.8 as well as the quaternary carbon at δ_C 43.7. The quaternary carbon at δ_C 140.1 showed HMBC correlations with the methine hydrogen at δ_H 2.19 (δ_C 54.8), the methylene hydrogens at δ_H 1.92 (δ_C 24.8) and the methyl hydrogens at δ_H 1.11 (δ_C 24.6). The methyl hydrogens at δ_H 1.11 (δ_C 24.6) had HMBC correlations with the methylene carbon at δ_C 29.7 as well as the quaternary carbons at δ_C 41.3, δ_C 43.7 and δ_C 140.1. The HMBC and COSY correlations (where applicable) supported the closure of a ring that fused to the 2nd ring, thus accounted for the fifth degree of unsaturation (3rd ring). (***Figure 2.34***)

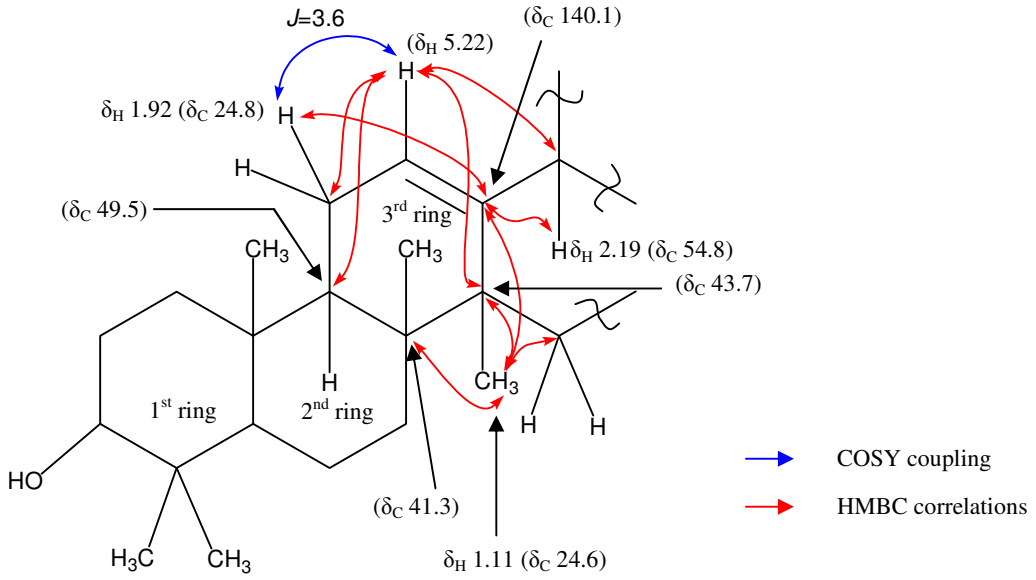

Figure 2.34: Closure of the 3rd ring for [51] based on COSY and HMBC correlations

In the COSY spectrum, the methylene hydrogens at δ_H 1.09 and δ_H 1.92 (δ_C 29.7) showed correlations with the methylene hydrogen at δ_H 2.03 (δ_C 25.8). In the ^{1}H NMR spectrum, the methylene hydrogen at δ_H 2.03 (δ_C 25.8) showed multiplicity of triplet of doublet with coupling constant (*J*) of 3.6 Hz and 13.2 Hz. Both the methylene hydrogens at δ_H 1.09 (δ_C 29.7) and δ_H 2.03 (δ_C 25.8) had HMBC correlations with the quaternary carbon at δ_C 50.0. HMBC correlation were also observed between the methylene hydrogen at δ_H 2.03 (δ_C 25.8) with the methine carbon at δ_C 54.8. The HMBC and COSY correlations supported the closure of a ring that fused to the 3rd ring, thus accounting for one additional degree of unsaturation. Therefore, this accounted for the sixth degree of unsaturation (4th ring). **(*Figure 2.35*)**

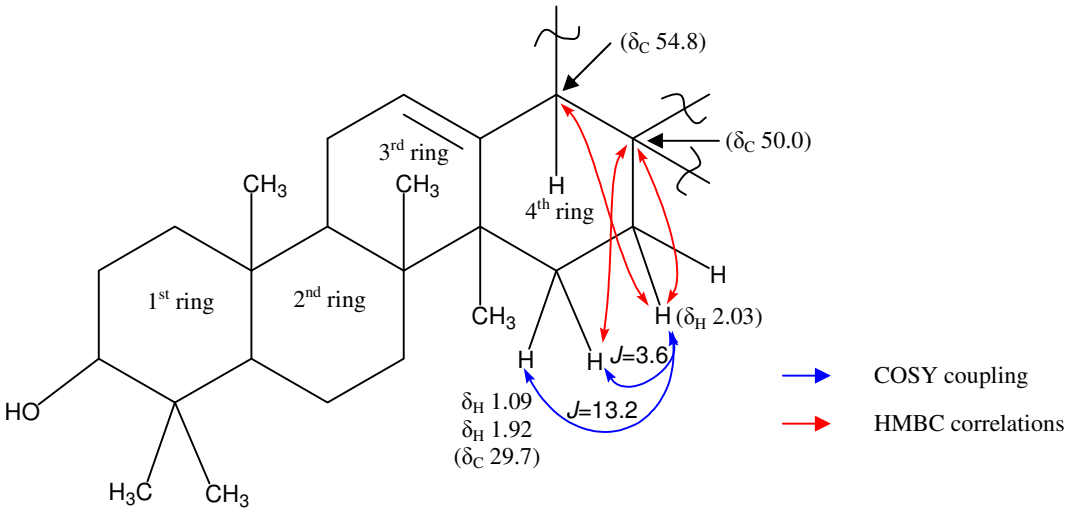

Figure 2.35: Closure of the 4th ring for [51] based on COSY and HMBC correlations

The methylene hydrogen at δ_H 2.03 (δ_C 25.8) also showed HMBC correlations with the quaternary carbon at δ_C 182.0. The chemical shift of the quaternary carbon at δ_C 182.0 was consistent with a carboxylic acid group (identified in the IR spectrum), which accounts for one hydrogen atom and two oxygen atoms.

The quaternary carbon at δ_C 182.0 showed HMBC correlations with the methine hydrogen at δ_H 2.19 (δ_C 54.8) and methylene hydrogens at δ_H 1.64 and δ_H 2.03 (δ_C 25.8). The HMBC correlations observed for the quaternary carbon at δ_C 182.0 indicated that it is likely to be attached to the quaternary carbon at δ_C 50.0. HMBC correlations were also observed between the quaternary carbon at δ_C 50.0 with the methylene hydrogens at δ_H 1.32 (δ_C 32.2) and δ_H 1.66 (δ_C 40.5). Both methylene hydrogens at δ_H 1.32 (δ_C 32.2) and δ_H 1.00 (δ_C 40.5) showed COSY correlations with each other. In the ^{1}H NMR spectrum, the methylene hydrogen at δ_H 1.00 (δ_C 40.5) showed a multiplicity of doublet of doublet with coupling constant (*J*) of 3.6 Hz and 13.2 Hz. The methylene hydrogen at δ_H 1.66 (δ_C 40.5) had HMBC correlation with the methine carbon at δ_H 1.68 (δ_C 38.6). HMBC correlations were also observed between the methine carbon at δ_C 38.6 with the methine hydrogen at δ_H 1.36 (δ_C 40.9). In the COSY spectrum, the methine hydrogen at δ_H 1.36 (δ_C 40.9) showed correlations with the methine hydrogen at δ_H 2.19 (δ_C 54.8). In the ^{1}H NMR spectrum, the methine hydrogen at δ_H 2.19 (δ_C 54.8) showed multiplicity of doublet with a coupling constant (*J*) of 11.4 Hz. This indicated that both methine hydrogens at δ_H 2.19 and δ_H 1.36 are in an axial-axial relationship. HMBC correlations were also observed between the methine hydrogen at δ_H 2.19 (δ_C 54.8) with the methine carbon at δ_C 40.9 and the methyl carbon at δ_C 18.1. This indicated that the methyl group at δ_H 0.87 (δ_C 18.1) is likely to be attached to the methine carbon at δ_C 40.9. This is supported by the multiplicity of doublet in the ^{1}H NMR spectrum. The methine carbon at δ_C 40.9 showed HMBC correlations with the methyl hydrogens at δ_H 0.95. HMBC correlations were also observed between the methyl hydrogens at δ_H 0.95 (δ_C 22.0) with the methylene carbons at δ_C 32.2 and δ_C 40.5. In the ^{1}H NMR spectrum, the methyl hydrogens at δ_H 0.95 showed a multiplicity of doublet, which indicates that the methyl group at δ_H 0.95 is likely to be attached to the methine carbon at δ_C 38.6. The HMBC and COSY correlations supported the closure of a ring that fused to the 4th ring, thus accounted for the seventh degree of unsaturation (5th ring). (***Figure 2.36***)

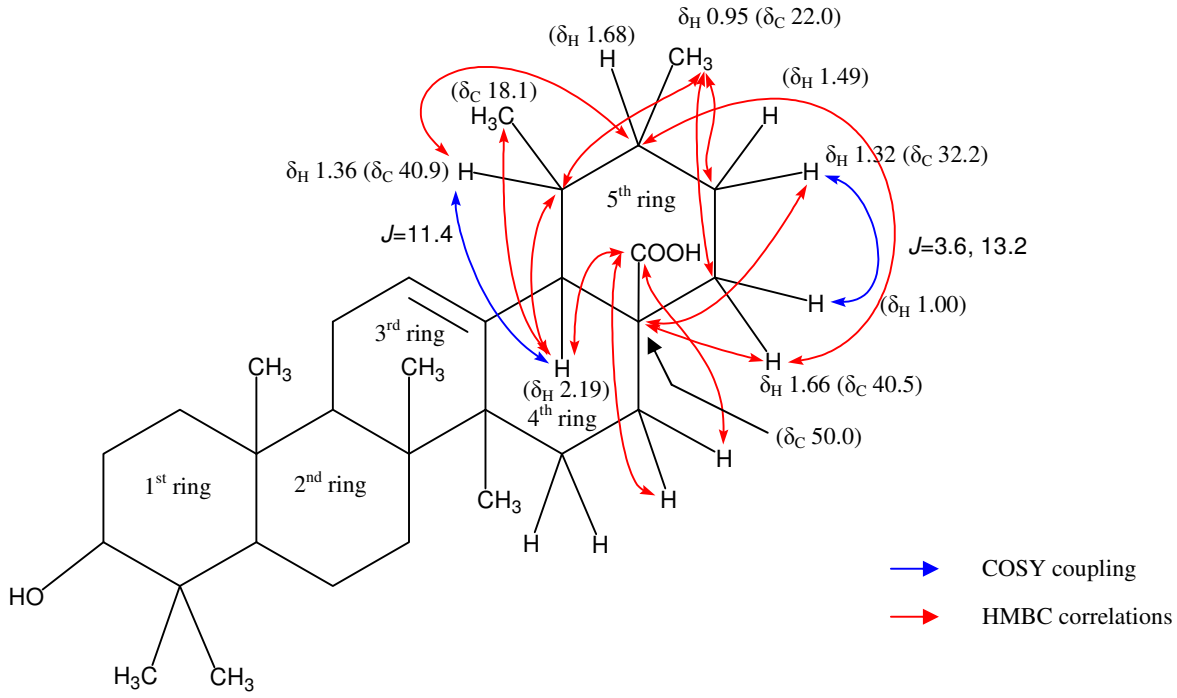

Figure 2.36: Closure of the 5th ring for [51] based on COSY and HMBC correlations

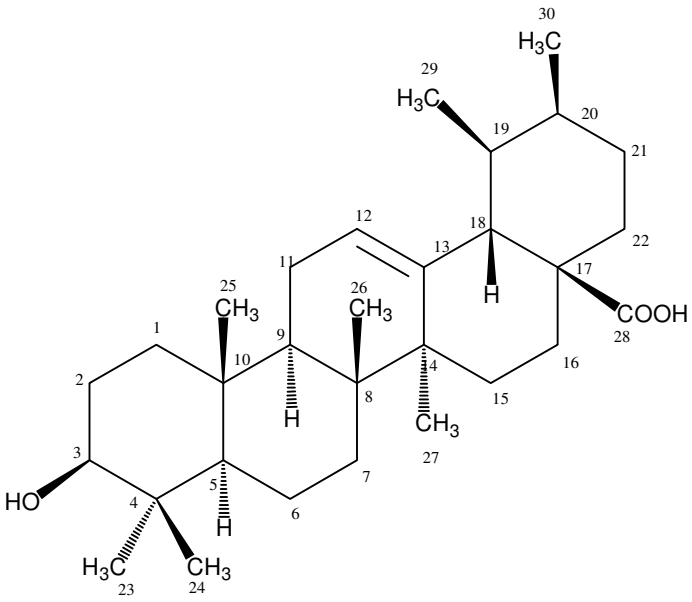

[51]

Table 2.7: Spectral data for [51]

C	δ_C	H	δ_H	I	M	*J*(Hz)	COSY	HMBC
C_{1*}	38.6	$H_{1\alpha}$ $H_{1\beta}$	1.68 1.62	1 1	m m		$H_{2\alpha}$	
C_2	28.4	$H_{2\alpha}$ $H_{2\beta}$	1.62 1.57	1 1	m m		$H_3, H_{1\alpha}$ H_3	C_{10}, C_4, C_1
C_3	80.2	H_3	3.14	1	dd	4.2, 11.4	$H_{2\alpha}, H_{2\beta}$	C_{23}, C_{24}
C_4	40.3							H_3, H_5, Me_{23}, Me_{24}
C_5	57.2	H_4	0.74	1	d	11.4	$H_{6\beta}$	C_3, C_9, C_4, C_1, C_7, C_{23}, C_6, C_{24}, C_{25}
C_6	19.9	$H_{6\alpha}$ $H_{6\beta}$	1.54 1.39	1 1	m m		 H_5	
C_7	34.8	$H_{7\alpha}$ $H_{7\beta}$	1.54 1.34	1 1	m m			
C_8	41.3							$H_{11\alpha}$, $H_{11\beta}$, Me_{27}, Me_{26}
C_9	49.5	H_9	1.56	1	m		$H_{11\alpha}, H_{11\beta}$	C_5, C_{14}, C_8, C_1, C_{11}, C_{26}, C_{25}
C_{10*}	40.9							$H_{2\beta}$
C_{11}	24.8	$H_{11\alpha}$ $H_{11\beta}$	1.92 1.92	1 1	m m		H_{12}, H_9 H_{12}, H_9	C_{13}, C_{12}, C_{18}, C_9, C_{14}, C_8
C_{12}	127.4	H_{12}	5.22	1	t	3.6	$H_{11\alpha}, H_{11\beta}$	$C_{18}, C_9, C_{14}, C_{11}$
C_{13}	140.1							$H_{18}, H_{11\alpha}, H_{11\beta}, Me_{27}$
C_{14}	43.7							H_{12}, H_{18}, H_9, $H_{16\beta}$, $H_{15\alpha}$, $H_{6\alpha}$, Me_{27}, Me_{26}
C_{15}	29.7	$H_{15\alpha}$ $H_{15\beta}$	1.92 1.09	1 1	m m		$H_{16\alpha}, H_{16\beta}$ $H_{16\alpha}, H_{16\beta}$	C_{17}, Me_{27} C_{17}
C_{16}	25.8	$H_{16\alpha}$ $H_{16\beta}$	2.03 1.64	1 1	td m	3.6, 13.2	$H_{15\alpha}, H_{15\beta}, {}_{16\beta}$ $H_{22\alpha}, H_{22\alpha}, {}_{16\alpha}$	$C_{28}, C_{18}, C_{17}, C_{15}$ C_{28}, C_{18}, C_{17}
C_{17}	50.0							H_{18}, $H_{22\alpha}$, $H_{21\beta}$, $H_{15\alpha}$, $H_{16\beta}$
C_{18}	54.8	H_{18}	2.19	1	d	11.4	H_{19}	C_{28}, C_{13}, C_{12}, C_{17}, C_{14}, C_{19}, C_{16}, C_{29}
C_{19*}	40.9	H_{19}	1.36	1	m		H_{18}	C_{20}
C_{20*}	38.6	H_{20}	1.68	1	m			H_{19}, $H_{22\alpha}$
C_{21}	32.2	$H_{21\alpha}$ $H_{21\beta}$	1.49 1.32	1 1	m m		 $H_{22\beta}$	
C_{22}	40.5	$H_{22\alpha}$ $H_{22\beta}$	1.66 1.00	1 1	m dd	 3.6, 13.2	 $H_{21\beta}$	C_{20}
C_{23}	29.2	Me_{23}	0.97	3	s		Me_{24}	C_3, C_5, C_4, C_{24}
C_{24}	16.8	Me_{24}	0.77	3	s		Me_{23}	C_3, C_5, C_4, C_{23}
C_{25}	16.5	Me_{25}	0.95	3	s			C_5, C_9
C_{26}	18.3	Me_{26}	0.84	3	s			C_9, C_{14}, C_8, C_{10}, C_7
C_{27}	24.6	Me_{27}	1.11	3	s			C_{13}, C_{14}, C_8, C_{15}
C_{28}	182.0							H_{18}, $H_{16\alpha}$, $H_{16\beta}$
C_{29}	18.1	Me_{29}	0.87	3	d			C_{18}, C_{19}
C_{30}	22.0	Me_{30}	0.95	3	d			C_{19}, C_{21}

* Interchangeable

[51] 600MHz (^{1}H and ^{13}C): δ (ppm) in CD_3OD

I = Integration
M = Multiplicity

The ROESY experiment unambiguously assigned the methyl hydrogens at δ_H 0.95 (δ_C 16.5), δ_H 0.77 (δ_C 16.8) and δ_H 0.84 (δ_C 18.3) to be on the same side of the molecule as there were strong ROESY correlations between these methyl hydrogens. **(*Figure 2.37*)**

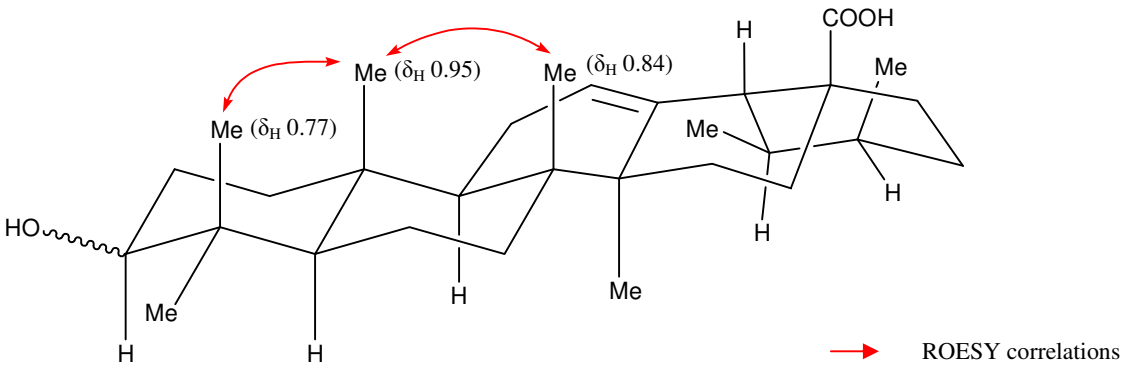

Figure 2.37: Stereochemical assignments of the methyl hydrogens for [51] based on ROESY correlations

The geminal methyl groups at δ_H 0.97 (δ_C 29.2) showed ROESY correlations with the methyl hydrogens at δ_H 0.77 (δ_C 16.8) as well as the methine hydrogens at δ_H 0.74 (δ_C 57.2) and δ_H 3.14 (δ_C 80.2). Therefore, the hydrogens at δ_H 0.74, δ_H 0.97 and δ_H 3.14 were assigned to be on the same side of the molecule. This indicated that the hydroxyl group attached to the methine carbon at δ_C 80.2 would be on the same side of the molecule with the methyl hydrogens at δ_H 0.77. **(*Figure 2.38*)**

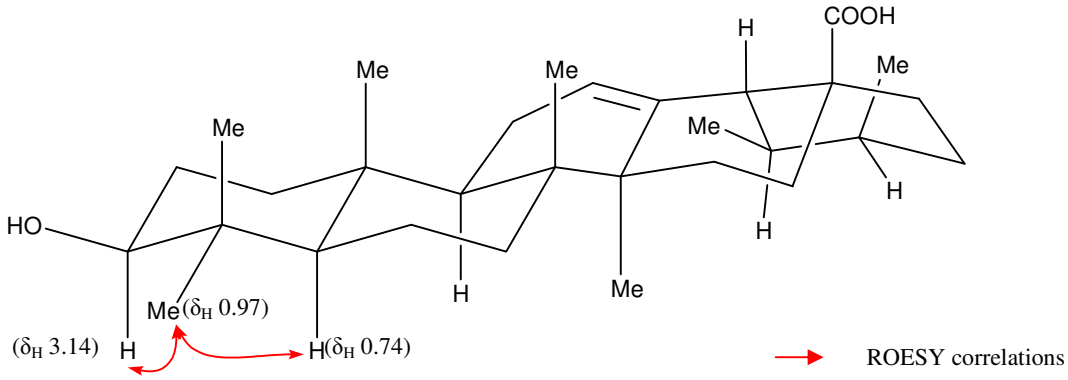

Figure 2.38: Stereochemical assignments of hydrogens at δ_H 3.14 and δ_H 0.74 for [51] based on ROESY correlations.

ROESY correlations were observed for both methine hydrogens at δ_H 0.74 (δ_C 57.2) and δ_H 1.56 (δ_C 49.5), followed by the methine hydrogen at δ_H 1.56 (δ_C 49.5) with the methyl

hydrogens at δ_H 1.11 (δ_C 24.6). The methyl hydrogens at δ_H 1.11 (δ_C 24.6) also showed ROESY correlations with the methine hydrogen at δ_H 1.36 (δ_C 40.9) and the methyl hydrogens at δ_H 0.87 (δ_C 18.1). This is consistent with the central cyclohexene ring being in a twist chair conformation. **(*Figure 2.39*)**

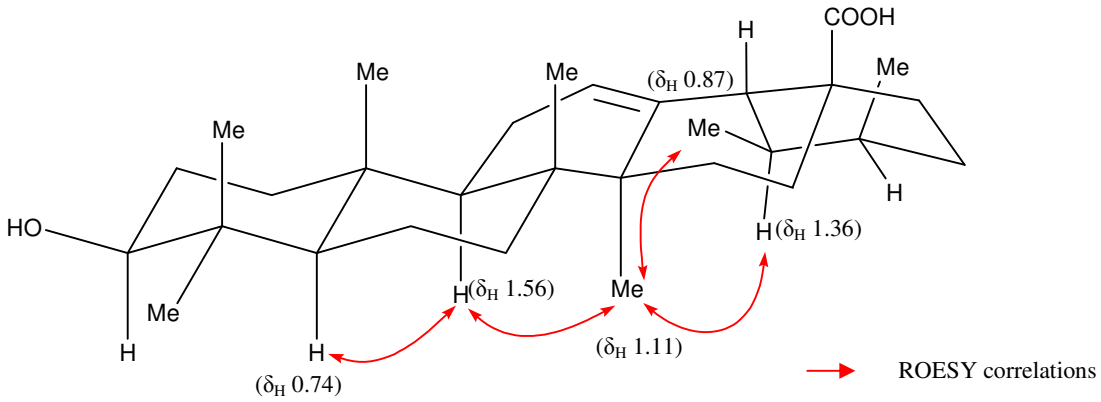

Figure 2.39: Stereochemical assignments of hydrogens at δ_H 0.87, δ_H 1.11, δ_H 1.36 and δ_H 1.56 for [51] based on ROESY correlations

The methyl hydrogens at δ_H 0.87 (δ_C 18.1) showed ROESY correlations with the methyl hydrogens at δ_H 0.95 (δ_C 22.0) and the methine hydrogen at δ_H 2.19 (δ_C 54.8). ROESY correlations were also observed between the methyl hydrogens at δ_H 0.95 (δ_C 22.0) with the methine hydrogen at δ_H 2.19 (δ_C 54.8). The ROESY correlations indicated that both the methyl hydrogens at δ_H 0.87 (δ_C 18.1) and δ_H 0.95 (δ_C 22.0) as well as the methine hydrogen at δ_H 2.19 (δ_C 54.8) would be on the opposite side of the methine hydrogen at δ_H 1.36 (δ_C 40.9). **(*Figure 2.40*)**

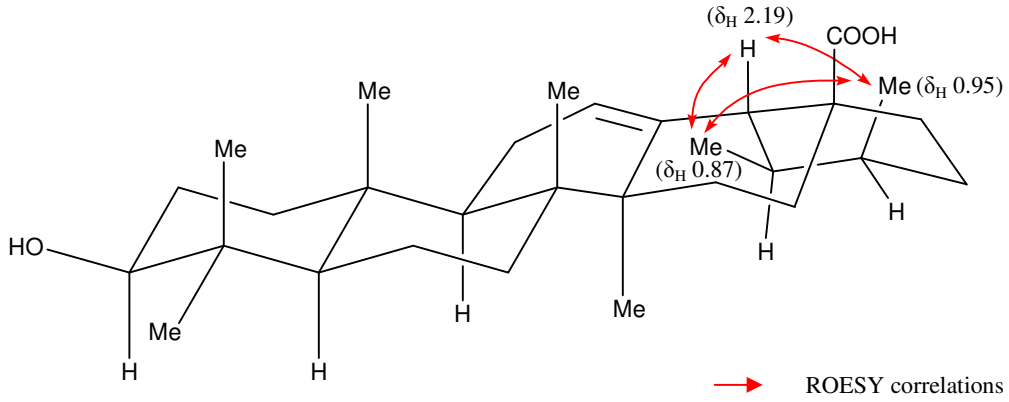

Figure 2.40: Stereochemical assignments of hydrogens at δ_H 0.87 and δ_H 0.95 and δ_H 2.19 for [51] based on ROESY correlations

Table 2.8: ROESY correlations for [51]

Proton	ROESY	Proton	ROESY
$H_{1\alpha}$		$H_{16\alpha}$	H_{19}, $H_{15\beta}$, Me_{27}
$H_{1\beta}$		$H_{16\beta}$	
$H_{2\alpha}$	H_3	H_{18}	H_{12}, Me_{30}, Me_{29}
$H_{2\beta}$	H_3	H_{19}	Me_{27}
H_3	H_5, $H_{2\alpha}$, $H_{2\beta}$, Me_{23}	$H_{21\alpha}$	
H_5	H_3, H_9, Me_{23}	$H_{21\beta}$	
$H_{6\alpha}$		$H_{22\alpha}$	
$H_{6\beta}$		$H_{22\beta}$	
$H_{7\alpha}$		Me_{23}	H_3, H_5
$H_{7\beta}$		Me_{24}	Me_{25}
H_9	H_5, Me_{27}	Me_{25}	Me_{26}, Me_{24}
$H_{11\alpha}$	H_{12}, $H_{1\alpha}$, Me_{26}, Me_{25}	Me_{26}	Me_{25}
$H_{11\beta}$	H_{12}	Me_{27}	$H_{9\alpha}$, $H_{19\alpha}$, $H_{16\alpha}$, Me_{29}
H_{12}	H_{18}, $H_{11\alpha}$, $H_{11\beta}$, Me_{29}	Me_{29}	$H_{18\alpha}$, Me_{27}, Me_{30}
$H_{15\alpha}$		Me_{30}	$H_{18\alpha}$
$H_{15\beta}$	$H_{7\beta}$, $H_{15\alpha}$, $H_{16\alpha}$		

[51] 600MHz (^{1}H): δ (ppm) in CD_3OD

The NMR assignments suggested that compound [51] is 20-*epi*-ursolic acid. As discussed in the ROESY correlations, the methyl group (δ_H 0.95) is positioned above the ring. In comparison, the stereochemistry of the equivalent methyl hydrogens in ursolic acid [15] is inverted.

20-*epi*-Ursolic acid has been prepared synthetically but no ^{13}C NMR data was reported.[46] Therefore, the ^{13}C chemical shifts of compound [51] are compared only with ursolic acid [15]. This is shown in ***Table 2.9***. The ^{13}C chemical shifts for compound [51] are similar but not the same as the literature report on ursolic acid [15].[47] However, compound [51] is not ursolic acid based on the ROESY assignment as discussed, but an isomer of ursolic acid.

Table 2.9: Comparison of the ^{13}C chemical shifts between [51] and ursolic acid [15]

C	δ_C [51]	δ_C [15][47]
C_1	38.6	37.4
C_2	28.4	28.0
C_3	80.2	77.9
C_4	40.3	39.4
C_5	57.2	55.8
C_6	19.9	19.0
C_7	34.8	33.7
C_8	41.3	40.1
C_9	49.5	48.1
C_{10}	40.9	37.6
C_{11}	24.8	23.9
C_{12}	127.4	125.6
C_{13}	140.1	139.2
C_{14}	43.7	42.7
C_{15}	29.7	28.6
C_{16}	25.8	24.8
C_{17}	50.0	47.9
C_{18}	54.8	53.4
C_{19}	40.9	39.55
C_{20}	38.6	39.5
C_{21}	32.2	31.2
C_{22}	40.5	39.3
C_{23}	29.2	29.3
C_{24}	17.1	16.2
C_{25}	16.5	17.9
C_{26}	18.3	18.0
C_{27}	24.6	24.3
C_{28}	182.0	179.3
C_{29}	18.1	17.1
C_{30}	22.0	22.1

An optical rotation of compound [51] was conducted for further confirmation of the structure for [51]. Compound [51] was found to have $[\alpha]_D^{23}$ + 87.2° (c 0.19, methanol), which corresponds with the reported literature on 20-*epi*-ursolic acid with the value of $[\alpha]_D$ + 92°.[46] The optical rotation value for compound [51] is also in the range of the literature reports on ursolic acid.[48,49] However, the actual optical rotation for ursolic acid [15] is inconclusive as there are more than 20 optical rotation values reported, ranging from $[\alpha]_D$ + 21.4°[48] to $[\alpha]_D$ + 126.7°.[48] Therefore, it is hard to compare the optical rotation value of compound [51] with the reported literature on ursolic acid.

From the literature, the melting point for 20-*epi*-ursolic acid has been reported to be 270 – 282 °C.[46] However, this does not correspond with the melting point of compound [51], which is 238 – 240 °C. The melting point of compound [51] is in the range of the literature reports for ursolic acid [15]. Again, the actual melting point of ursolic acid is also inconclusive as there is a wide range of melting point reported in more than 20 literature reports, ranging from 228°C[50] to 307°C[51]. The melting point for the reported 20-*epi*-ursolic acid was also in the range of the melting point for ursolic acid [15][52]. Therefore there is likelihood that compound [51], 20-*epi*-ursolic acid might have a different melting point with the reported literature for 20-*epi*-ursolic acid. There is a possibility that there might be a range of melting point for 20-*epi*-ursolic acid as seen for ursolic acid [15]. Only one literature on 20-*epi*-ursolic acid was reported.[46] Therefore, there is no other comparison that can be made to clarify the melting point of 20-*epi*-ursolic acid to be only in the range of be 270 – 282 °C. In addition, the 20-*epi*-ursolic acid is synthetically made and was not isolated from natural sources.[46] Therefore, there is also a possibility that the melting point might be slightly different.

Despites all the comparison made, the ROESY assignments clearly show the stereochemistry to be that of 20-*epi*-ursolic acid.

Ursolic acid had been previously found in *Scaevola spinescens* and *Scaevola* species. However, the isomer of ursolic acid, 20-*epi*-ursolic acid has not been isolated from *Scaevola spinescens* or any other *Scaevola* species.

2.4.3 Methanol Extract

Fractionation and purification of compounds from methanol extract

A total of 71 g of methanol extract was obtained from the Soxhlet extraction. The methanol extract was then subjected to fractionation and purification by flash column chromatography. Preparative thin layer chromatography (PTLC) was used for futher purification on some of the compounds. The fractionation and purification of compounds from methanol extract are summarized in ***Figure 2.41***. Below are the details of the fractionation and purification of compounds from the methanol extract.

- Three batches (approximately 22 g each) were subjected to flash column chromatography (100 mm column diameter) using a series of increasing polarity solvents to yield 17 fractions, M01-M17 (***Figure 2.41***).

- Fraction M09 (444 mg) was then subjected to further flash column chromatography (30 mm column diameter) using a series of increasing polarity solvents to yield 15 sub-fractions, M0901-M0915 (***Figure 2.41***).

- White amorphous solids precipitated from sub-fractions M0906, M0907, M0908 and M0911. These solids (designated M0906a, M0907a and M0911a respectively) were analyzed using 1D NMR spectrum. Sub-fractions M096a and M0907a were found to have similar NMR spectra. Therefore, only M0906a [53] and M0911a [54] were further analyzed using 2D NMR, melting point, mass spectrometry, FTIR and UV-visible spectroscopy.

- Fraction M10 (367 mg) was subjected to further flash column chromatography (30 mm column diameter) using a series of increasing polarity solvents to yield 10 sub-fractions, M1001-M1010 (***Figure 2.41***).

- Sub-fraction M1004 (19 mg) was then subjected to preparative thin layer chromatography and developed three times using dichloromethane (***Figure 2.41***). Ten bands were observed visually, under UV light and using phosphomolybdic acid (PMA) staining. Each band on the TLC plate was scraped off and the silica of each scraped band was soaked overnight in methanol. The methanol filtrate of each band was then evaporated to dryness. The sample obtained from Band 2 (2 mg) [55], which was only visible under PMA staining on the TLC plate, was analyzed using 2D NMR spectrometer and was found to have similar NMR spectrum to that of sample M0906a [53]. The rest of the samples from other bands were not further analyzed as the amounts obtained were only about 1 mg or less.

Figure 2.41: Fractionation from 71 g of methanol extract

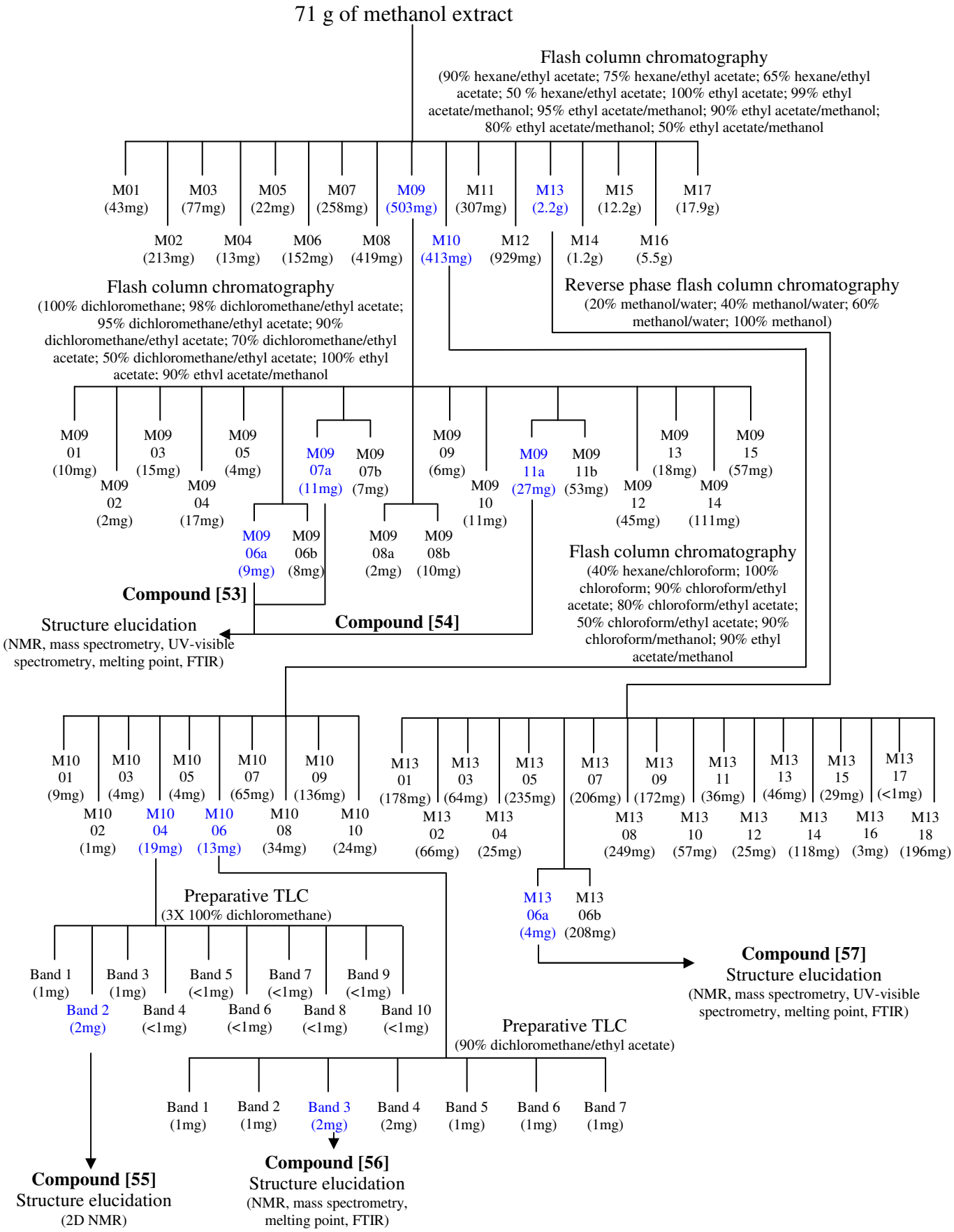

- Fraction M1006 (13 mg) was also subjected to preparative thin layer chromatography using a solvent system of 90% dichloromethane / 10% ethyl acetate (***Figure 2.41***). Seven bands were observed visually using UV light and PMA staining. Each band on the TLC plate was scraped off and the silica of each scraped band was soaked overnight in methanol. The methanol filtrate of each band was then evaporated to dryness. The sample obtained from Band 3 (2 mg) [56] was analyzed using 2D NMR, melting point, mass spectrometry and FTIR. This sample showed blue fluorescence under UV and visible under PMA staining. The rest of the samples from other bands were not further analyzed as the amounts obtained were only about 1 mg.

- Fraction M13 (2.1 g) was subjected to reversed-phase flash column chromatography (40 mm column diameter) using a series of solvents of reducing polarity to yield 18 sub-fractions, M1301-M1318 (***Figure 2.41***).

- A white solid (4 mg) [57] precipitated from fraction M1306a. This sample [57] was further analyzed using 2D NMR, melting point, mass spectrometry, FTIR and UV-visible spectroscopy.

Compounds found in methanol extract

Compound [56]

Compound [56] (2 mg) was isolated as a pale yellow, amorphous solid with a melting point of 170°C. The molecular formula was determined to be $C_{14}H_{14}O_4$ from the molecular ion peak at *m/z* 246.0889 (calculated 246.0892) in the high-resolution EI mass spectrum (HREIMS). This indicated that the compound had eight degrees of unsaturation. The IR spectrum indicated the presence of hydroxyl group(s) as there was an absorption at 3412 cm^{-1}. There was also an aborption at 1708 cm^{-1} which indicated the presence of carbonyl group(s) as well as the presence of double bond group(s) with an absorption at 1598 cm^{-1}.

The ^{13}C and DEPT NMR spectra indicated a total of 14 unique carbons; two methyls (δ_C 24.8, 25.8), one methylene (δ_C 28.6), one sp^3 methine (δ_C 90.9), four sp^2 methines (δ_C 96.7, 111.1, 123.8, 144.7), one quaternary sp^3 carbon (δ_C 69.9) and five quaternary sp^2 carbons (δ_C 112.0,

125.5, 155.0, 160.5, 163.3). All these resonances accounted for a partial molecular formula $C_{14}H_{13}$. The remaining one hydrogen atom and four oxygen atoms suggested the presence of a hydroxyl group. The nine sp^2 carbons (four double-bond functionalities and one carbonyl group) accounted for five degrees of unsaturation. This suggested that the compound contained 3 rings.

All the methyl, methylene and methine carbons identified in the DEPT NMR were assigned to their directly attached hydrogens using the HSQC experiment. The NMR assignments for [56] were mainly based on HMBC, ROESY and COSY (where applicable) correlations. These correlations are shown in ***Table 2.10*** and ***Table 2.11***.

In the COSY spectrum, the methine hydrogen at δ_H 6.20 (δ_C 111.1) showed correlations with the methine hydrogen at δ_H 7.92 (δ_C 144.7). The ^{1}H NMR spectrum showed that both hydrogens at δ_H 6.20 and δ_H 7.92 had a coupling constant (*J*) of 9.0 Hz which indicated a 1,2 orientation between the two hydrogens.

HMBC correlations were observed between the methine hydrogen at δ_H 6.20 (δ_C 111.1) with quaternary carbons at δ_C 112.0 and δ_C 160.50. The chemical shift of the quaternary carbon at δ_C 160.5 which is adjacent to the methine hydrogen at δ_H 6.20, suggested that oxygen group is likely to be attached to this quaternary carbon thereby causing the chemical shift of the adjacent hydrogen to be shifted upfield. Therefore, this accounts for one oxygen group (1st oxygen group). In addition, the hydrogen at δ_H 7.92 (δ_C 144.7) showed HMBC correlations with quaternary carbons at δ_C 112.0, δ_C 155.0 and δ_C 160.5 as well as methine carbon at δ_C 123.8. The chemical shift of a quaternary carbon at δ_C 155.0 suggested that oxygen group is likely to be attached to this quaternary carbon. Therefore, this accounts for another oxygen group (2nd oxygen group). The HMBC correlations between the two hydrogens at δ_H 6.20 and δ_H 7.92 with the quaternary carbons at 112.0, δ_C 155.0 and δ_C 160.5 supported the closure of a ring, thus accounting for one additional degree of unsaturation. Therefore, this accounted for the sixth degree of unsaturation (1st ring). **(*Figure 2.42*)**

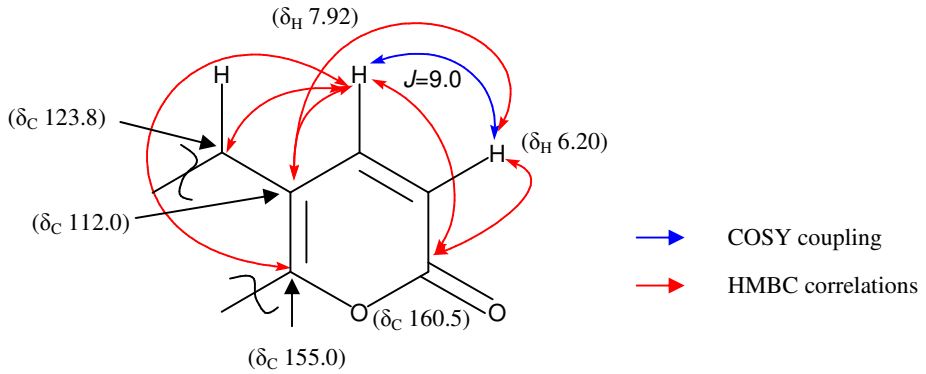

Figure 2.42: Closure of 1st ring for [56] based on COSY and HMBC correlations

In the COSY spectrum, the methine hydrogen at δ_H 7.47 (δ_C 123.8) showed correlations with the hydrogen at δ_H 3.15. The methylene hydrogen at δ_H 3.15 (δ_C 28.6) also had COSY correlations with methine hydrogen at δ_H 4.69 (δ_C 90.9).

HMBC correlations were observed between the methine hydrogen at δ_H 7.47 (δ_C 123.8) with the quaternary carbons at δ_C 155.0 and δ_C 163.3 as well as the methine carbon at δ_C 144.7 and the methylene carbon at δ_C 28.6. The methine hydrogen at δ_H 6.78 (δ_C 96.7) showed HMBC correlations with quaternary carbons at δ_C 112.0, δ_C 125.5, δ_C 155.0 and δ_C 163.3. The HMBC correlations supported the closure of a ring that fused to the 1st ring to form a coumarin system, thus accounting for one additional degree of unsaturation. Therefore, this accounted for the seventh degree of unsaturation (2nd ring). **(*Figure 2.43*)**

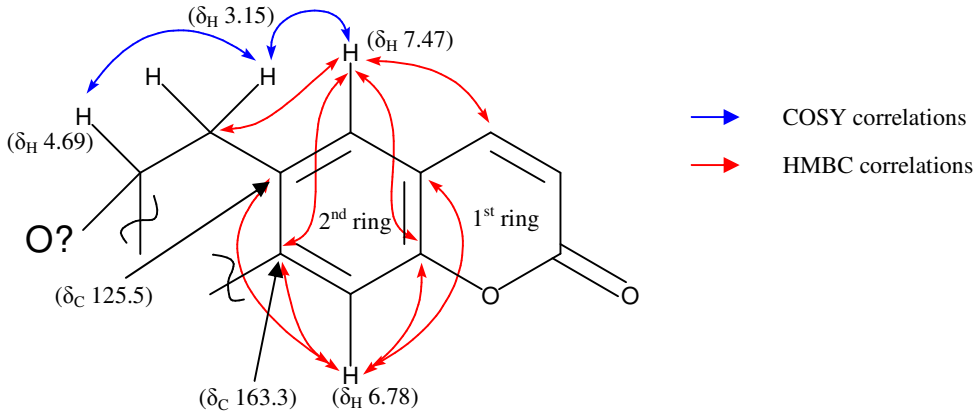

Figure 2.43: Closure of 2nd ring for [56] based on COSY and HMBC correlations

The methine hydrogen at δ_H 4.69 (δ_C 90.9) showed HMBC correlations with two methyl groups at δ_C 24.8 and δ_C 25.8. HMBC correlations were observed between the methylene

hydrogen at δ_H 3.15 with the quaternary carbon at δ_C 69.9 and the methine carbon at δ_C 90.9. The chemical shift of the quaternary carbon at δ_C 69.9 suggested that an oxygen group is likely to be attached to this carbon. Based on the chemical shift of the quaternary carbon at δ_C 69.9 and δ_C 163.3, these carbons are likely to be connected through an oxygen group to form the 3rd ring, which accounted for the eight degree of unsaturation. This oxygen group accounts for the 3rd oxygen group. Therefore, the unassigned oxygen group would be an hydroxyl group. (***Figure 2.44***)

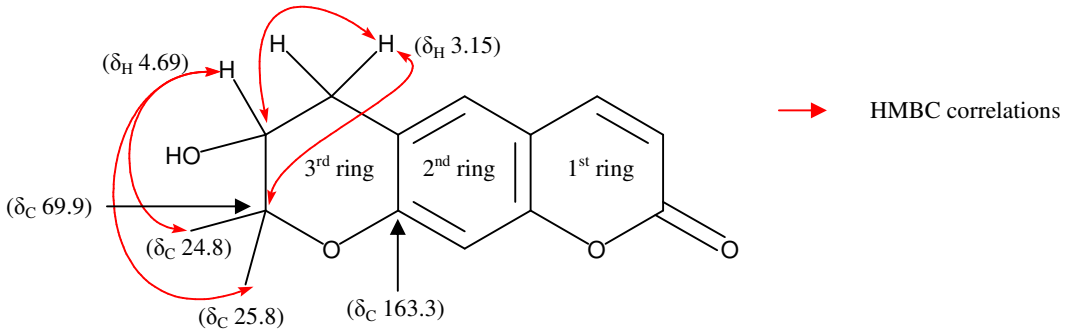

Figure 2.44: Closure of 3rd ring for [56] based on HMBC correlations

Table 2.10: Spectral data for [56]

C	δ_C	H	δ_H	I	M	J(Hz)	COSY	HMBC
C_2	160.5							$H_{3\alpha}$, $H_{4\alpha}$
C_3	111.1	H_3	6.20	1	d	9.0	H_4	C_2, C_{4a}
C_4	144.7	H_4	7.92	1	d	9.0	H_3	C_2, C_{4a}, C_5, C_{10a}
C_{4a}	112.0							$H_{4\alpha}$, $H_{5\alpha}$, $H_{10\alpha}$
C_5	123.8	H_5	7.47	1	s		$H_{6\alpha}$	C_4 C_6 C_{9a} C_{10a}
C_{5a}	125.5							$H_{10\alpha}$
C_6	28.6	$H_{6\alpha}$ $H_{6\beta}$	3.15	2	m		H_5, H_7	C_7, C_8
C_7	90.9	H_7	4.69	1	t	9.0	$H_{6\alpha}$	Me_{11}, Me_{12}
C_8	69.9							
C_{9a}	163.3							$H_{5\alpha}$, $H_{10\alpha}$
C_{10}	96.7	H_{10}	6.78	1	s			C_{4a}, C_{5a}, C_{9a}, C_{10a}
C_{10a}	155.0							$H_{4\alpha}$,$H_{5\alpha}$, $H_{10\alpha}$
C_{11}	25.8	Me_{11}	1.13	3	s			C_7, C_8
C_{12}	24.8	Me_{12}	1.12	3	s			C_7, C_8

[56] 600MHz (^{1}H and ^{13}C): δ (ppm) in d_6-DMSO

I = Integration
M = Multiplicity

In the ROESY spectrum, the methyl hydrogens at δ_H 1.12 showed correlations with the methine hydrogen at δ_H 4.69. The methine hydrogen at δ_H 4.69 had ROESY correlations with the methylene hydrogen at δ_H 3.15. ROESY correlations were also observed between the methine hydrogen at δ_H 7.47 with the methine hydrogen at δ_H 7.92 and the methylene hydrogen at δ_H 3.15. Therefore, all these hydrogens are on the same face of the pyran ring. (***Figure 2.45***) The ROESY correlations are shown in ***Table 2.10***.

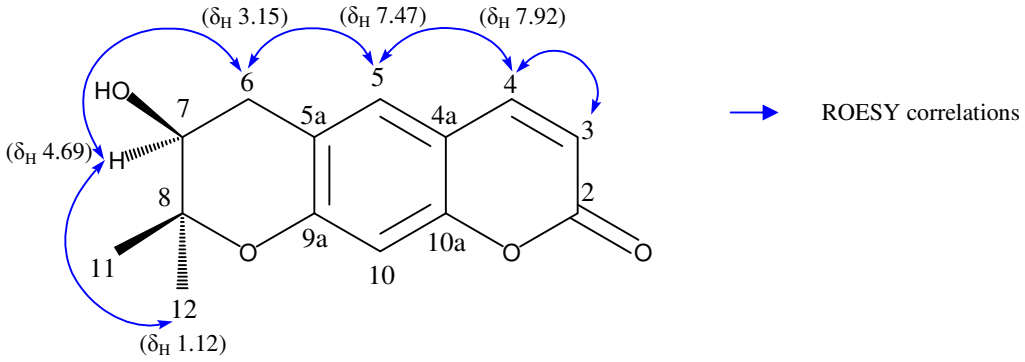

Figure 2.45: ROESY correlations for [56] to show relative stereochemistry

Table 2.11: ROESY correlations for [56]

Proton	ROESY
H_3	H_4
H_4	H_5, H_3
H_5	H_4, H_6, H_6
$H_{6\alpha}$	H_7, Me_{12}
$H_{6\beta}$	H_7, Me_{12}
H_7	H_6, H_6, Me_{12}
H_{10}	
Me_{11}	
Me_{12}	H_6, H_7

[57] 600MHz (^{1}H): δ (ppm) in d_6-DMSO

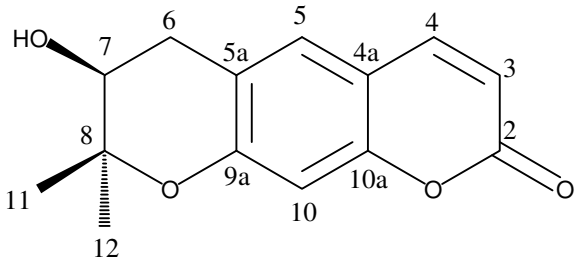

[56]

The NMR assignments confirmed compound [56] to be decursinol [58]. The ^{1}H chemical shifts for fraction M100603 [56] are broadly consistent with one of the literature reports of (-)-

decursinol (***Table 2.12***).[53] The ^{13}C chemical shifts for compound [56] are also broadly consistent with another literature report on (-)-decursinol (***Table 2.13***).[54] Both literature reports are based on NMR spectra obtained in deuterated chloroform. Compound [56] did not dissolve well in either deuterated chloroform or deuterated methanol, therefore this sample was dissolved in deuterated DMSO. Although no direct comparison can be made, the broad consistency of the ^{1}H and ^{13}C chemical shifts between (-)-decursinol and compound [56] supported that compound [56] is decursinol.

The optical rotation for compound [56] was not determined as the sample was insufficient for the experiment. An optical rotation was attempted with the concentration of compound [56] at 0.01g/100mL. However, the results were irreproducible and inconsistent as the sample was clearly too dilute.

Table 2.12: ^{1}H chemical shift values between [56] and [58]

H	δ_H [56]	δ_H [58][53]
Solvent	d_6-DMSO	$CDCl_3$
$H_{3\alpha}$	6.20	6.24
$H_{4\alpha}$	7.92	7.60
$H_{5\alpha}$	7.47	7.30
$H_{6\alpha}$	3.15	3.15
$H_{10\alpha}$	6.78	6.80
$Me_{11/12}$	1.13/1.12	1.34/1.45

[56] 600MHz (^{1}H): δ (ppm) in d_6-DMSO

Table 2.13: ^{13}C chemical shift values between [56] and [58]

C	δ_C [56]	δ_C [58][54]
Solvent	d_6-DMSO	$CDCl_3$
C_2	160.5	161.0
C_3	111.1	112.7
C_4	144.7	142.7
C_{4a}	112.0	112.5
C_5	123.8	128.6
C_{5a}	125.5	116.4
C_6	28.6	30.6
C_7	90.9	68.9
C_8	69.9	78.0
C_{9a}	163.3	156.2
C_{10}	96.7	104.8
C_{10a}	155.0	153.6
C_{11}	25.8	25.1
C_{12}	24.8	21.9

[56] 600MHz (^{1}H and ^{13}C): δ (ppm) in d_6-DMSO

Compound [57]

Compound [57] (4mg) was isolated as a pale yellow, amorphous solid with a melting point of 260 - 265°C. The Negative Ion Atmospheric Pressure Chemical Ionization (APCI) method was used on an LTQ Orbitrap^{TM} mass spectrometer to obtain the negative ion spectrum of this sample. A mass of 447.0936 was determined, indicating a molecular formula of $C_{21}H_{20}O_{11}$. The calculated mass for $C_{21}H_{20}O_{11}$ – H is 447.0927. The molecular formula indicated that the compound had twelve degrees of unsaturation. The absorption at 3451cm^{-1} and 3495 cm^{-1} in the IR spectrum indicated the presence of hydroxyl group(s). The IR spectrum also indicated the presence of a carbonyl group as there was an absorption at 1659 cm^{-1} and a double bond due to the absorption at 1597 cm^{-1} and 1609 cm^{-1}. An absorption in the UV at 352 nm (in methanol) indicated the presence of conjugated double bonds.

The ^{13}C and DEPT NMR spectra indicated a total of 21 unique carbons; one methylene (δc 62.89), five sp^3 methines (δc 71.7, 75.2, 78.3, 78.8, 102.1), six sp^2 methines (δc 96.5, 101.1, 103.5, 106.9, 109.9, 120.6), and nine quaternary sp^2 carbons (δc 107.5, 121.6, 154.8, 159.4, 159.4, 163.3, 165.1, 168.9, 184.4). All these resonances accounted for a partial molecular formula $C_{21}H_{13}$. The remaining seven hydrogen atoms and eleven oxygen atoms suggested the presence of multiple hydroxyl groups. The fifteen sp^2 carbons (seven double-bond functionalities and one carbonyl group) accounted for eight degrees of unsaturation. This suggested that the compound contained 4 rings.

All the methyl, methylene and methine carbons identified in the DEPT NMR were assigned to their directly attached hydrogens using the HSQC experiment. The NMR assignments for [57] were mainly based on HMBC, ROESY and COSY (where applicable) correlations. These correlations are shown in ***Table 2.14*** and ***Table 2.15***.

In the COSY spectrum, the methine hydrogens at δ_H 6.47 (δ_C 101.1) and δ_H 6.80 (δ_C 96.5) showed correlations with each other. The ^{1}H NMR spectrum showed that both methine hydrogens at δ_H 6.47 and δ_H 6.80 had a coupling constant (*J*) of 2.4 Hz. The coupling constant is consistent with a 1,3 orientation for an aromatic system. The chemical shifts of both methine hydrogens, which are shifted upfield, indicate that they are adjacent to electronegative elements. In this case, it would be an oxygen group or groups.

HMBC correlations were observed between the methine hydrogen at δ_H 6.47 (δ_C 101.1) with the quaternary carbons at δ_C 107.5, δ_C 163.3 and δ_C 165.1. In addition, the methine hydrogen at δ_H 6.80 (δ_C 96.5) showed HMBC correlations with the quaternary carbons at δ_C 101.1, δ_C 107.5, δ_C 159.4 and δ_C 165.1. The HMBC correlations as well as the COSY coupling supported the closure of an aromatic ring, thus accounting for one additional degree of unsaturation. Therefore, this accounted for the ninth degree of unsaturation (1st ring).

The chemical shifts of the quaternary carbons at δ_C 159.4, δ_C 163.3 and δ_C 165.1 which are adjacent to the methine hydrogens at δ_H 6.47 and δ_H 6.80, suggested that oxygen groups are likely to be attached to these quaternary carbons thereby causing the chemical shifts of the adjacent methine hydrogens to be shifted upfield by resonance. **(*Figure 2.46*)**

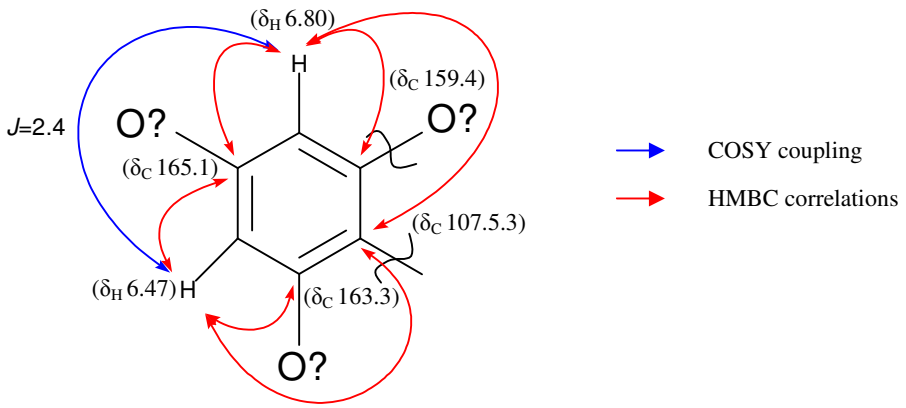

Figure 2.46: Closure of the 1st ring for [57] based on COSY and HMBC correlations

The hydrogen at δ_H 6.56 showed HMBC correlations with quaternary carbons at δ_C 107.5, δ_C 121.6, δ_C 168.9 and δ_C 184.4. The HMBC correlations supported the closure of an additional ring that fused to the 1st ring. Therefore, this ring closure accounted for the tenth degree of unsaturation (2nd ring).

The chemical shift of the quaternary carbon at δ_C 184.4 indicated that it is a carbonyl carbon of a ketone. Therefore, this accounts for one oxygen group (1st oxygen group).

The chemical shift of the quaternary carbon at δ_C 168.9 indicated that an oxygen group is likely to be attached to this quaternary carbon. The chemical shifts for both quaternary carbon

at δ_C 159.4 (from 1st aromatic ring) and δ_C 168.9 (from 2nd aromatic ring) suggested that they are connected through an oxygen group. Therefore, this accounted for another oxygen group (2nd oxygen group). (***Figure 2.47***)

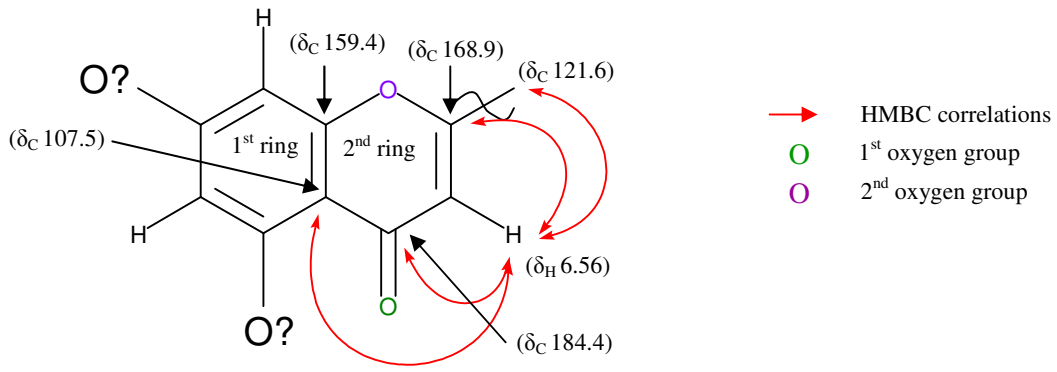

Figure 2.47: Closure of the 2nd ring for [57] based on HMBC correlations

In the COSY spectrum, the methine hydrogen at δ_H 7.36 (δ_C 120.6) showed correlations with the methine hydrogens at δ_H 7.16 (δ_C 106.9) and δ_H 6.68 (δ_C 109.9). The ^{1}H NMR spectrum showed that both methine hydrogens at δ_H 7.36 and δ_H 7.16 had a coupling constant (*J*) of 2.4 Hz, which indicated a 1,3 orientation between these two hydrogens. In addition, the methine hydrogen at δ_H 7.36 also had a coupling constant (*J*) of 8.4 Hz, which indicated a 1,2 orientation between the methine hydrogen at δ_H 7.36 with δ_H 6.68. The chemical shift of the methine hydrogen at δ_H 6.68 and δ_H 7.16 which are slightly upfield indicated that they are close to an electronegative element, an oxygen group or groups.

HMBC correlations are observed between the methine hydrogen at δ_H 7.36 with quaternary carbons at δ_C 106.9, δ_C 121.6 and δ_C 159.4. The methine hydrogen at δ_H 7.16 showed HMBC correlations with quaternary carbons at δ_C 120.6, δ_C 121.6, δ_C 154.8 and δ_C 159.4. The methine hydrogen at δ_H 6.68 showed HMBC correlations with quaternary carbons at δ_C 154.8, δ_C 159.4 and δ_C 168.9. The COSY coupling and HMBC correlations observed among those methine hydrogens supported the closure of an aromatic ring. Therefore, this accounted for the eleventh degree of unsaturation (3rd ring).

The chemical shifts of quaternary carbons at δ_C 154.8 and δ_C 159.4 indicated that oxygen groups are likely to be attached to these quaternary carbons thereby causing the chemical

shifts of the adjacent methine hydrogens (δ_H 7.16 and δ_H 6.68) to be shifted upfield. **(*Figure 2.48*)**

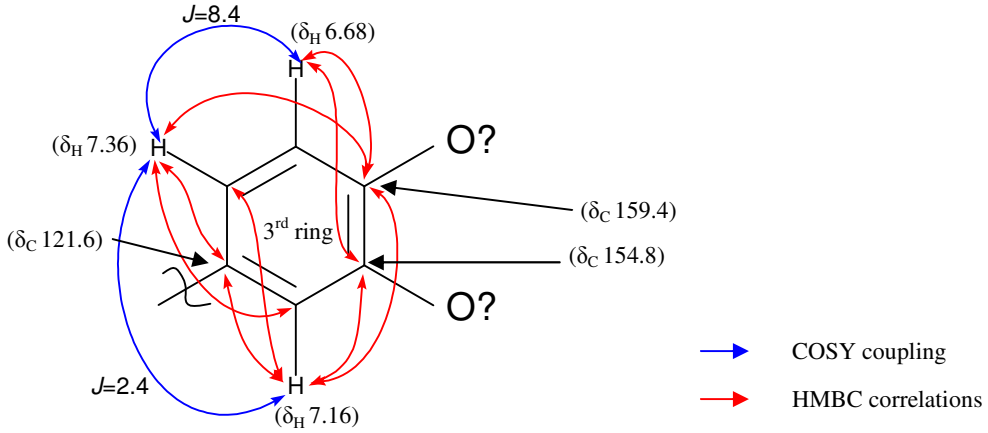

Figure 2.48: Closure of 3rd ring for [57] based on COSY and HMBC correlations

HMBC correlations were observed between the methine hydrogen at δ_H 6.68 with the quaternary carbon at δ_C 168.9 and the methine hydrogen at δ_H 6.56 with quaternary carbon at δ_C 121.6. The HMBC correlation observed showed that the 3rd ring is joined to the 2nd ring through the quaternary carbon at δ_C 121.6 and δ_C 168.9. **(*Figure 2.49*)**

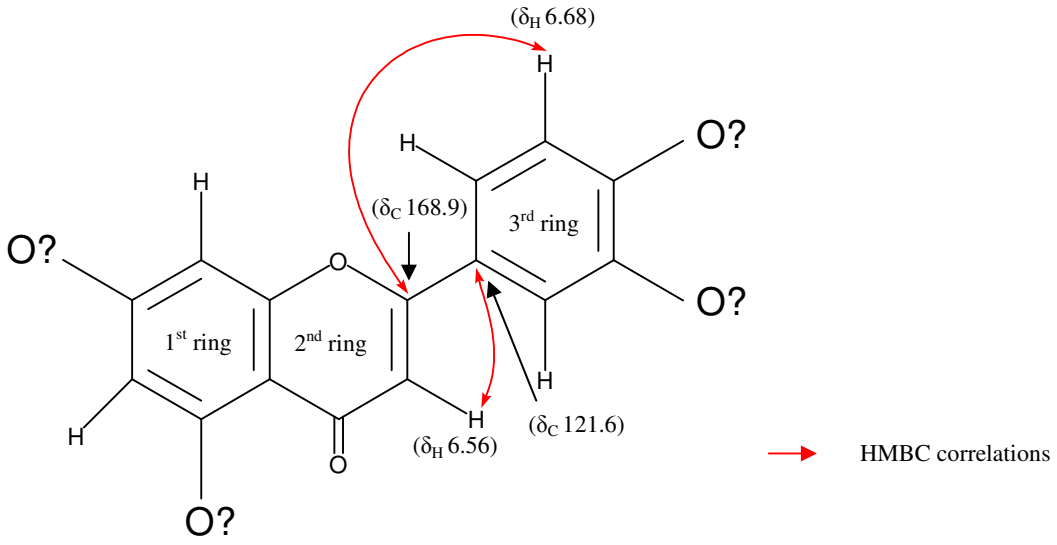

Figure 2.49: Fusing of the 3rd ring to the 2nd ring for [57] based on HMBC correlations

In the COSY spectrum, the methine hydrogen at δ_H 5.06 (δ_C 102.1) had correlations with δ_H 3.48 (δ_C 75.2) which then also had correlations with δ_H 3.49 (δ_C 78.3). The methine hydrogen at δ_H 3.49 also had COSY correlations with δ_H 3.41 (δ_C 71.1) followed by COSY correlations

between hydrogens at δ_H 3.41 and δ_H 3.54 (δ_C 78.8). COSY correlations are also observed between the methine hydrogen at δ_H 3.54 with the methylene hydrogen at δ_H 3.71 (δ_C 62.8).

The chemical shifts of all these hydrogens indicate that they are adjacent to an electronegative element. In this case, it would be multiple oxygen groups. The chemical shifts for δ_H 5.06 (δ_C 102.1), which is shifted downfield compared to the chemical shifts of other hydrogens / carbons indicates two oxygen groups are likely to be attached to this carbon.

HMBC correlations were observed between the hydrogen at δ_H 3.48 (δ_C 75.2) with sp^3 methine carbons at δ_C 102.1 and δ_C 78.3. The methine hydrogen at δ_H 3.49 (δ_C 78.3) showed HMBC correlations with sp^3 methine carbons at δ_C 75.2 and δ_C 71.7. HMBC correlations are also observed between the hydrogen at δ_H 3.41 (δ_C 71.7) with sp^3 methine carbon at δ_C 78.8 and δ_C 62.8 as well as δ_H 3.54 (δ_C 78.8) with an sp^3 methine carbon at δ_C 71.7. The methylene hydrogen at δ_H 3.71 showed HMBC correlations with sp^3 methine carbons at δ_C 71.7 and δ_C 78.8 while the methylene hydrogen at δ_H 3.92 showed HMBC correlations with an sp^3 methine carbon at δ_C 71.7.

The COSY and HMBC correlations observed supported the closure of a ring, which would account for the twelfth degree of unsaturation (4th ring). The ^{1}H NMR showed distinct signals for a sugar unit, possibly a pyranose. This is also supported by the COSY correlations as well as the chemical shifts of the hydrogens. **(*Figure 2.50*)**

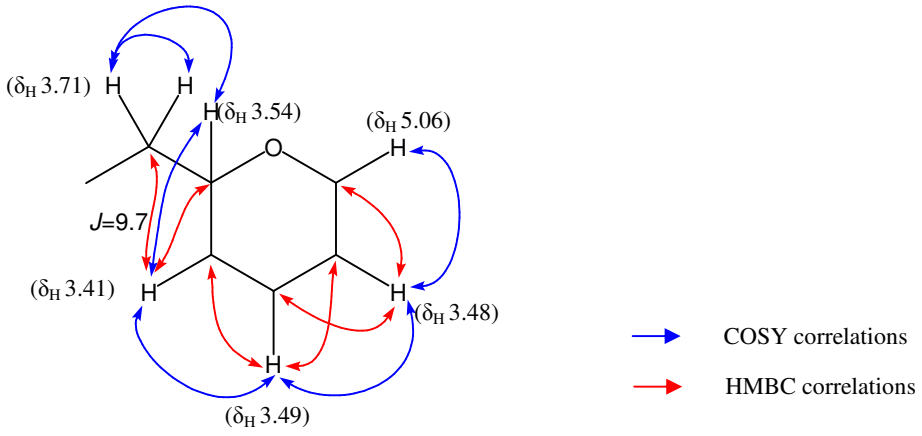

Figure 2.50: Closure of a sugar unit ring for [57] based on COSY coupling

In the ^{1}H NMR spectrum, the methine hydrogen at δ_H 5.06 had a coupling constant (J) of 7.2 Hz which indicates an axial-axial coupling with the methine hydrogen at δ_H 3.48. The methine hydrogen at δ_H 5.06 showed ROESY correlations with methine hydrogens at δ_H 3.49 and δ_H 3.54, indicating that these hydrogens are on the same face of the ring. In the ^{1}H NMR spectrum, the methine hydrogen at δ_H 3.54 appeared to be a multiplet but resolved into doublet of doublet of doublet upon Lorentzian / Gaussian resolution enhancement (LB = -2 and GF = 0.2) using SpinWorks 3 (δ_H 3.54, ddd, J = 2.3, 5.6, 9.7 Hz) (See ***Appendix A***). In the ^{1}H NMR spectrum, the methine hydrogen at δ_H 3.54 had a coupling constant (J) of 9.7 Hz which indicates an axial-axial coupling with methine hydrogen at δ_H 3.41. Therefore, the pyranose sugar could be positively identified as a β-glucoside. The pyranose sugar consists of an oxygen group and four hydroxyl groups. Therefore, this accounts for five oxygen groups (3rd - 7th oxygen group). **(*Figure 2.51*)**

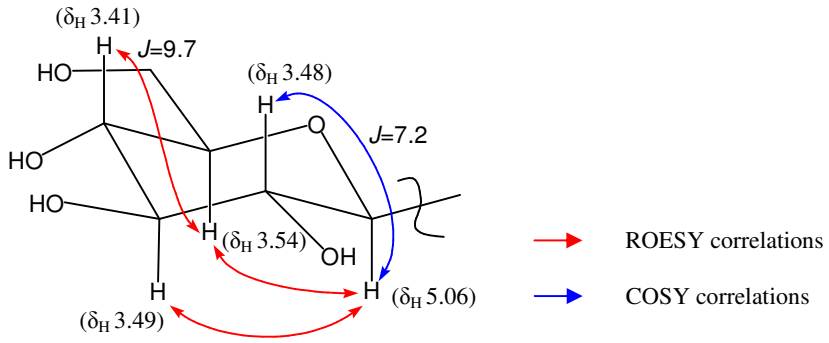

Figure 2.51: Stereochemical assignments for [57] based on ROESY correlations

In the HMBC spectrum, the methine hydrogen at δ_H 5.06 showed HMBC correlation with the methine carbon at δ_C 165.1. The methine hydrogen at δ_H 5.06 also showed ROESY correlations with the methine hydrogens at δ_H 6.47 and δ_H 6.80. Therefore, the 4th ring is connected to the 1st ring through an oxygen group. This oxygen group accounts for the 8th oxygen group. **(*Figure 2.52*)**

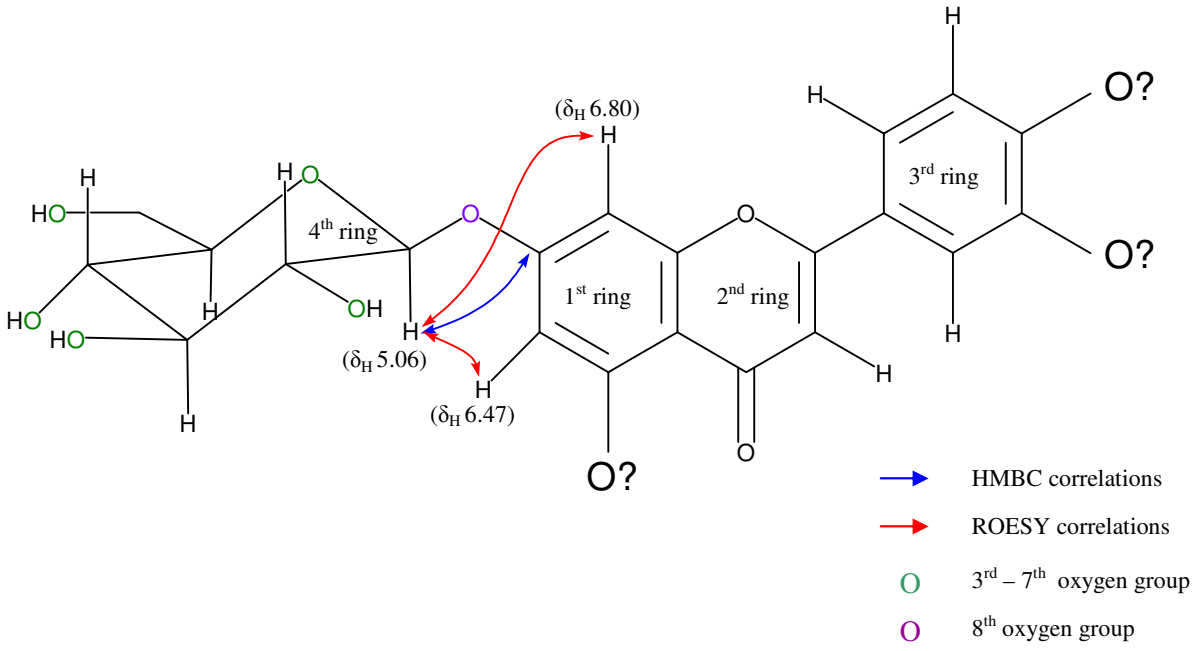

Figure 2.52: Connection between the 4th and the 1st ring for [57] based on ROESY and HMBC correlations

The molecular formula of the four assigned rings accounted for $C_{21}H_{17}O_8$ with three unassigned oxygen group. Therefore, the three unassigned oxygen group would be hydroxyl groups as this would give the exact molecular formula of the compound which is $C_{21}H_{20}O_{11}$.

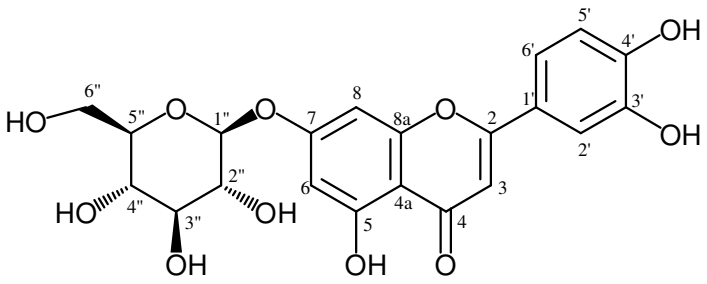

[57]

Table 2.14: Spectral data for [57]

C	δ_C	H	δ_H	I	M	J(Hz)	COSY	HMBC
C_2	168.9							H_3, $H_{2'}$, $H_{6'}$
C_3	103.5	H_3	6.56	1	s			$C_{1'}$, C_2, C_4, C_{4a}
C_4	184.4							H_3
C_{4a}	107.5							H_3, H_6, H_8
C_5	163.3							H_6
C_6	101.1	H_6	6.47	1	d	2.4	$H_{8\alpha}$	C_{4a}, C_5, C_7, C_8
C_7	165.1							H_6, H_8, $H_{1''}$
C_8	96.5	H_8	6.80	1	d	2.4	$H_{6\alpha}$	C_{4a}, C_6, C_7, C_{8a}
C_{8a*}	159.48							H_8
$C_{1'}$	121.6							H_3, $H_{1'}$, $H_{5'}$
$C_{2'}$	106.9	$H_{2'}$	7.16	1	d	2.4	$H_{6'\alpha}$	$C_{1'}$, $C_{3'}$, $C_{4'}$, $C_{6'}$
$C_{3'}$	154.8							$H_{2'}$, $H_{5'}$
$C_{4'*}$	159.46							$H_{2'}$, $H_{5'}$, $H_{6'}$
$C_{5'}$	109.9	$H_{5'}$	6.68	1	d	8.4	$H_{6'\alpha}$	C_2, $C_{3'}$, $C_{4'}$
$C_{6'}$	120.6	$H_{6'}$	7.36	1	dd	2.4, 8.4	$H_{2'\alpha}$, $H_{5'\alpha}$	$C_{1'}$, $C_{2'}$, $C_{4'}$
$C_{1''}$	102.1	$H_{1''}$	5.06	1	d	7.2	$H_{2''\alpha}$	C_7
$C_{2''}$	75.2	$H_{2''}$	3.48	1	m		$H_{1''\alpha}$, $H_{3''\alpha}$	$C_{1''}$, $C_{3''}$
$C_{3''}$	78.3	$H_{2''}$	3.49	1	m		$H_{2''\alpha}$, $H_{4''\alpha}$	$C_{2''}$, $C_{4''}$
$C_{4''}$	71.7	$H_{3''}$	3.41	1	m		$H_{3''\alpha}$, $H_{5''\alpha}$	$C_{5''}$, $C_{6''\alpha}$
$C_{5''}$	78.8	$H_{4''}$	3.54	1	ddd	2.3, 5.6, 9.7	$H_{4''\alpha}$, $H_{6''\alpha}$	$C_{4''}$, $C_{5''}$
$C_{6''}$	62.8	$H_{6''\alpha}$	3.71	1	dd	5.6, 12.0	$H_{5''\alpha}$, $H_{6''\beta}$	$C_{4''}$, $C_{5''}$
		$H_{6''\beta}$	3.92	1	dd	2.3, 12.0	$H_{6''\alpha}$	$C_{4''}$

* Interchangeable [57] 600MHz (^{1}H and ^{13}C): δ (ppm) in CD_3OD

I = Integration

M = Multiplicity

Table 2.15: ROESY correlations for [57]

Proton	ROESY	Proton	ROESY
H_3	$H_{2'}$, $H_{6'}$	$H_{2''}$	
H_6	$H_{1''}$	$H_{3''}$	$H_{1''}$
H_8	$H_{1''}$	$H_{4''}$	
$H_{2'}$	H_3	$H_{5''}$	$H_{1''}$
$H_{5'}$	$H_{6'}$	$H_{6''\alpha}$	$H_{6''\beta}$
$H_{6'}$	H_3, $H_{5'}$	$H_{6''\beta}$	$H_{5''}$, $H_{6''\alpha}$
$H_{1''}$	$H_{3''}$, $H_{5''}$		

[57] 600MHz (^{1}H): δ (ppm) in CD_3OD

The NMR assignments confirmed that compound [57] is luteolin-7-*O*-glucoside [44]. This compound has been previously isolated from *Scaevola spinescens* by Nobbs.[6] Comparison of the ^{13}C chemical shifts values for compound [57] with other literature reports of luteolin-7-*O*-glucoside [44] has been done and these are shown in **Table 2.16**. They have similar ^{13}C chemical shifts but not identical as the solvents used are different. Four out of the five previous reports used d_6-DMSO and one of the reports is based on pyridine-d_5 + D_2O solvent. Therefore, no direct comparison can be made. However, the similar ^{13}C chemical shifts as well as the NMR assignments are consistent with the structure of luteolin-7-*O*-glucoside [44].

Table 2.16: ^{13}C chemical shift values between [57] and [44]

C	δ_C [57]	δ_C [44][6]	δ_C [44][55]	δ_C [44][56]	δ_C [44][57]	δ_C [44][58]
Solvent	CD_3OD	d_6-DMSO	d_6-DMSO	d_6-DMSO	d_6-DMSO	pyridine-d_5 + D_2O
C_2	168.9	164.4	164.9	164.9	164.5	164.2
C_3	103.5	103.1	103.6	103.3	103.2	104.4
C_4	184.4	181.8	182.4	182.2	181.6	183.3
C_{4a}	107.5	105.2	105.8	105.6	105.5	106.9
C_5	163.3	161.0	161.6	161.4	161.1	162.5
C_6	101.1	99.4	100.0	99.8	99.7	101.02
C_7	165.1	162.9	163.4	163.27	162.9	166.0
C_8	96.5	94.6	95.2	95.0	94.9	96.2
C_{8a}	159.4*	156.8	157.4	157.2	156.9	158.2
$C_{1'}$	121.6	121.2	121.8	121.3	121.6	123.0
$C_{2'}$	106.9	113.5	114.0	113.7	113.7	115.0
$C_{3'}$	154.8	145.7	146.3	146.2	145.7	147.9
$C_{4'}$	159.4*	149.9	150.4	150.8	149.7	152.0
$C_{5'}$	109.9	115.9	116.5	116.3	116.0	117.3
$C_{6'}$	120.6	119.1	119.7	119.5	119.0	120.3
$C_{1''}$	102.1	100.0	100.3	100.2	100.0	102.0
$C_{2''}$	75.2	73.0	73.8	73.4	73.2	74.8
$C_{3''}$	78.3	76.3	76.8	76.7	76.5	78.1
$C_{4''}$	71.7	69.5	70.0	69.9	69.7	71.4
$C_{5''}$	78.8	77.1	77.6	77.5	77.2	75.9
$C_{6''}$	62.8	60.5	61.1	60.9	60.8	65.6

[57] 600MHz (^{13}C): δ (ppm) in CD_3OD

* Assignments may be reversed

2.4.4 Aqueous Extracts

Fractionation and purification of compounds from aqueous extract

A total of 46 g of aqueous extract was obtained from the decoction method and 71 g of aqueous extract from Soxhlet extraction. Each of these aqueous extracts were then separately dissolved in 70% v/v methanol before being subjected to liquid-liquid partitioning with hexane, followed by dichloromethane and ethyl acetate. Each of the aqueous extracts was partitioned twice with each of the solvents to increase the yield of partitioned products.

Aqueous extract (decoction)

Liquid-liquid partitioning of the aqueous extract from the decoction method gave 21 mg of hexane extract, 1.2 g of dichloromethane extract and 7.6 g of ethyl acetate extract. Evaporation of the aqueous methanol extract gave 33.5 g. The fractionation and purification of compounds from each of the partitioned extracts are summarized in ***Figure 2.53***. Below are the details of the fractionation and purification of compounds from each of the partitioned extracts.

- The dichloromethane extract (1.2 g) from the partitioning was subjected to reversed-phase flash column chromatography (40 mm column diameter) using a series of decreasing polarity solvents to yield 10 fractions, Aq(Dct)D01-Aq(Dct)D10 (***Figure 2.53***).

- The ethyl acetate extract (7.6 g) from the partitioning was subjected to reversed-phase column chromatography (40 mm column diameter) using a series of decreasing polarity solvents to yield 11 fractions, Aq(Dct)EA01-Aq(Dct)EA11 (***Figure 2.53***).

- The aqueous methanol residue (33.5 g) from the partitioning was subjected to reversed-phase column chromatography (40 mm column diameter) using a series of decreasing polarity solvents to yield 11 fractions, Aq(Dct)AM01-Aq(Dct)AM11 (***Figure 2.53***).

Figure 2.53: Fractionation from 46 g of decoction aqueous extract

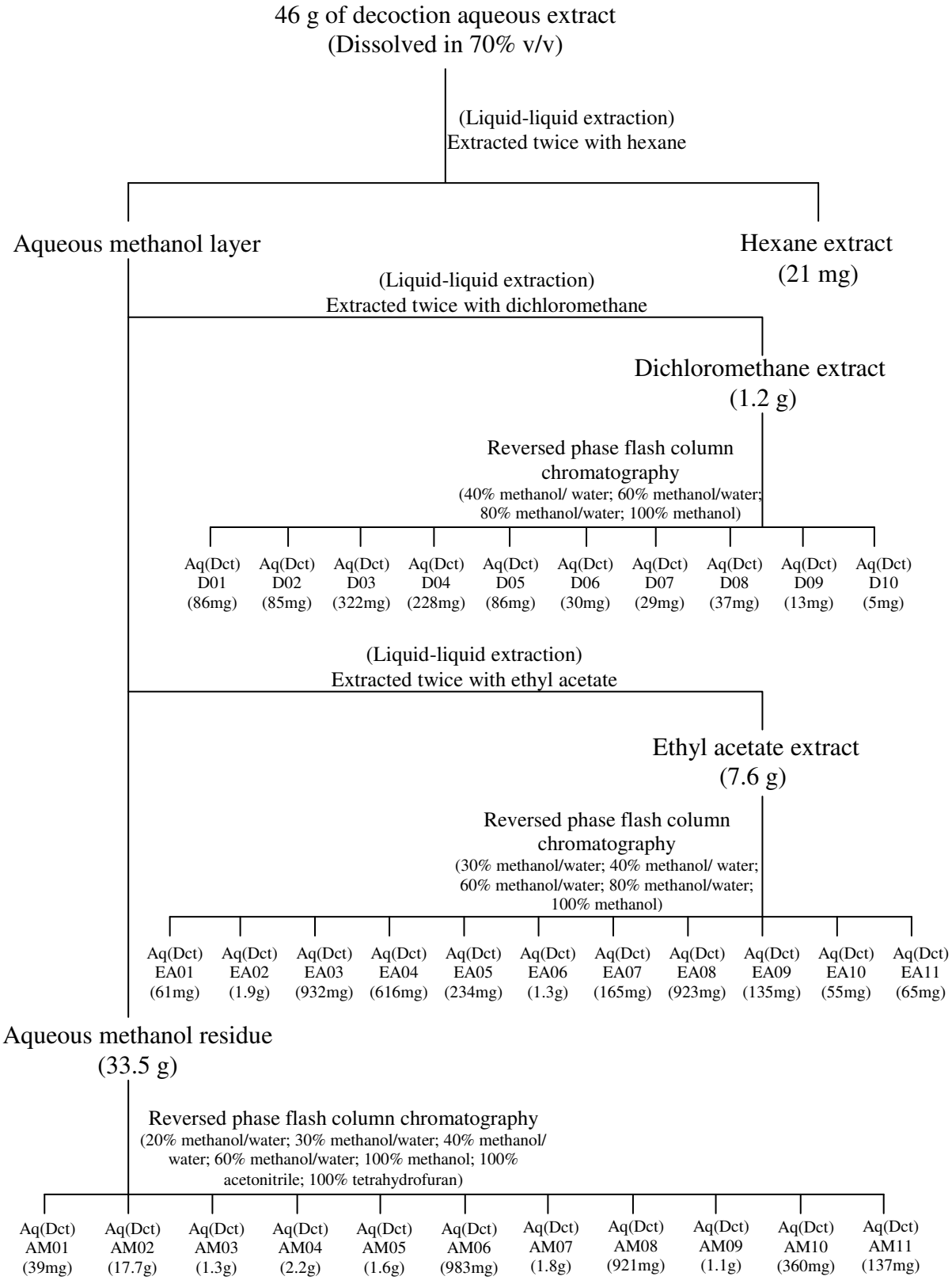

Aqueous extract (soxhlet)

Liquid-liquid partitioning of the aqueous extract from the Soxhlet method gave 27 mg of hexane extract, 1.9 g of dichloromethane extract, 6.2 g of ethyl acetate extract and 52 g of aqueous methanol residue upon evaporation. The fractionation and purification of compounds from each of the partitioned extracts are summarized in ***Figure 2.54***. Below are the details of the fractionation and purification of compounds from each of the partitioned extracts.

- The dichloromethane extract (1.9 g) from the partitioning was subjected to reversed-phase flash column chromatography (40 mm column diameter) using a series of decreasing polarity solvents to yield 14 fractions, Aq(Sox)D01-Aq(Sox)D14 (***Figure 2.54***). When solution of fraction Aq(Sox)D02 was left standing, colourless solids [59] (15 mg) crystallized out of solution. Only the ^{1}H NMR spectrum was acquired for compound [59].

- The ethyl acetate extract (6.2 g) from the partitioning was subjected to reversed-phase flash column chromatography (40 mm column diameter) using a series of decreasing polarity solvents to yield 11 fractions, Aq(Sox)EA01-Aq(Sox)EA11 (***Figure 2.54***). When solution of fraction Aq(Sox)EA02 was left standing, colourless solids [60] (125 mg) crystallized out of solution. Therefore, the colourless solids [60] was further analyzed using 2D NMR, melting point, mass spectrometry, FTIR and UV-visible spectroscopy to determine the structure. Compound [60] was found to have a similar ^{1}H NMR with compound [59].

- The aqueous methanol residue (52 g) from the partitioning was subjected to reversed-phase flash column chromatography (40 mm column diameter) using a series of decreasing polarity solvents to yield 11 fractions, Aq(Sox)AM01-Aq(Sox)AM11 (***Figure 2.54***).

Figure 2.54: Fractionation from 71 g of Soxhlet aqueous extract

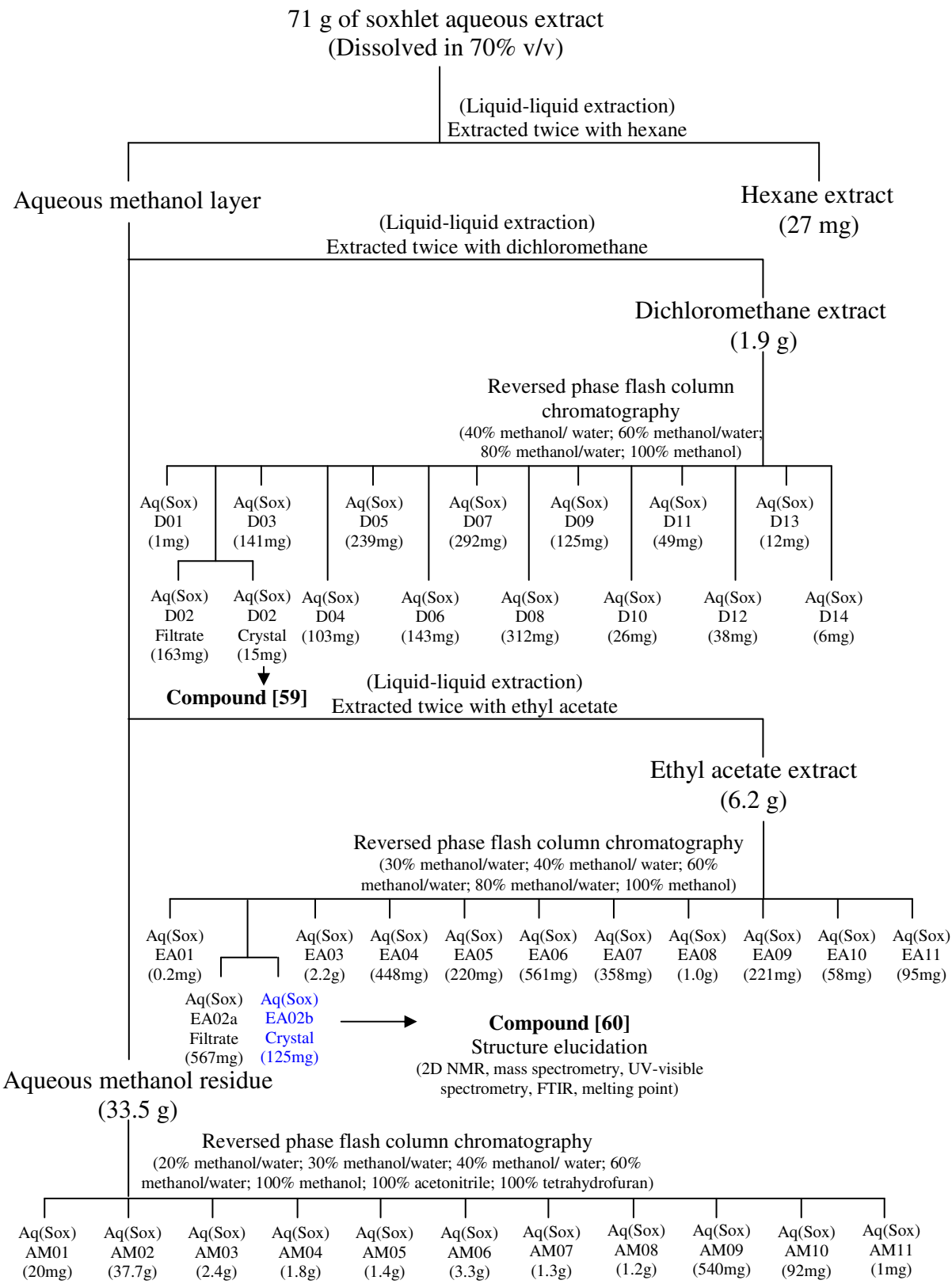

Compounds found in aqueous extracts

Compound [60]

Compound [60] (26 mg) was isolated as colourless crystals with a melting point of 230 - 233°C. Positive ion electrospray ionization mass spectrometry (ESI-MS) showed a mass at 166.0751. The calculated mass of $C_6H_{12}O_5$ + H is 165.0762, which supported the mass obtained from positive ion ESI-MS. This indicated that the compound had one degree of unsaturation. The adsorption at 3306 cm^{-1} in the IR spectra indicated the presence of hydroxyl group(s).

The ^{13}C and DEPT NMR spectra indicated a total of 6 unique carbons; one methylene (δ_C 35.20) and five sp^3 methines (δ_C 70.52, 70.83, 72.90, 74.17, 76.49). All these resonances accounted for a partial molecular formula C_6H_7. The remaining five hydrogen atoms and five oxygen atoms suggested the presence of hydroxyl groups. This is supported by the infrared spectra.

All the methyl, methylene and methine carbons identified in the DEPT NMR were assigned to their directly attached hydrogens using the HSQC experiment. The NMR assignments for [60] were mainly based on COSY coupling. These correlation are shown in ***Table 2.17***.

In the COSY spectrum, the methylene hydrogens at δ_H 1.86 and δ_H 2.04 (δ_C 35.2) showed coupling with each other. Both methylene hydrogens also coupled with δ_H 4.07 (δ_C 70.5) and δ_H 3.80 (δ_C 70.8). The methylene hydrogen at δ_H 2.04 (δ_C 35.2) also coupled with δ_H 3.98 (δ_C 74.1). COSY couplings were also observed between the methine hydrogen at δ_H 4.07 with δ_H 3.98, δ_H 1.86 and δ_H 2.04, as well as δ_H 3.98 with δ_H 3.76 and δ_H 2.04. The methine hydrogen at δ_H 3.80 showed COSY couplings with the hydrogens at δ_H 3.62, δ_H 1.86 and δ_H 2.04. COSY couplings were also observed between the methine hydrogens at δ_H 3.76 (δ_C 72.9) and δ_H 3.62 (δ_C 76.4). The COSY spin system data supported the closure of a ring. Therefore, it accounted for one degree of unsaturation. **(*Figure 2.55*)**

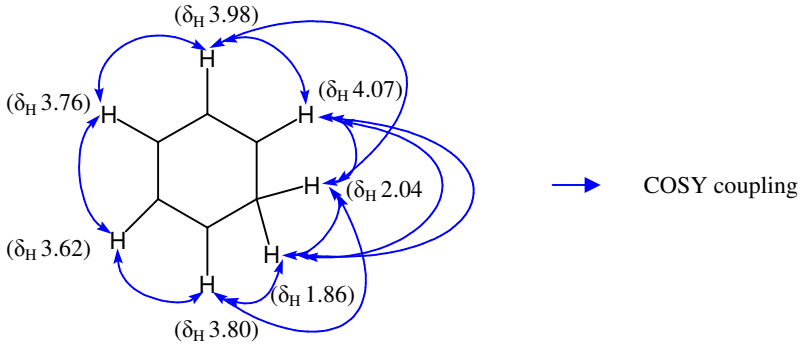

Figure 2.55: Closure of a ring for [60] based on COSY coupling

The coupling constants for the hydrogens can be used to determine the relative stereochemistry of the assigned signals. The ^{1}H NMR spectrum shows that the methine hydrogen at δ_H 3.76 had a coupling constant (*J*) of 9.6 Hz with the hydrogen at δ_H 3.62, indicating that these two hydrogens are in an axial-axial relationship. The coupling constant of 9.6 Hz and 11.5 Hz for the methine hydrogen at δ_H 3.80 indicated axial-axial coupling with both hydrogens at δ_H 1.86 and δ_H 3.62. Since the methylene hydrogen at δ_H 1.86 has been assigned as axial, therefore, the geminal methylene hydrogen at δ_H 2.04 must be equatorial. The coupling constant of 14.4 Hz between the methylene hydrogens at δ_H 1.86 and δ_H 2.04 a supported a 2*J* geminal coupling. In the ^{1}H NMR spectrum, the methine hydrogen at δ_H 4.07 had a coupling constant (*J*) of 3.6 Hz with both methylene hydrogens. This indicated that the methine hydrogen at δ_H 4.07 is in an equatorial position as it supported the equatorial-equatorial coupling constant with the methylene hydrogen at δ_H 2.04 and axial-equatorial coupling constant with the methylene hydrogen at δ_H 1.86. The methine hydrogen at δ_H 3.98 is the last hydrogen to be assigned, either axial or equatorial. The ^{1}H NMR spectrum shows that the methine hydrogen at δ_H 3.98 had a coupling constant (*J*) of 3.6 Hz with the methine hydrogens at δ_H 3.76 and δ_H 4.07. Therefore, the methine hydrogen at δ_H 3.98 has to be equatorial as it supported the equatorial-equatorial relationship with the methine hydrogen at δ_H 4.07 and axial-equatorial relationship with the methine hydrogen at δ_H 3.76. This is also supported by the long range coupling constant of 1.2 Hz between the two hydrogens at δ_H 3.98 and δ_H 2.04. (***Figure 3.56***)

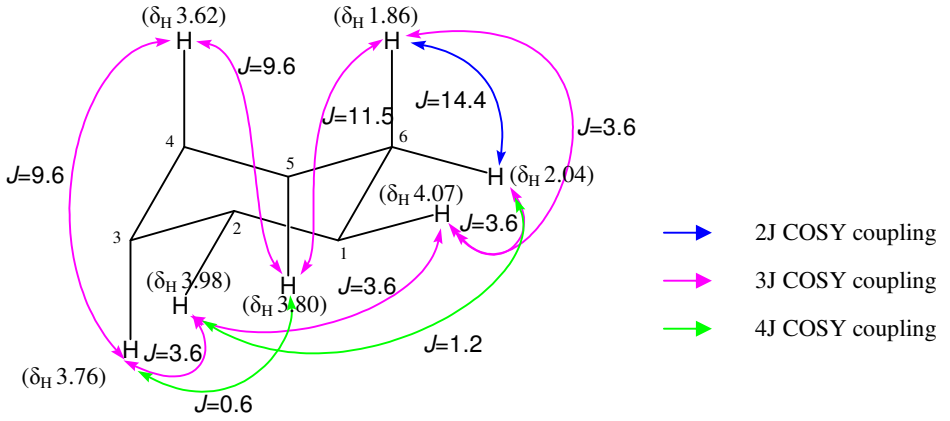

Figure 2.56: Assignment of relative stereochemistry for [60] based on COSY coupling

Thus, the overall structure of compound [60] can be illustrated in two different representations that are shown in ***Figure 2.57***.

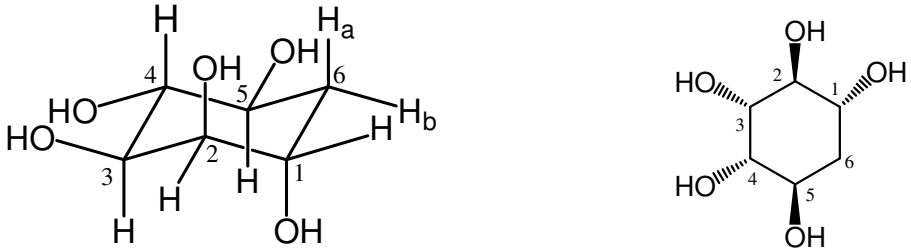

[60]

Figure 2.57: Different representations indicating the relative stereochemistry for [60]

Table 2.17: Spectral data for [60]

C	δ_C	H	δ_H	I	M	*J*(Hz)	COSY	HMBC
C_1	70.5	$H_{1\alpha}$	4.07	1	q	3.6	$H_{2\alpha}$, $H_{6\alpha}$, $H_{6\beta}$	C_2, C_3, C_5
C_2	74.1	$H_{2\alpha}$	3.98	1	td	1.2, 3.6	$H_{1\alpha}$, $H_{3\alpha}$, $H_{6\beta}$	C_1, C_3, C_4, C_6
C_3	72.9	$H_{3\alpha}$	3.76	1	ddd	0.6, 3.6, 9.6	$H_{2\alpha}$, $H_{4\alpha}$	C_4, C_5
C_4	76.4	$H_{4\alpha}$	3.62	1	t	9.6	$H_{3\alpha}$, $H_{5\alpha}$	C_3, C_5, C_6
C_5	70.8	$H_{5\alpha}$	3.80	1	dddd	0.6, 4.8, 9.6, 11.5	$H_{4\alpha}$, $H_{6\alpha}$, $H_{6\beta}$	C_4, C_6
C_6	35.2	$H_{6\alpha}$	1.86	1	ddd	3.6, 11.5, 14.4	$H_{1\alpha}$, $H_{5\alpha}$, $H_{6\beta}$	C_1, C_4, C_5
		$H_{6\beta}$	2.04	1	dddd	1.2, 3.6, 4.8, 14.4	$H_{1\alpha}$, $H_{2\alpha}$, $H_{5\alpha}$, $H_{6\alpha}$	C_1, C_2, C_4, C_5

[60] 600MHz (^{1}H and ^{13}C): δ (ppm) in D_2O

I = Integration
M = Multiplicity

The NMR assignments suggested that compound [60] is 2-*deoxy*-chiro-inositol. An optical rotation of compound [60] was conducted for further confirmation of the structure for [60]. Compound [60] was found to have $[\alpha]_D^{22.5}$ + 23.6° (c 0.22, water), which corresponds with the reported literature on 2-*deoxy*-D-chiro-inositol with the value of $[\alpha]_D$ + 23.2°.[59] This compound had previously been isolated from *Scaevola spinescens* by Nobbs.[6] The melting point range also matches the values found in Nobbs's thesis as well as in the literature.[6,60] Thefore, these confirmed that compound [60] can be identified as 2-*deoxy*-D-chiro-inositol.

CHAPTER 3

Antibacterial Assay

3.1 Introduction

The in vitro antibacterial activity of the plant extracts was determined using a broth micro-dilution assay based on minimum inhibitory concentration (MIC) and minimum bactericidal concentrations (MBC). MIC is the lowest concentration of antibacterial agent that completely inhibits the growth of microorganism in the micro-dilution wells as detected by the unaided eye after overnight incubation.[61] Once an MIC has been performed, MBC can subsequently be determined. MBC is the lowest concentration of antibacterial agent that has bacterial killing effects. Gram-positive and Gram-negative bacteria were used for antibacterial testing.

The Gram-positive bacteria used for antibacterial testing were *Staphylococcus aureus* (ATCC 25923) and *Streptococcus pyogenes* (ATCC 10389). *Escherichia coli* (ATCC 25922) and *Pseudomonas aeruginosa* (ATCC 27853) were the Gram-negative bacteria used for antibacterial testing. The selection of these Gram-positive and Gram-negative bacteria are based on the uses of the plant by the Aboriginal people. These bacteria are commonly found in many important human diseases. *Staphylococcus aureus* and *Streptococcus pyogenes* are the cause of many human diseases ranging from mild skin infections to life-threatening systemic diseases.[62,63] Previous research done on childhood infections in tropical north Australia showed that these bacteria are also important pathogens in indigenous communities.[64] *Escherichia coli* and *Pseudomonas aeruginosa* can cause a variety of different types of infections including urinary tract infections (UTIs).[62] UTIs, predominantly caused by *Escherichia coli* are the most common bacterial infections found in most women nowadays.[65,66] Besides that, *Escherichia coli* is also an important pathogen in the general community and indigenous communities, causing infectious diarrhea.[64]

Ampicillin was used as a known inhibitor in the assay with an MIC of 0.5 – 2.0 µg/mL against *Staphylococcus aureus* (ATCC 25923), which was in accordance with published reference ranges for *Staphylococcus aureus* (ATCC 29213) and 0.06 – 0.25 µg/mL against *Streptococcus pyogenes* (ATCC 10389), which was in accordance with published reference ranges for *Streptococcus pneumoniae* (ATCC 49619).[67] Gentamicin was used as a known inhibitor in the assay with an MIC of 0.65 µg/mL against *Escherichia coli* (ATCC 25922) and 1.30 µg/mL against *Pseudomonas aeruginosa* (ATCC 27853), which was in accordance with published reference ranges for these strains.[67]

The scoring of good antibacterial activity for the extracts tested in this research is based on the criteria for 'activity' in the review of Cos *et al.*[68] A stringent criteria for activity is set to IC_{50} values below 100 µg/mL for extracts and below 25 µM for pure compounds.[68] Therefore, any antibacterial activity observed below 100 µg/mL is considered good. This value was used as a general guideline as there are other criteria such as the microorganism used, which can also affect the antibacterial activity. Different pathogens have specific sensitivities to the aspecific or toxic action of chemical molecules.[68]

All the extracts (depending on the availability of the extracts) isolated in this thesis were tested for antibacterial activity using the broth micro-dilution assay to determine the MIC and subsequently the MBC on the selected extracts or compounds that showed promising antibacterial activity (***Table 3.1***).

Table 3.1: Antibacterial testing on the crude extracts of *Scaevola spinescens* (Activities reported in µg/mL)

Crude extract	Microorganism							
	Staphylococcus aureus ATCC 25923		*Streptococcus pyogenes* ATCC 10389		*Escherichia coli* ATCC 25922		*Pseudomonas aeruginosa* ATCC 27853	
	MIC	MBC	MIC	MBC	MIC	MBC	MIC	MBC
Hexane	NA	NA	500	1000	NA	NA	NA	NA
Ethyl acetate	1000	1000	250-500	500	NA	NA	NA	NA
Methanol	NA	NA	4000	4000	NA	NA	NA	NA
Aqueous (Soxhlet)	NA	NA	NA	NA	NA	NA	NA	NA
Aqueous (Decoction)	NA	NA	NA	NA	NA	NA	NA	NA

NA : No activity

3.2 Hexane Extract

The crude hexane extract showed activity against *Streptococcus pyogenes* (ATCC 10389) with MIC at 500 µg/mL and MBC at 1000 µg/mL. This suggested that the bacteria might be inhibited but not killed at the concentration of 500 µg/mL. No activity was observed against *Staphylococcus aureus* (ATCC 25923), *Escherichia coli* (ATCC 25922) and *Pseudomonas aeruginosa* (ATCC 27853) at a maximum concentration of 1000 µg/mL (***Table 3.1***).

Twenty-two fractions (H01-H22) were isolated by flash column chromatography of the hexane crude extract. However, not all of the hexane fractions were tested against *Streptococcus pyogenes* (ATCC 10389) due to insufficient amount of samples for testing. Only the first nine fractions (H01-H09) were tested for antibacterial activity against *Streptococcus pyogenes* (ATCC 10389) (***Figure 3.1***). The remaining thirteen fractions were not tested as those samples have been used for further chromatographic fractionation. Among the nine fractions tested for antibacterial activity against *Streptococcus pyogenes* (ATCC 10389), only sample H04 was found to be active with MIC at 500 -1000 µg/mL (***Figure 3.1***). The MIC value was still above the criteria for good activity (100 µg/mL). Therefore, no further investigation was done on sub-fractions from sample H04.

Figure 3.1: Antibacterial testing on the crude extract of hexane as well as its sub-fractions (MIC value) (MBC value)

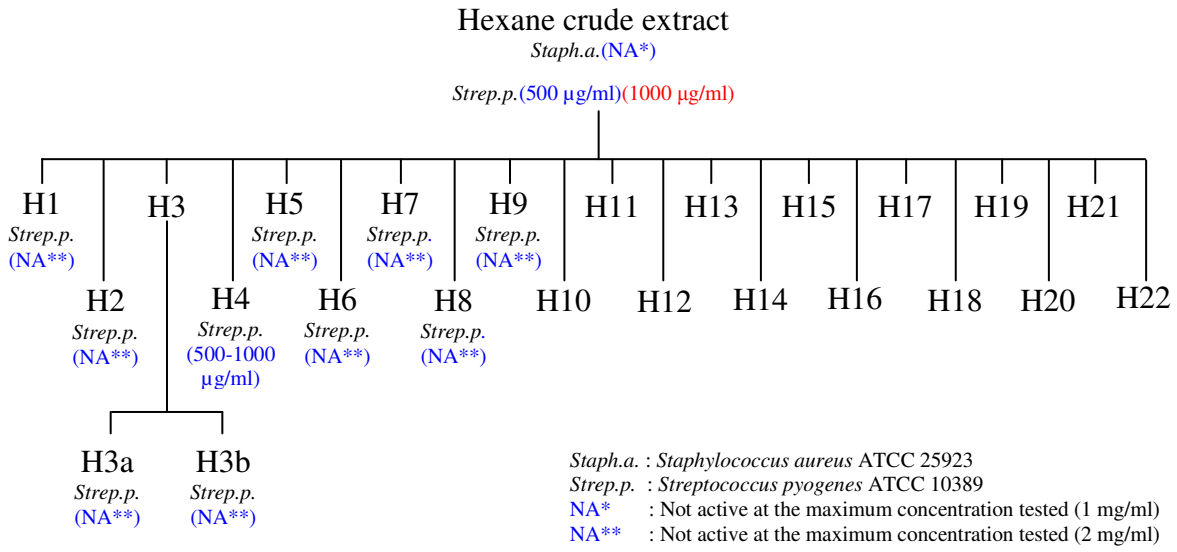

3.3 Ethyl acetate Extract

The crude ethyl acetate extract showed activity against both Gram-positive bacteria. Both MIC and MBC observed against *Staphylococcus aureus* (ATCC 25923) was 1000 µg/mL. This indicated that 1000 µg/mL of ethyl acetate crude extract had a bactericidal effect on *Staphylococcus aureus* (ATCC 25923). The MIC of the extract against *Streptococcus pyogenes* (ATCC 10389) was between 250 – 500 µg/mL with MBC observed at 500 µg/mL. There was no antibacterial activity observed against either of the Gram-negative bacteria at a maximum concentration of 1000 µg/mL (***Table 3.1***). Based on the assay, the ethyl acetate extract has better bactericidal effect against *Streptococcus pyogenes* (ATCC 10389). Therefore, the ethyl acetate fractions isolated from flash column chromatography were tested only against *Streptococcus pyogenes* (ATCC 10389).

A total of twenty-six fractions (See **Chapter** 2) were isolated from the two batches of ethyl acetate crude extract using flash column chromatography. However, only sixteen out of twenty-six ethyl acetate fractions were tested against *Streptococcus pyogenes* (ATCC 10389) for any antibacterial activity at a maximum concentration of 2000 µg/mL (***Figure 3.2***). The selection of samples to be tested was based on the amount available for testing. Some of the samples are insufficient for testing as they have been used for further chromatographic fractionation.

Among the sixteen fractions tested, fraction EA10, EA11 and EA12 showed good antibacterial activity against *Streptococcus pyogenes* (ATCC 10389) with MIC ranging from 62.5 – 250 µg/mL (***Figure 3.2***). These three fractions were then tested against *Staphylococcus aureus* (ATCC 25923) at a maximum concentration of 4000 µg/mL. Only fraction EA12 showed antibacterial activity against *Staphylococcus aureus* (ATCC 25923) with an MIC of 4000 µg/mL. The results show that these fractions have better antibacterial activity against *Streptococcus pyogenes* (ATCC 10389) compared to *Staphylococcus aureus* (ATCC 25923). Therefore, the sub-fractions of these three fractions were further tested only against *Streptococcus pyogenes* (ATCC 10389) (***Figure 3.2***).

Figure 3.2: Antibacterial testing on the crude extract of ethyl acetate as well as its sub-fractions (MIC value)(MBC value)

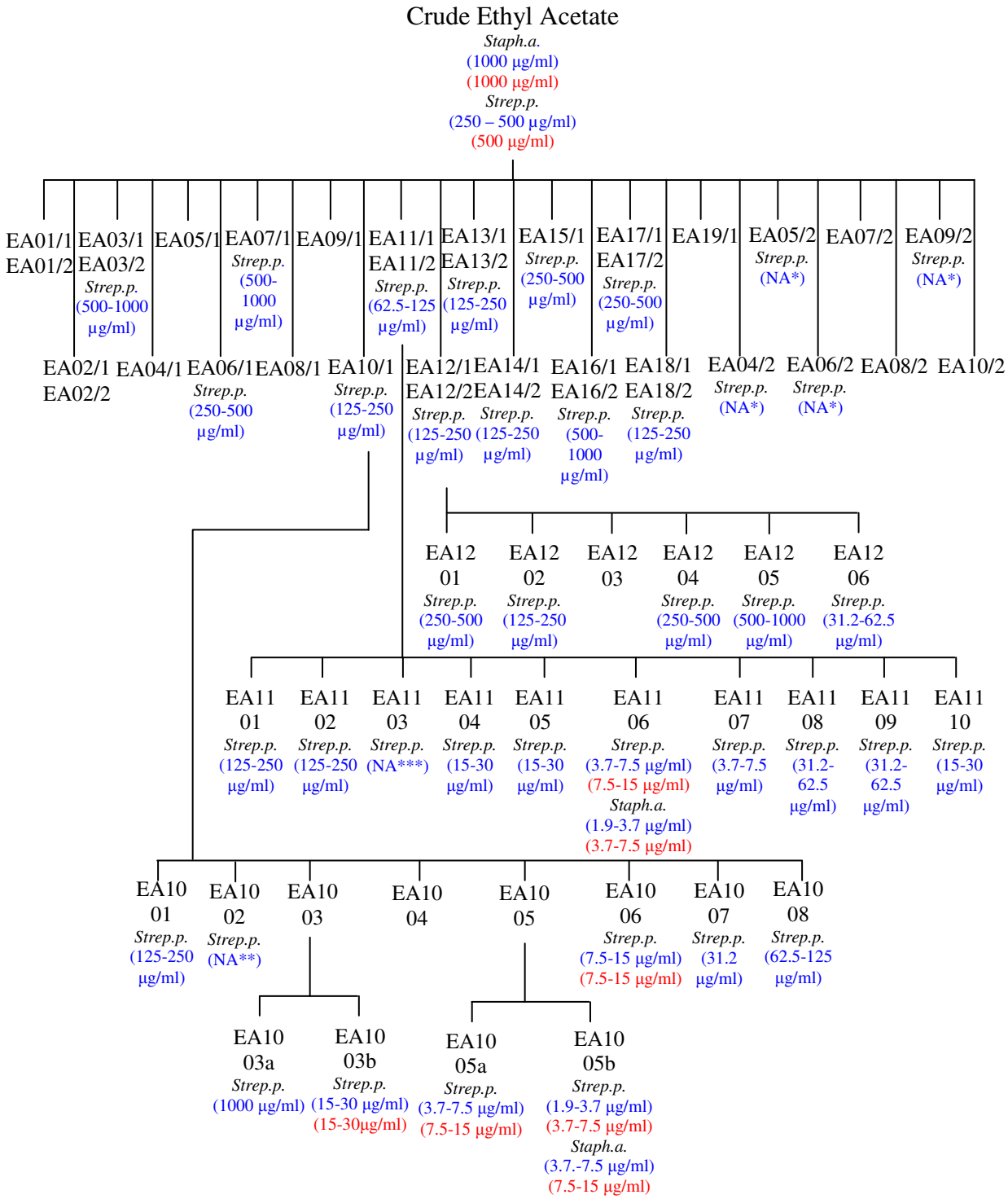

Staph.a. : *Staphylococcus aureus* ATCC 25923
Strep.p. : *Streptococcus pyogenes* ATCC 10389
NA* : Not active at the maximum concentration tested (2 mg/ml)
NA** : Not active at the maximum concentration tested (1 mg/ml)
NA*** : Not active at the maximum concentration tested (500 µg/ml)

Some of the sub-fractions from the EA10 extract (EA1003b, EA1005a, EA1005b and EA1006) showed good antibacterial activity against *Streptococcus pyogenes* (ATCC 10389) with MIC ranging from 1.9 – 30 μg/mL (***Figure 3.2***). The MBC of these sub-fractions were also observed ranging from 1.9 – 15 μg/mL (***Figure 3.2***). Sub-fraction EA1005b [51] which showed MIC of 1.9 – 3.7 μg/mL (4.16 – 8.11 μM) and MBC of 3.7 – 7.5 μg/mL (8.11 – 16.4 μM) against *Streptococcus pyogenes* (ATCC 10389) has been identified as 20-*epi*-ursolic acid. Sub-fraction EA1005b [51] also has good antibacterial activity against *Staphylococcus aureus* (ATCC 25923) with MIC of 3.7 – 7.5 μg/mL (8.11 – 16.4 μM) and MBC of 7.5 – 15 μg/mL (16.4 – 32.8 μM). Initially, fraction EA10 did not show any significant antibacterial activity against *Staphylococcus aureus* (ATCC 25923). The results of the purified extract later showed good antibacterial activity against this Gram-positive bacterium. This is probably due to the amount of sub-fraction EA1005b [51] (60 μg/mL) in fraction EA10 which is too little to be detected and therefore has little ability to inhibit the growth of *Staphylococcus aureus* (ATCC 25923). There is also a possibility that the interactions with other components in the crude fractions block or antagonize its effects. Unlike *Staphylococcus aureus* (ATCC 25923), *Streptococcus pyogenes* (ATCC 10389) is more sensitive therefore, can be easily inhibited even in a low amount of active compound. However, sub-fraction EA1005b [51] still did not show any activity against either Gram-negative bacteria at a maximum concentration of 60 μg/mL (***Figure 3.2***).

Among the sub-fractions from EA11 that were tested, sub-fraction EA1106 and EA1107 showed good antibacterial activity against *Streptococcus pyogenes* (ATCC 10389) with MIC of 3.7 – 7.5 μg/mL. There is a possibility that these two sub-fractions with similar MIC values might have similar active compounds as EA1107 is the sub-fraction obtained after EA1106. Sub-fraction EA1106 was then subjected for further antibacterial testing against *Staphylococccus aureus* (ATCC 25923) and both Gram-negative bacteria. Sub-fraction EA1106 showed good antibacterial activity against *Staphylococcus aureus* (ATCC 25923) with MIC of 1.9 – 3.7 μg/mL and MBC of 3.7 – 7.5 μg/mL. Initially, fraction EA11 from which this compound was extracted did not show any significant antibacterial activity against this Gram-positive bacterium. Similar to EA1005b, the relative amount of sub-fraction EA1106 might be too little to be detected at an earlier stage, therefore no inhibition of growth was observed against *Staphylococcus aureus* (ATCC 25923). *Staphylococcus aureus* (ATCC 25923) is generally more resistant compared to *Streptococcus pyogenes* (ATCC 10389).

Therefore, a more concentrated amount of active compound is needed to observe any growth inhibition for *Staphylococcus aureus* (ATCC 25923). However, in some cases, the MICs were about the same, depending on the active compounds of an extract. Sub-fraction EA1106 did not have any antibacterial activity against either of the Gram-negative bacteria at a maximum concentration of 30 μg/mL (***Figure 3.2***).

Five out of the six sub-fractions from EA12 were tested against *Streptococcus pyogenes* (ATCC 10389). Among those tested, sub-fraction EA1206 showed good antibacterial activity with MIC of 31.2 – 62.5 μg/mL. However, no further antibacterial assay was performed on this sub-fraction. This sub-fraction could be further fractionated in the near future to isolate the active compounds that have good antibacterial activity against *Streptococcus pyogenes* (ATCC10389). Sub-fraction EA1203 was not tested due to insufficient amount for antibacterial testing (***Figure 3.2***).

3.4 Methanol Extract

The methanol crude extract showed some antibacterial activity against *Streptococcus pyogenes* (ATCC 10389) with MIC of 4000 µg/mL. No antibacterial activity was observed against either of the Gram-negative bacteria at a maximum concentration of 4000 µg/mL (***Table 3.1***).

However, a study done by Nobbs has shown that three methanol fractions of *Scaevola spinescens* have antibacterial activity (at maximum concentration of 60 mg/disc using disc diffusion assay).[6] From a clinical perspective, compounds with MIC values over 1 mg/mL using broth or agar dilution methodologies are not considered as a potential antibacterial agent since a number of relatively inert substances may show antibacterial activity at this high concentration.[69] The antibacterial activity observed by Nobbs was at a high concentration. There could be a lot of possibilities that contribute to the antibacterial activity at this high concentration. It is hard to determine what the actual available concentration in these previously conducted diffusion assays were.

The dilution assay has more advantages compared to the diffusion assay, namely the test compound concentration in the medium is defined and has significant reductions in test compound concentration.[70] As observed in Nobbs' work, the higher test concentration is required for the diffusion assay. Besides that, the antibacterial activity observed in the diffusion assay is dependent upon the ability of test compounds to migrate across the agar.

To verify the findings found by Nobbs, the antibacterial activity of the methanol crude extract has been tested using a broth micro-dilution assay. The antibacterial activities of methanol fractions were further tested although the MIC value of methanol crude extract was observed at a maximum concentration of 4000 µg/mL. There was a possibility that the total percentage of active compounds in the methanol crude extract was too little to be effective at this stage.

Seventeen fractions (M01-M17) have been isolated from the methanol crude extract using flash column chromatography. Only eight out of seventeen methanol fractions were further tested on *Streptococcus pyogenes* (ATCC 10389) for any antibacterial activity (at a maximum concentration of 4000 µg/mL). (***Figure 3.3***) The selected fractions (M09, M10 and M13) are

in the range where pure compounds (M0906a, M0907a, M100603, M1306a) have been isolated. This approach was to target the compounds already isolated.

Among those methanol fractions tested, fraction M13 showed moderate antibacterial activity with MIC of 125 – 250 μg/mL (***Figure 3.3***). This fraction is of interest as a pure compound, identified as luteolin-7-*O*-glucoside was isolated from this fraction. Therefore, all of the M13 sub-fractions, except the pure compound, were further tested against *Streptococcus pyogenes* (ATCC 10389). This is because the amount of pure compound isolated was insufficient for antibacterial assay.

The sub-fractions from M1303 to M1310 did not show any antibacterial activity against *Streptococcus pyogenes* (ATCC 10389) at a maximum concentration of 2000 μg/mL. Therefore, there is a possibility that luteolin-7-*O*-glucoside (fraction M1306a) might not have any antibacterial activity against *Streptococcus pyogenes* (ATCC 10389). Research done by Chiruvella *et al* showed that luteolin-7-*O*-glucoside (10 mg/mL) did not have antibacterial activity against *Staphylococcus aureus* and *Pseudomonas aeruginosa* using the agar well diffusion methanol.[33] Therefore, no further antibacterial testing was done on these two microorganisms. Nevertheless, luteolin-7-*O*-glucoside (10 mg/mL) has previously been found to have antibacterial activity against *Bacillus subtilis* and Gram-negative bacteria including *Klebsiella pneumoniae*, *Salmonella typhimurium*, *Proteus vulgaris* and *Escherichia coli*.[33] This shows that luteolin-7-*O*-glucoside has antibacterial properties that are specific to certain bacteria (typically Gram-negative bacteria). Besides having antibacterial properties, luteolin-7-*O*-glucoside (10 mg/mL) was also found to have antifungal activity against *Aspergillus fumigatus*, *Aspergillus niger* and *Aspergillus alternata*.[33]

The sub-fractions M1302 and from M1311 to M1314 showed antibacterial activity against *Streptococcus pyogenes* (ATCC 10389). Among these sub-fractions, M1313 and M1314 showed good antibacterial activity with MIC of 15 – 30 μg/mL. However, active pure compounds from these sub-fractions have not yet been isolated.

Figure 3.3: Antibacterial testing on the crude extract of methanol as well as its sub-fractions (MIC) (MBC)

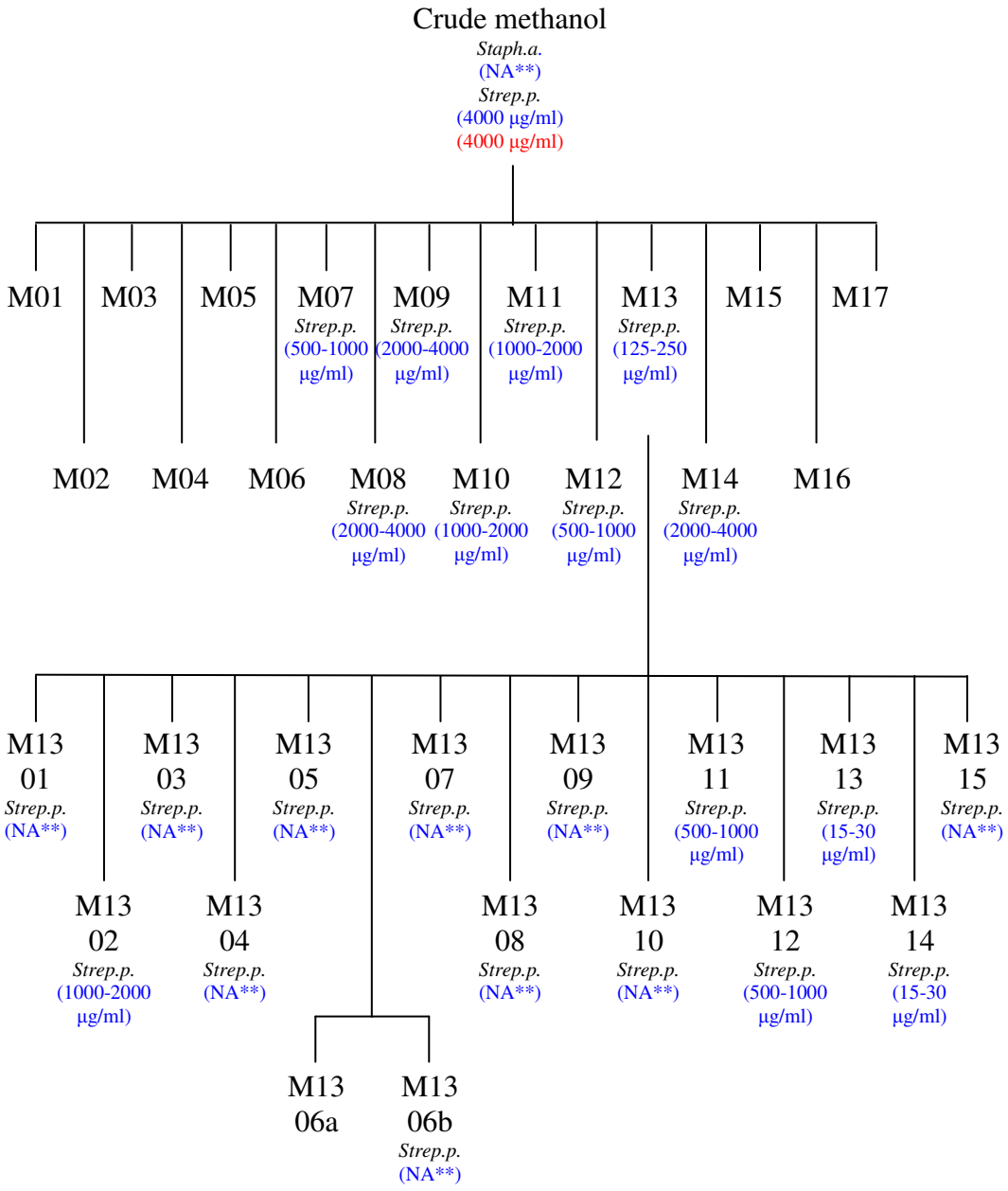

Staph.a. : *Staphylococcus aureus* ATCC 25923
Strep.p. : *Streptococcus pyogenes* ATCC 10389
NA* : Not active at the maximum concentration tested (1 mg/ml)
NA** : Not active at the maximum concentration tested (2 mg/ml)

3.5 Aqueous Extracts

Both aqueous extracts (decoction and Soxhlet extraction) did not show any activity against either Gram-positive (at a maximum concentration of 4000 µg/mL) or Gram-negative bacteria (at a maximum concentration of 1000 µg/mL). However, both aqueous extracts were sequentially extracted using liquid-liquid extraction (hexane, dichloromethane, ethyl acetate and methanol) and these extracts were further tested for any antibacterial activity. There is a possibility that the active compounds were present at too low a concentration to be detected at this stage.

Aqueous extract (decoction)

The hexane extract [Aq(Dct)H] from liquid-liquid partitioning of the aqueous decoction did not show any antibacterial activity for Gram-positive and Gram-negative bacteria at a maximum concentration of 1000 µg/mL (***Figure 3.4***). Due to insufficient amount of samples no further tests were done for this extract on a higher concentration.

The dichloromethane extract [Aq(Dct)D] from liquid-liquid partitioning of the aqueous decoction showed antibacterial activity against *Streptococcus pyogenes* (ATCC 10389) with an MIC of 1000 – 2000 µg/mL. No antibacterial activity was observed against *Staphylococcus aureus* (ATCC 25923) and either of the Gram-negative bacteria at a maximum concentration of 1000 µg/mL. Therefore, the sub-fractions from this extract were further tested against *Staphylococcus aureus* (ATCC10389). However, only eight out of ten sub-fractions were tested as there were two sub-fractions that were insufficient for antibacterial testing. Four out of the eight sub-fractions tested showed antibacterial activity. Among those four sub-fractions, fraction Aq(Dct)D07 showed reasonable antibacterial activity with an MIC of 250 – 500 µg/mL. This fraction needs to be fractionated in the future so as to isolate the active pure compounds that contribute to the antibacterial activity (***Figure 3.4***).

The ethyl acetate extract [Aq(Dct)EA] from liquid-liquid partitioning of the aqueous decoction did not show any antibacterial activity against *Staphylococcus aureus* (ATCC 25923) and either of the Gram-negative bacteria at a maximum concentration of 1000 µg/mL. This extract

also did not show any antibacterial activity against *Streptococcus pyogenes* (ATCC 10389) at a maximum concentration of 4000 µg/mL. Therefore, the sub-fractions of this extract were not further examined (***Figure 3.4***).

The aqueous methanol residue [Aq(Dct)AM] from liquid-liquid partitioning of the aqueous decoction showed antibacterial activity against *Staphylococcus aureus* (ATCC 25923) with an MIC of 500-1000 µg/mL. No antibacterial activity was observed against *Streptococcus pyogenes* (ATCC 10389) at a maximum concentration of 4000 µg/mL. Both Gram-negative bacteria were not tested for this extract as it has clearly shown no activity in the crude extract as well as the hexane, dichloromethane and ethyl acetate partition extracts. The sub-fractions of this extract were further tested against *Staphylococcus aureus* (ATCC 25923). Nine out of eleven sub-fractions tested showed positive results. Among those results observed, Aq(Dct)AM05 showed reasonable antibacterial activity against *Streptococcus pyogenes* (ATCC 10389) with an MIC of 125 – 250 µg/mL. This fraction can be further fractionated in the future to isolate active pure compounds that contribute to the antibacterial activity (***Figure 3.4***).

Figure 3.4: Antibacterial testing on the extracts from liquid-liquid partitioning of the aqueous decoction as well as its sub-fractions (MIC)

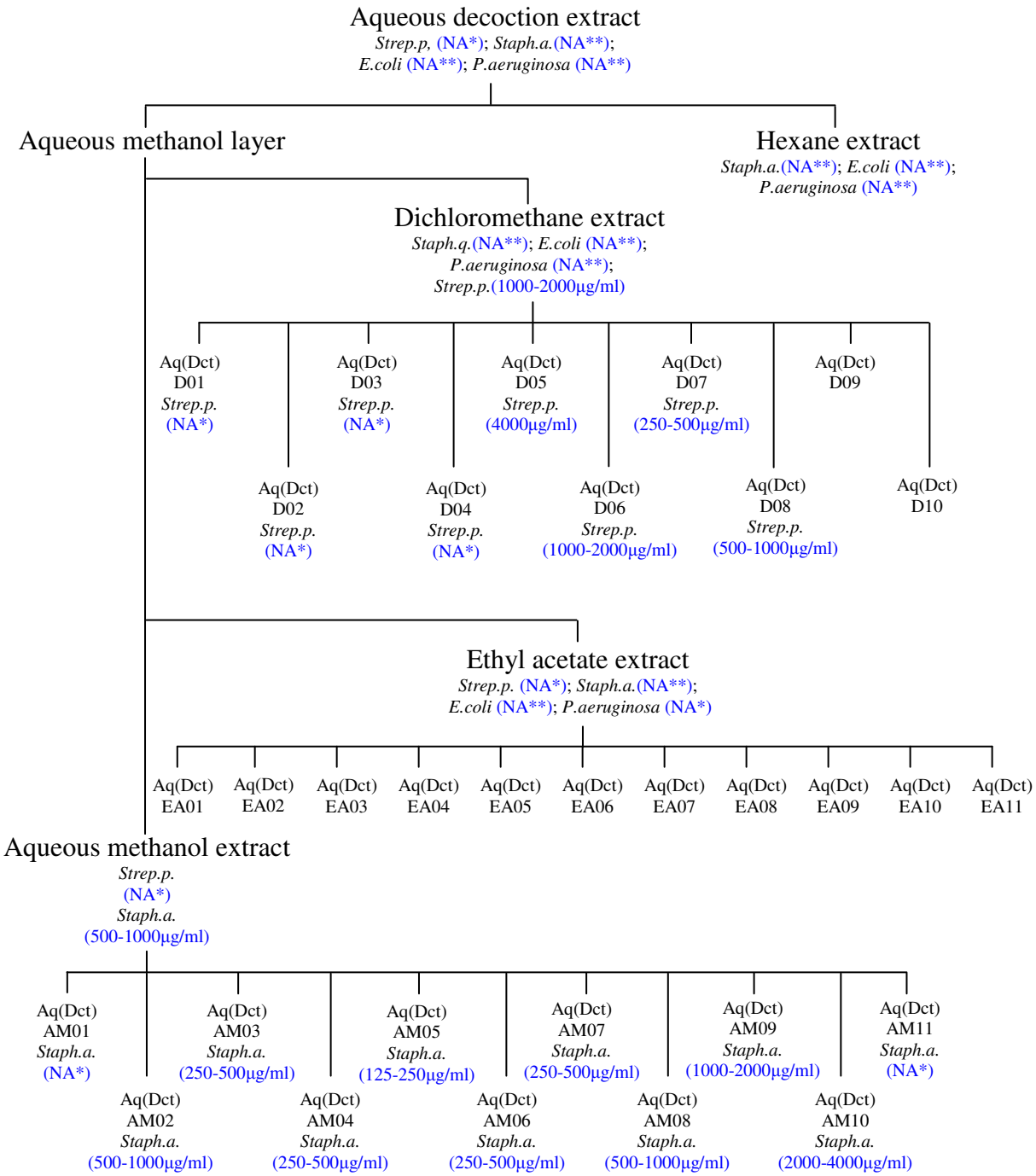

Staph.a.	: *Staphylococcus aureus* ATCC 25923
Strep.p.	: *Streptococcus pyogenes* ATCC 10389
E.coli	: *Escherichia coli* ATCC 25922
P.aeruginosa	: *Pseudomonas aeruginosa* ATCC 27853
NA*	: Not active at the maximum concentration tested (4 mg/ml)
NA**	: Not active at the maximum concentration tested (1 mg/ml)

Aqueous extract (soxhlet)

The hexane extract [Aq(Sox)H] from liquid-liquid partitioning of the aqueous Soxhlet extract showed good antibacterial activity against *Streptococcus pyogenes* (ATCC 10389) with an MIC of 62.5 – 125 μg/mL and a reasonable antibacterial activity against *Staphylococcus aureus* (ATCC 25923) with an MIC of 250 – 500 μg/mL. This extract was not further fractionated due to the insufficient amount of sample. Therefore, the active compounds in this extract cannot be determined at this point of time (***Figure 3.5***).

The dichloromethane extract [Aq(Sox)D] from liquid-liquid partitioning of the aqueous Soxhlet extract had antibacterial activity against *Streptococcus pyogenes* (ATCC 10389) and *Staphylococcus aureus* (ATCC 25923) with MIC of 1000 – 2000 μg/mL. Only eleven out of fourteen sub-fractions of this extract were further tested on both Gram-positive bacteria due to insufficient amount available for testing. Nine out of the sub-fractions tested showed antibacterial activity against *Staphylococcus aureus* (ATCC 25923) with a range of MIC between 500 to 4000 μg/mL. Among those sub-fraction tested, Aq(Sox)D10 and Aq(Sox)D11 showed good antibacterial activity against *Streptococcus pyogenes* (ATCC 10389) with MIC of 15 – 30 μg/mL. There was better antibacterial activity observed against *Streptococcus pyogenes* (ATCC 10389) compared to *Staphylococcus aureus* (ATCC 25923). These two sub-fractions are of interest for further testing. Therefore, further fractionation on these two sub-fractions can be done in the future to isolate the active compounds that contribute to the antibacterial activity (***Figure 3.5***).

The ethyl acetate extract [Aq(Sox)EA] from liquid-liquid partitioning of the aqueous soxhlet showed antibacterial activity against *Staphylococcus aureus* (ATCC 25923) with MIC of 250 – 500 μg/mL. No antibacterial activity was observed against *Streptococcus pyogenes* (ATCC 10389) at a maximum concentration of 4000 μg/mL. Therefore, the sub-fractions of this extract were only further tested against *Staphylococcus aureus* (ATCC 25923). All except one of the sub-fractions were tested as the amount was insufficient for antibacterial testing (***Figure 3.5***).

Two out of eleven sub-fractions tested did not show any antibacterial activity. One of them was the isolated pure compound, identified as 2-deoxy-D-chiro-inositol. However, the filtrate

where this pure compound was isolated showed antibacterial activity with MIC of 500 – 1000 μg/mL. (***Figure 3.5***).

Among those sub-fractions that were tested positive, fraction Aq(Sox)EtoAc08 showed good antibacterial activity with MIC of 62.5 – 125 μg/mL. Therefore, this extract has been further fractionated into 6 fractions and those fractions were then tested for antibacterial activity. Among those 6 fractions tested, fraction Aq(Sox)EtoAc0805 showed good antibacterial activity with MIC of 31.25 – 62.5 μg/mL. This fraction is deemed desirable for further isolation to determine the active compound that contributes to the antibacterial activity. However, the active compounds have not yet been isolated due to the limitation of time (***Figure 3.5***).

The aqueous methanol residue [Aq(Sox)AM] from liquid-liquid partitioning of the aqueous Soxhlet extract had antibacterial activity against *Staphylococcus aureus* (ATCC 25923) with MIC of 500 – 1000 μg/mL. No antibacterial activity was observed against *Streptococcus pyogenes* (ATCC 10389) at a maximum concentration of 4000 μg/mL. Only ten out of eleven sub-fractions from this extract were further tested against *Staphylococcus aureus* (ATCC 25923) due to insufficient amount of sample available for testing. All of the sub-fractions tested showed antibacterial activity against *Staphylococcus aureus* (ATCC 25923) with MIC ranging from 125 to 2000 μg/mL. Further purification of these fractions needs to be performed to isolate the active compounds that contribute to antibacterial activity.

Figure 3.5: Antibacterial testing on the extracts from liquid-liquid partitioning of the aqueous soxhlet as well as its sub-fractions (MIC)

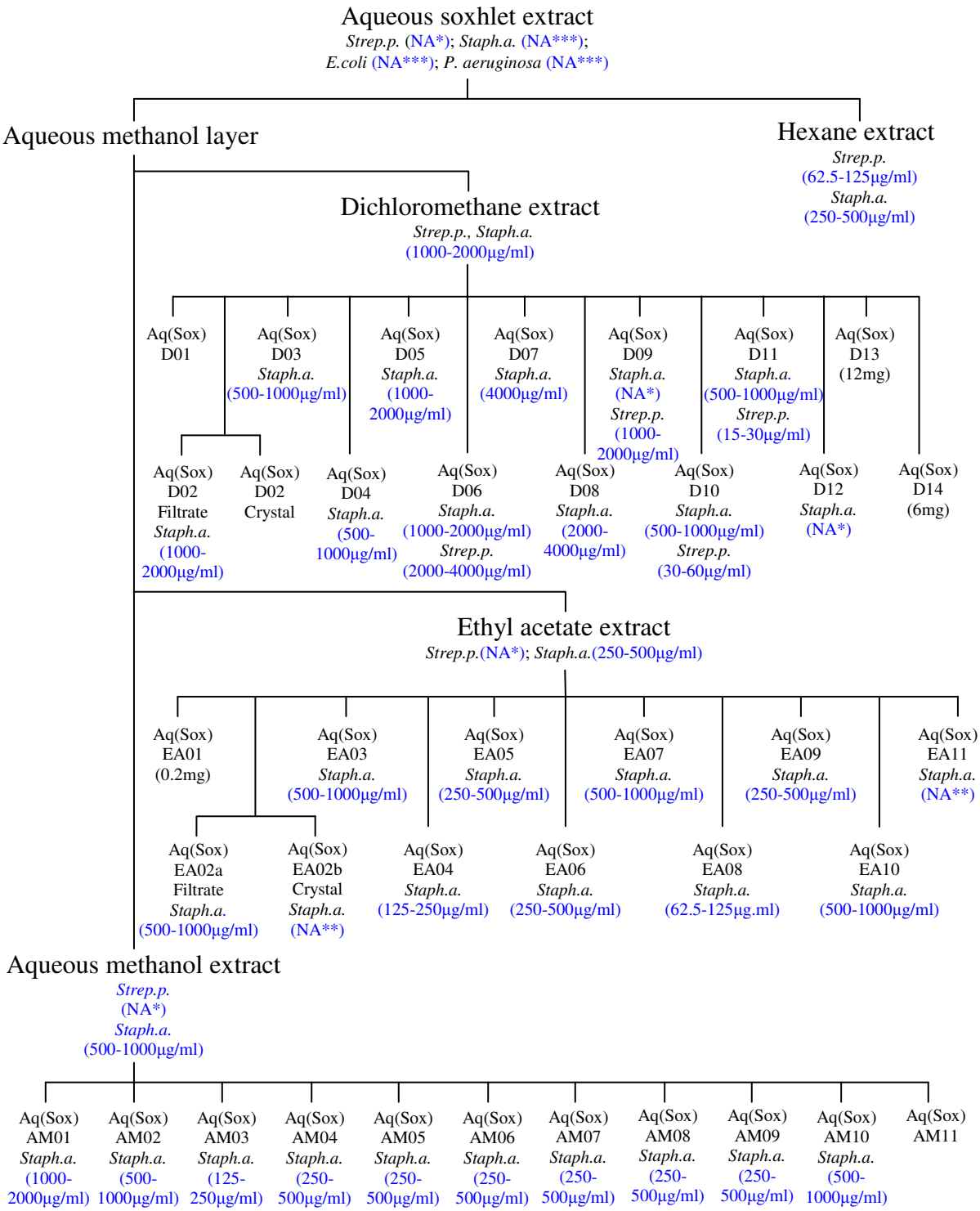

Staph.a. : *Staphylococcus aureus* ATCC 25923
Strep.p. : *Streptococcus pyogenes* ATCC 10389
E.coli : *Escherichia coli* ATCC 25922
P.aeruginosa : *Pseudomonas aeruginosa* ATCC 27853
NA* : Not active at the maximum concentration tested (4 mg/ml)
NA** : Not active at the maximum concentration tested (2 mg/ml)
NA*** : Not active at the maximum concentration tested (1 mg/ml)

3.6 Discussion

Generally, the initial crude extracts show less activity compared to the fractionated extracts. In some of the cases observed, the antibacterial activity is only present in the fractionated extracts and not in the initial crude extracts. This is probably due to the active compounds in the crude extracts being in a low concentration and thus, not able to be detected by the antibacterial assay. There is also a possibility that interactions with other components in the crude extracts antagonize its effect. The antibacterial activity in an extract should be greater in the purified compound. However, it is not unusual for the initial extract to show greater activity than any of the fractions obtained with bioassay-guided fractionation.[71] In cases like this, the possibility of synergy should be considered and if possible, checked by testing the bioactivity of the combined fractions.[71]

Differential solubility can be a problem, particularly when the extract is not water soluble, in which case methanol or dimethylsulfoxide (DMSO) may need to be used.[71] However, these solvent must be used at a very low concentration. This is to prevent any possible killing effect from the solvent instead of the extract itself. A DMSO medium control was carried out in each assay to show that the concentration used to dissolve the extracts is not responsible for the killing effect. Therefore, any inhibition or killing effects observed are solely due to the active compounds in the extracts.

Based on the results of the assay, none of the extracts tested on either of the Gram-negative bacteria showed any antibacterial activity. This is probably due to the cell envelope of the bacteria. Gram-positive bacteria have a relatively simple cell envelope that consists of two or three layers.[72] Whereas in Gram-negative bacteria, the cell envelope is a highly complex, multilayered structure.[72] This makes the active compounds from the extracts harder to penetrate through the cell envelope of Gram-negative bacteria. Therefore, Gram-negative bacteria are harder to kill compared to Gram-positive bacteria.

Among all the samples tested, the ethyl acetate fractions showed the greatest antibacterial activity. This is clearly observed in the purified compound of EA1005b as well as EA1106 with MIC ranging from 1.9 to 7.5 μg/mL (4.16 – 16.4 μM) against *Streptococcus pyogenes* (ATCC 10389) and *Staphylococcus aureus* (ATCC 25923).

The sub-fraction [Aq(Sox)EA0805] also showed promising antibacterial activity with MIC of 31.25 – 62.5 μg/mL. The promising results from this aqueous extract supported the claimed used by the Aboriginal people on this plant to cure stomach ache, urinary problems and pain in the alimentary tract as well as boils, skin rashes and sores. These cures are usually related to microbial infections.

Bioassay-guided fractionation is one of the ways to identify possible active compounds. Any fractions that have antibacterial activity with MIC below 100 μg/mL are deemed desirable for further antibacterial testing in the sub-fractions, which might lead to identification of active pure compounds.

CHAPTER 4

Experimental

4.1 General experimental procedures

- Analytical TLC was performed using Merck Kieselgel 60 F254 silica on aluminium backing sheets. Preparative TLC was performed using Merck pre-coated Kieselgel 60 F254 silica on glass plates (20 cm x 20 cm) with the thickness of 0.25 mm.

- Normal phase flash chromatography was performed using Davisil Chromatographic Silica Media for separation and purification application (40 – 63 micron). Chem-supply sand acid washed was used in packing the normal phase flash chromatography. Reversed-phase flash chromatography was performed using Waters Preparative C18 125 Å (55 – 105 micron), which contained dimethyloctadecylsilyl bonded amorphous silica.

- Visualization of TLC plates was done using ultraviolet radiation at 254 nm and staining reagents such as phosphomolybdic acid, vanillin, anisaldehyde and potassium permanganate solution.

- Melting points were obtained using a Reichert hot-stage microscope (0° - 350°C).

- UV/ visible spectra were acquired on an SP-8001 Metertech UV/Vis spectrophotometer.

- Infrared spectra were acquired on a Perkin Elmer spectrum BX FT-IR system.

- 1D and 2D NMR spectra were acquired on a Varian INOVA 600 MHz spectrometer. Chemical shifts were referenced to residual solvent resonances.

- High and low resolution mass spectra analysis was conducted at the Central Science Laboratory, Tasmania using a Kratos Concept ISQ magnetic sector mass spectrometer (positive ion mode unless indicated otherwise). Negative Ion Atmospheric Pressure Chemical Ionization (APCI) method was used on an LTQ Orbitrap^{TM} mass spectrometer to obtain negative ion spectra.

- Optical rotation values were acquired on an AP-100 Automatic polarimeter.

- A 0.5 McFarland standard bacterial cell suspension was determined using a VITEK colorimeter.

4.2 Plant material

The aerial parts of the plant (leaves and branches) were collected in April 2007 on the Morgan-Eudunda road, 10km west of Morgan. A voucher specimen was deposited at the State Herbarium of South Australia, Adelaide. –Voucher Number AD99702040

4.3 Extraction and isolation

The aerial parts (leaves and branches) of *Scaevola spinescens* (1.6 kg) were air-dried. The total loss of moisture was about 160 g. The ground up samples were mixed then divided into two lots, one with about 2/3 of the total sample (Sample A) and the other with about 1/3 of the total sample (Sample B).

Sample A was sequentially extracted using Soxhlet extraction based on increasing polarity solvents, starting from hexane (2.5 L), then ethyl acetate (2.5 L), methanol (2.5 L) and lastly distilled water (2.5 L). The solvents for each extraction that were evaporated to dryness *in vacuo* at 40°C gave 8g of hexane extract, 15 g of ethyl acetate extract and 71 g of methanol extract. The distilled water that was evaporated to dryness *in vacuo* at 60°C gave 71 g of aqueous extract (soxhlet).

Sample B was extracted using the decoction method. The samples were soaked in warm water (the level of the water is 3 cm above the sample) for half an hour, heated to boiling, then simmered for about 45 minutes with constant stirring. The samples were then filtered using a Buchner funnel and the water from the filtrate was evaporated to dryness *in vacuo* at 60°C using a rotary evaporator. Sample B was re-extracted twice using the same procedure to increase the yield of extracted material. This extraction yielded 46 g of aqueous extract (decoction).

4.3.1 Hexane extract

The hexane extract (8 g) was subjected to flash column chromatography (100 mm column diameter) using a series of increasing polarity solvents. The sample was loaded onto the column in a minimum volume of 50% hexane / 50% dichloromethane then eluted sequentially with 2 L of each of the following solvent systems:

50% hexane / 50% dichloromethane

50% hexane / 45% dichloromethane / 5% ethyl acetate

50% hexane / 40% dichloromethane / 10% ethyl acetate

50% hexane / 50% ethyl acetate

20% hexane / 80% ethyl acetate

100% ethyl acetate

90% ethyl acetate / 10% methanol

80% ethyl acetate / 20% methanol

A total of 32 x 500 mL fractions were collected. After TLC analysis, appropriate fractions were combined to give 22 fractions, H01-H22.

Fraction H10 (500 mg) was resubjected to flash column chromatography (40 mm column diameter). The sample was loaded onto the column in a minimum volume of 60% hexane / 38% dichloromethane / 2% ethyl acetate then eluted sequentially with 60% hexane / 38% dichloromethane / 2% ethyl acetate (800 mL) then 60% hexane / 35% dichloromethane / 2% ethyl acetate (800 mL) to give 40 x 40 mL fractions. After TLC analysis, appropriate fractions were combined to give 12 sub-fractions, H1001-H1012.

Sub-fraction H1010 (150 mg) was resubjected to flash column chromatography (20 mm column diameter). The sample was loaded onto the column in a minimum volume of 5% hexane / 95% dichloromethane then eluted with the same solvent (200 mL) to give 20 x 10 mL fractions. After TLC analysis, appropriate fractions were combined to give 5 sub-fractions, H101001-H101005.

Fraction H11 (980 mg) was resubjected to flash column chromatography (50 mm column diameter). The sample was pre-absorbed with a small quantity of silica and added as a dry mixture onto the column, then eluted with 100% dichloromethane then 50% hexane / 45%

dichloromethane / 5% ethyl acetate to give 40 x 50 mL fractions. After TLC analysis, appropriate fractions were combined to give 14 sub-fractions, H1101-H1114.

Fraction H12 (900 mg) was resubjected to flash column chromatography (50 mm column diameter). The sample was loaded onto the column in a minimum volume of 50% hexane / 45% dichloromethane / 5% ethyl acetate then eluted sequentially with 50% hexane / 45% dichloromethane / 5% ethyl acetate then 50% hexane / 40% dichloromethane / 10% ethyl acetate to give 40 x 50 mL fractions. After TLC analysis, appropriate fractions were combined to give 14 sub-fractions, H1201-H1214.

Fraction H14 (580 mg) was resubjected to flash column chromatography (40 mm column diameter). The sample was pre-absorbed with a small quantity of silica and added as a dry mixture onto the column, then eluted with 20% hexane / 70% dichloromethane / 10% ethyl acetate, 90% dichloromethane / 10% ethyl acetate then 80% dichloromethane / 20% ethyl acetate to give 60 x 30 mL fractions. After TLC analysis, appropriate fractions were combined to give 16 sub-fractions, H1401-H1216.

The sub-fractions H1007, H1008 and H1103 with similar ^{1}H NMR profile were combined (456 mg) and crystallized from hot dichloromethane. The white solids (56 mg) that crystallized out of solution were then re-crystallized again from hot dichloromethane to give fine, white crystals (31 mg). The sub-fractions H101003 and H1205 with similar ^{1}H NMR profile were combined (53 mg) and crystallized from hot dichloromethane to give fine, white crystals (7 mg). The ^{1}H NMR profile of these crystals was found to be similar to compound isolated from fraction H1007, H1008 and H1103. These compounds were combined [49] and further characterized using 2D NMR, melting point, mass spectrometry, FTIR and UV-visible spectroscopy. The structure for compound [49] was identified as 18-*epi*-taraxerol. Details of the data are presented below.

When a solution of fraction H1407 was left standing, white solids (15 mg) crystallized out of solution. This white precipitate was then re-crystallized from hot dichloromethane to give a white amorphous solid (11 mg) [50]. Compound [50] was further characterized using 2D NMR, melting point, mass spectrometry, FTIR and UV-visible spectroscopy. The structure for compound [50] was identified as myricadiol. Details of the data are presented below.

Compounds

18-*epi*-taraxerol [49]

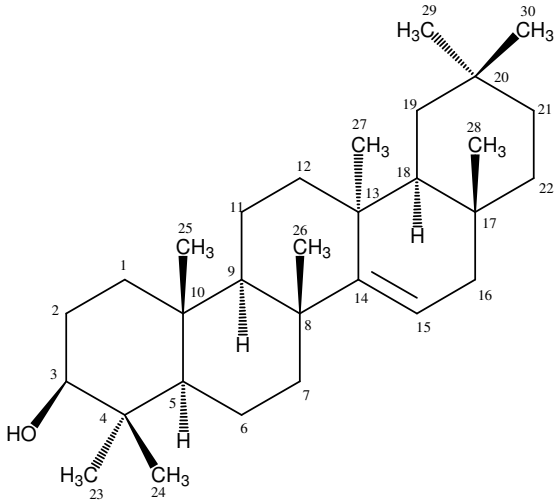

[49]

38 mg of [49] was recrystallized from fractions H1007, H1008, H101003, H1103 and H1205 as fine white crystals. **MP:** 282 - 283°C. **IR:** ν_{max} (nujol) 3480 cm^{-1} (OH), 1641 cm^{-1} (C=C). **^{1}H NMR** (600 MHz, $CDCl_3$); δ_H: 0.78 [1H, dd, $J_{5,6}$ = 2.4 Hz, 12.0 Hz , H(5)], 0.80 [3H, s, Me(24)], 0.82 [3H, s, Me(28)], 0.91 [3H, s, Me(27)], 0.91 [3H, s, Me(30)], 0.92 [3H, s, Me(25)], 0.93 [1H, m, H(1β)], 0.95 [3H, s, Me(29)], 0.96 [1H, m, H(18)], 0.97 [1H, m, H(19β)], 0.98 [3H, s, Me(23)], 1.01 [1H, m, H(22β)], 1.09 [3H, d, Me(26)], 1.24 [1H, m, H(21β)], 1.31 [1H, m, H(19α)], 1.33 [1H, m, H(21α)], 1.34 [1H, m, H(7β)], 1.36 [1H, m, H(22α)], 1.41 [1H, m, H(9)], 1.47 [1H, m, H(11β), 1.47 [1H, m, H(6β)], 1.55 [1H, m, H(12β)], 1.57 [1H, m, H(2β)], 1.59 [1H, m, H(1α)], 1.60 [1H, m, H(2α)], 1.61 [1H, m, H(6α)], 1.61 [1H, m, H(12α)], 1.63 [1H, m, H(11α)], 1.63 [1H, m, H(16β)], 1.91 [1H, dd, $J_{15,16\alpha}$ = 3.0 Hz, $J_{16\alpha,16\beta}$ = 15.0 Hz, H(16α)], 2.03 [1H, dd, $J_{6,7}$ = 6.6 Hz, 12.0 Hz, H(7α)], 3.19 [1H, m, H(3)], 5.53 [1H, dd, $J_{15,16\alpha}$ = 3.0 Hz , $J_{15,16\beta}$ = 7.4 Hz, H(15)]. **^{13}C NMR** (600 MHz, $CDCl_3$); δ_C: 15.41 [C(25*)], 15.44 [C(24*)], 17.4 [C(11)], 18.7 [C(6)], 21.3 [C(27)], 25.9 [C(26)], 27.1 [C(2)], 27.9 [C(23)], 28.7 [C(20)], 29.8 [C(28)], 29.9 [C(30)], 33.0 [C(21)], 33.3 [C(29)], 33.6 [C(12)], 35.1 [C(22)], 35.7 [C(17)], 36.6 [C(19)], 37.71 [C(1*)], 37.74 [C(16*)], 37.5 [C(13)], 38.0 [C(10)], 38.7 [C(4)], 38.9 [C(8)], 41.3 [C(7)], 48.7 [C(18)], 49.2 [C(9)], 55.5 [C(27)], 79.0 [C(3)], 116.8 [C(15)], 158.0 [C(14)]. **LREIMS** *m/z* 426 [M^+, 15%], 411 [18%], 302 [42%], 287 [48%], 269 [30%], 204 [100%], 189 [45%], 147 [35%], 135 [68%]. **HREIMS** *m/z* 426.3858 (calculated for $C_{30}H_{50}O$, 426.3861).

* Assignments may be reversed.

Myricadiol [50]

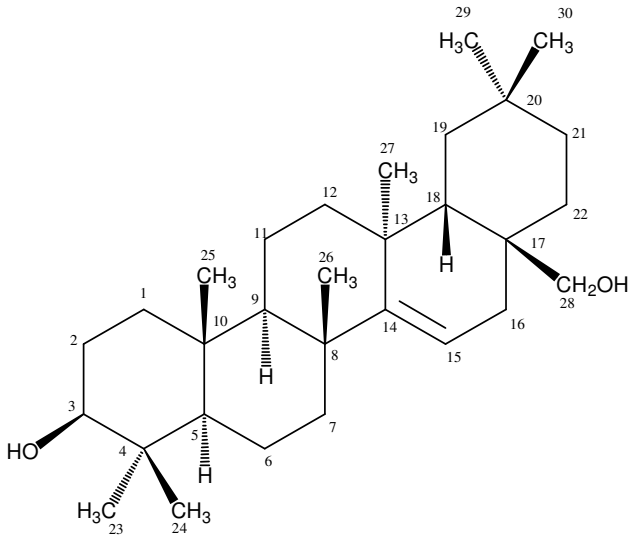

[50]

11 mg of [50] was isolated from fraction H1407 as a white, amorphous solid. **MP:** 265 - 270°C. **IR:** ν_{max} (nujol) 3340 cm^{-1} (OH). **^{1}H NMR** (600 MHz, $CDCl_3$); δ_H: 0.57 [1H, dd, $J_{18,19\beta}$ = 3.6 Hz, $J_{18,19\alpha}$ = 13.8 Hz, H(18)], 0.77 [1H, dd, $J_{5,6}$ = 2.4 Hz, 12.6 Hz, H(5)], 0.79 [3H, s, Me(24)], 0.89 [3H, s, Me(30)], 0.91 [3H, s, Me(25)], 0.961 [3H, s, Me(27)], 0.964 [3H, s, Me(29)], 0.97 [3H, s, Me(23)], 1.00 [1H, dd, $J_{18,19\beta}$ = 3.6 Hz, $J_{9\beta,19\alpha}$ = 13.2 Hz, H(19β)], 1.06 [3H, s, Me(26)], 1.24 [1H, m, H(21β)], 1.26 [1H, m, H(21α)], 1.33 [1H, td, $J_{6,7\beta}$ = 3.0 Hz, $J_{7\beta,7\alpha}$ = 12.6 Hz, H(7β)], 1.41 [1H, m, H(19α)], 1.42 [1H, m, H(9)], 1.47 [1H, m, H(22β)], 1.50 [1H, m, H(22α)], 1.58 [1H, m, H(1β)], 1.59 [1H, m, H(2β)], 1.60 [1H, m, H(2α)], 1.61 [1H, m, H(1α)], 1.62 [1H, m, H(12β)], 1.66 [1H, m, H(12α)], 1.70 [1H, dd, $J_{16\beta,15}$ = 3.0 Hz, $J_{16\beta,16\alpha}$ = 15.0 Hz, H(16β)], 2.01 [1H, dt, $J_{6,7\alpha}$ = 3.0 Hz, $J_{7\alpha,7\beta}$ = 12.6 Hz, H(7α)], 2.14 [1H, dd, $J_{15,16\alpha}$ = 8.4 Hz, $J_{16\alpha,16\beta}$ = 15.0 Hz, H(16α)], 3.10 [1H, d, $J_{28\beta,28\alpha}$ = 10.8 Hz, H(28β)], 3.16 [1H, dd, $J_{3,2}$ = 4.8 Hz, 10.8 Hz, H(3)], 3.24 [1H, d, $J_{28\alpha,28\beta}$ = 10.8 Hz, H(28α)], 5.51 [1H, dd, $J_{15,16\beta}$ = 3.0 Hz, $J_{15,16\alpha}$ = 8.4 Hz, H(15)]. **^{13}C NMR** (600 MHz, $CDCl_3$); δ_C: 15.2 [C(25)], 15.3 [C(24)], 17.1 [C(11)], 18.5[C(6)], 21.3 [C(27*)], 25.8 [C(26)], 26.9 [C(2)], 27.6 [C(22)], 27.8 [C(23)], 28.3 [C(20)], 29.6 [C(30)], 30.4 [C(16)], 33.2 [C(12)], 32.4 [C(21)], 33.3 [C(29*)], 35.6 [C(16)], 37.2 [C(13)], 37.5 [C(1)], 37.7 [C(10)], 38.5 [C(4)], 38.8 [C(8)], 40.2 [C(17)], 41.1 [C(7)], 44.6 [C(18)], 48.9 [C(9)], 55.3 [C(5)], 64.8 [C(28)], 78.5 [C(3)], 115.6 [C(15)], 158.6 [C(14)]. **LREIMS** *m/z* 442 [M^+, 4%], 411 [57%], 302 [40%], 287 [45%], 203 [55%], 189 [100%]. **HREIMS** *m/z* 411.3633 (calculated for $C_{29}H_{47}O$, 411.3626).

* Assignments may be reversed.

4.3.2 Ethyl acetate extract

Two batches of the ethyl acetate extract (~ 7.5 g each time) were subjected to flash column chromatography (100 mm column diameter) using increasing polarity solvents. The sample was loaded onto the column in a minimum volume of 50% hexane / 50% dichloromethane then eluted sequentially with 2 L of each of the following solvent systems:

50% hexane / 50% dichloromethane

50% hexane / 40% dichloromethane / 10% ethyl acetate

50% hexane / 50% ethyl acetate

50% hexane / 30% ethyl acetate / 20% methanol

40% hexane / 40% ethyl acetate / 20% methanol

90% ethyl acetate / 10% methanol

80% ethyl acetate / 20% methanol

A total of 28 x 500 mL fractions were collected. After TLC analysis, appropriate fractions were combined to give 19 fractions, EA01/1-EA19/1 and 17 fractions respectively, EA01/2-EA17/2.

Fraction EA10 (690 mg) was resubjected to flash column chromatography (40 mm column diameter) using increasing polarity solvents. The sample was pre-absorbed with a small quantity of silica and added as a dry mixture onto the column then eluted sequentially with 600 mL of each of the following solvent systems:

40% hexane / 50% dichloromethane / 10% ethyl acetate

30% hexane / 50% dichloromethane / 20% ethyl acetate

20% hexane / 50% dichloromethane / 30% ethyl acetate

100% ethyl acetate

A total of 80 x 30 mL fractions were collected. After TLC analysis, appropriate fractions were combined to give 8 fractions, EA1001-EA1008.

When solutions of fractions EA1003 and EA1005 were left standing, white solids crystallized out of each solution. The white solids were labeled as EA1003a (7 mg) and EA1005a (8 mg). The filtrate from fraction EA1005 (EA1005b) was tested for purity by ^{1}H NMR as this compound showed good antibacterial activity and was found reasonably good for further characterization. Therefore, EA1005b [51] was further characterized using 2D NMR, melting

point, mass spectrometry, FTIR and UV-visible spectroscopy. Compound [51] was identified as 20-*epi*-ursolic acid. Details of the data are presented below.

Fraction EA11 (416 mg) was resubjected to flash column chromatography (40 mm column diameter) using increasing polarity solvents. The sample was pre-absorbed with a small quantity of silica and added a dry mixture onto the column then eluted sequentially with 600 mL of each of the following solvent systems:

95% dichloromethane / 5% ethyl acetate

20% hexane / 70% dichloromethane / 10% ethyl acetate

20% hexane / 60% dichloromethane / 20% ethyl acetate

70% dichloromethane / 30% ethyl acetate

100% ethyl acetate

95% ethyl acetate / 5% methanol

A total of 120 x 30 mL fractions were collected. After TLC analysis, appropriate fractions were combined to give 10 fractions, EA1101-EA1110.

Sub-fraction EA1106 [52] was then further characterized using 2D NMR, melting point, mass spectrometry, FTIR and UV-Visible spectroscopy. However, the structure of compound [52] is yet to be determined.

Compound

20-*epi*-Ursolic acid [51]

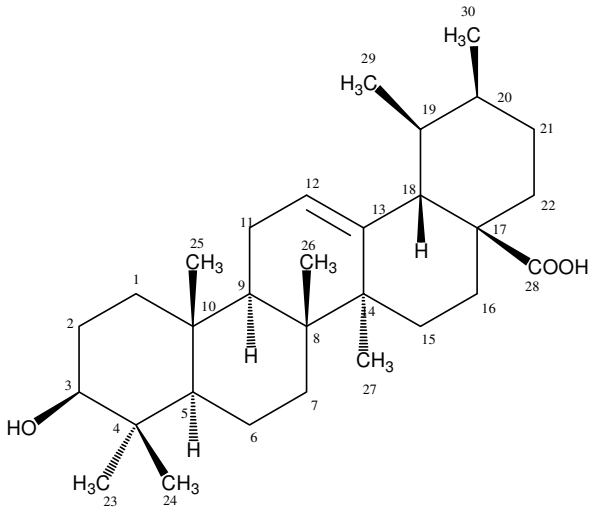

[51]

118 mg of [51] was isolated from fraction EA1005b as a white, amorphous solid. **MP:** 238 - 240°C. **$[\alpha]_D$:** +87.2° (c 0.19, methanol). **IR:** ν_{max} (nujol) 3401cm^{-1} (OH), 2850 cm^{-1} (OH), 1686 cm^{-1} (C=O). **^{1}H NMR** (600 MHz, CD_3OD); δ_H : 0.74 [1H, d, $J_{5,6\beta}$ = 11.4 Hz, H(5)], 0.77 [3H, s, Me(24)], 0.84 [3H, s, Me(26)], 0.87 [3H, d, Me(29)], 0.95 [3H, d, Me(30)], 0.95 [3H, s, Me(25)], 0.97 [3H, s, Me(23)], 1.00 [1H, dd, $J_{21,22\beta}$ = 3.6 Hz, 13.2 Hz, H(22β)], 1.09 [1H, m, H(15β)], 1.11 [3H, s, Me(27)], 1.32 [1H, m, H(21β)], 1.34 [1H, m, H(7β)], 1.36 [1H, m, H(19)], 1.39 [1H, m, H(6β)], 1.49 [1H, m, H(21α)], 1.54 [1H, m, H(7α)], 1.54 [1H, m, H(6α)], 1.56 [1H, m, H(9)], 1.57 [1H, m, H(2β)], 1.62 [1H, m, H(2α)], 1.62 [1H, m, H(1β)], 1.64 [1H, m, H(16β)], 1.66 [1H, m, H(22α)], 1.68 [1H, m, H(20)], 1.68 [1H, m, H(1α)], 1.92 [1H, m, H(11α)], 1.92 [1H, m, H(11β)], 1.92 [1H, m, H(15α)], 2.03 [1H, td, $J_{16\alpha,15}$ = 3.6 Hz, 13.2 Hz, H(16α)], 2.19 [1H, d, $J_{18,19}$ = 11.4 Hz, H(18)], 3.14 [1H, dd, $J_{3,2}$ = 4.2 Hz, 11.4 Hz, H(3)], 5.22 [1H, t, $J_{12,11}$ = 3.6 Hz, H(12)]. **^{13}C NMR** (600 MHz, CD_3OD); δ_C : 16.5 [C(25)], 16.8 [C(24)], 18.1 [C(29)], 18.3 [C(26)], 19.9 [C(6)], 22.0 [C(30)], 24.6 [C(27)], 24.8 [C(11)], 25.8 [C(16)], 28.4 [C(2)], 29.2 [C(23)], 29.7 [C(15)], 32.2 [C(21)], 34.8 [C(7)], 38.6 [C(1*)], 38.6 [C(20*)], 40.3 [C(4)], 40.5 [C(22)], 40.9 [C(19*)], 40.9 [C(10*)], 41.3 [C(8)], 43.7 [C(14)], 49.5 [C(9)], 50.0 [C(17)], 54.8 [C(18)], 57.2 [C(5)], 80.2 [C(3)], 127.4 [C(12)], 140.1 [C(13)], 182.0 [C(28)]. **LREIMS** *m/z* 456 [M^+, <1%], 248 [100%], 208 [25%], 203 [70%], 133 [50%]. **HREIMS** *m/z* 456.3599 (calculated for $C_{30}H_{48}O_3$, 456.3603).

* Assignments may be reversed.

4.3.3 Methanol extract

Three batches (approximately 22 g each) were subjected to flash column chromatography (100 mm column diameter) using increasing polarity solvents. The sample was pre-absorbed with a small quantity of silica and added as a dry mixture onto the column then eluted sequentially with 2 L of each of the following solvent systems:

90% hexane / 10% ethyl acetate
75% hexane / 25% ethyl acetate
65% hexane / 35% ethyl acetate
50% hexane / 50% ethyl acetate
100% ethyl acetate
99% ethyl acetate / 1% methanol
95% ethyl acetate / 5% methanol
90% ethyl acetate / 10% methanol
80% ethyl acetate / 20% methanol
50% ethyl acetate / 50% methanol

A total of 40 x 500 mL fractions were collected. After TLC analysis, appropriate fractions were combined to give 18 fractions, M01-M18.

Fraction M09 (444 mg) was resubjected to flash column chromatography (30 mm column diameter). The sample was pre-absorbed with a small quantity of silica and added as a dry mixture onto the column then eluted sequentially with 100% dichloromethane (800 mL), 98% dichloromethane / 2% ethyl acetate (500 mL), 95% dichloromethane / 5% ethyl acetate (500 mL), 90% dichloromethane / 10% ethyl acetate (500 mL), 70% dichloromethane / 30% ethyl acetate (500 mL), 50% dichloromethane / 50% ethyl acetate (400 mL), 100% ethyl acetate (400 mL) and 90% ethyl acetate / 10% methanol (400 mL) to give 80 x 50 mL fractions. After TLC analysis, appropriate fractions were combined to give 15 sub-fractions, M0901-M0915.

White amorphous solids precipitated from sub-fractions M0906, M0907, M0908 and M0911. These solids (designated M0906a, M0907a and M0911a respectively) were analyzed using 1D NMR. Sub-fractions M096a and M0907a were found to have similar NMR spectra. Therefore, only M0906a [53] and M0911a [54] were further analyzed using 2D NMR, melting point,

mass spectrometry, FTIR and UV-visible spectroscopy. However, the structures of compound [53] and [54] are yet to be determined.

Fraction M10 (367 mg) was resubjected to flash column chromatography (30 mm column diameter). The sample was pre-absorbed with a small quantity of silica and added as a dry micture onto the column then eluted sequentially with 40% hexane / 60% chloroform (900 mL), 100% chloroform (400 mL), 90% chloroform / 10% ethyl acetate (300 mL), 80% chloroform / 20% ethyl acetate (200 mL), 50% chloroform / 50% ethyl acetate (200 mL), 90% chloroform / 10% methanol (200 mL) and 90% ethyl acetate / 10% methanol (200 mL) to give 48 x 50 mL fractions. After TLC analysis, appropriate fractions were combined to give 10 sub-fractions, M1001-M1010.

Sub-fraction M1004 (19 mg) was then subjected to preparative thin layer chromatography and developed three times using dichloromethane. Ten bands were observed visually, under UV light and using Phosphomolybdic acid (PMA) staining. Each band on the TLC plate was scraped off and the silica of each scraped band was soaked overnight in methanol. The methanol filtrate of each band was then evaporated to dryness. Only sample from Band 2 (2 mg) [55] was analyzed using 2D NMR as the rest of the samples obtained were only about 1 mg or less. This sample was only visible under PMA staining. Compound [55] was found to have similar ^{1}H NMR and ^{13}C NMR with compound [53]. However, the structures of both compounds are yet to be determined.

Sub-fraction M1006 (13 mg) was also subjected to preparative thin layer chromatography using a solvent system of 90% dichloromethane / 10% ethyl acetate. Seven bands were observed visually, under UV light and using PMA staining. Each band on the TLC plate was scraped off and the silica of each scraped band was soaked overnight in methanol. The methanol filtrate of each band was then evaporated to dryness. The pure compound obtained from Band 3 (2 mg) [57] was analyzed using 2D NMR, melting point, mass spectrometry and FTIR. The rest of the samples obtained were not characterized as they only contained about 1 mg. This sample showed blue florescence under UV and was visible under PMA staining. Compound [56] was identified as decursinol. Details of the data are presented below.

Fraction M13 (2.1 g) was resubjected to reversed-phase flash column chromatography (40 mm column diameter) using increasing polarity solvents. The sample was pre-absorbed with small quantity of C-18 silica and added it as a dry mixture onto the column then eluted sequentially with 1 L of each of the following solvent systems:

20% methanol / 80% water

40% methanol / 60% water

60% methanol / 40% water

100% methanol

A total of 80 x 500 mL fractions were collected. After TLC analysis, appropriate fractions were combined to give 18 fractions, M1301-M1318.

A white solid (4 mg) [57] precipitated from fraction M1306a. Compound [57] was further analyzed using 2D NMR, melting point, mass spectrometry, FTIR and UV-visible spectroscopy. Compound [57] was identified as luteolin-7-*O*-glucoside. Details of the data are presented below.

Compounds

Decursinol [56]

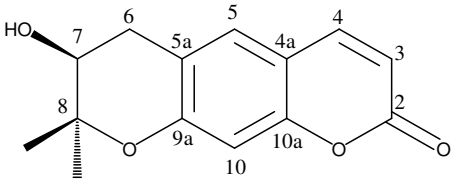

[56]

2 mg of [56] was isolated from fraction M100603 as a pale yellow, amorphous solid. **MP**: 170°C. **IR**: ν_{max} (nujol) 3412 cm^{-1} (OH), 1708 cm^{-1} (C=O), 1598 cm^{-1} (C=C). **^{1}H NMR** (600 MHz, d_6-DMSO); δ_H: 1.12 [3H, s, Me(12)], 1.13 [3H, s, Me(11)], 3.15 [2H, s, H(6)], 4.69 [1H, t, $J_{6,7}$ = 9.0 Hz, H(7)], 6.20 [1H, d, $J_{3,4}$ = 9.0 Hz, H(3)], 6.78 [1H, s, H(10)], 7.47 [1H, s, H(5)], 7.92 [1H, d, $J_{3,4}$ = 9.0 Hz, H(4)]. **^{13}C NMR** (600 MHz, d_6-DMSO); δ_C: 24.8 [C(12)], 25.8 [C(11)], 28.6 [C(6)], 69.9 [C(8)], 90.9 [C(7)], 96.7 [C(10)], 111.1 [C(3)], 112.0 [C(4a)], 123.8 [C(5)], 125.5 [C(5a)], 144.7 [C(4)], 155.0 [C(10a)], 160.5 [C(2)], 163.3 [C(9a)]. **LREIMS** *m/z* 246 [M^+, 35%], 213 [25%], 187 [100%], 175 [14%], 160 [27%], 131 [15%]. **HREIMS** *m/z*: 246.0889 (calculated for $C_{14}H_{14}O_4$, 246.0892).

Luteolin-7-*O*-glucoside [57]

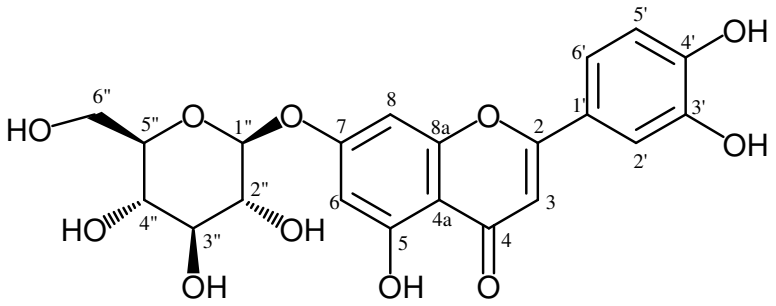

[57]

4 mg of [57] was isolated from fraction M1306a as pale yellow, amorphous solid. **MP**: 260 – 265 °C. **IR**: ν_{max} (nujol) 3495 cm^{-1} (OH), 3451 cm^{-1} (OH), 1659 cm^{-1} (C=O), 1609 cm^{-1} (C=C), 1597 cm^{-1} (C=C). **UV**: λ_{max} (methanol) 352 nm. **^{1}H NMR** (600 MHz, CD_3OD); δ_H: 3.41 [1H, m, H(4")], 3.48 [1H, m, H(2")], 3.49 [1H, m, H(3")], 3.54 [1H, ddd, $J_{5",6"\beta}$ = 2.3 Hz, $J_{5",6"\alpha,}$ = 5.6 Hz, $J_{4",5"}$ = 9.7 Hz, H(5")], 3.71 [1H, dd, $J_{5",6"\alpha}$ = 5.6 Hz, $J_{6"\beta,6"\alpha}$ = 12.0 Hz, H(6"α)], 3.92 [1H, dd, $J_{5",6"\beta}$ = 2.3 Hz, $J_{6"\alpha,6"\beta}$ = 12.0 Hz, H(6"β)], 5.06 [1H, d, $J_{1",2"}$ = 7.2 Hz, H(1")], 6.47 [1H, d, $J_{6,8}$ = 2.4 Hz, H(6)], 6.56 [1H, s, H(3)], 6.68 [1H, d, $J_{5',6'}$ = 8.4 Hz, H(5')], 6.80 [1H, d, $J_{6,8}$ = 2.4 Hz, H(8)], 7.16 [1H, d, $J_{2',6'}$ = 2.4 Hz, H(2')], 7.36 [1H, dd, $J_{2',6'}$ = 2.4 Hz, H(6')]. **^{13}C NMR** (600 MHz, CD_3OD); δ_C: 62.8 [C(6")], 71.7 [C(4")], 75.2 [C(2")], 78.3 [C(3")], 78.8 [C(5")], 96.5 [C(8)], 101.1 [C(6)], 102.1 [C(1")], 103.5 [C(3)], 106.9 [C(2')], 107.5 [C(4a)], 109.9 [C(5')], 120.6 [C(6')], 121.6 [C(1'), 154.8 [C(3')], 159.46 [C(4'*)], 159.48 [C(8a*)], 163.3 [C(5)], 165.1 [C(7)], 168.9 [C(2)], 184.4 [C(4)]. **APCI MS** (Negative ion) *m/z*: 447.0936 (calculated for $C_{21}H_{20}O_{11}$ – H, 447.0927), 285.0406 (100%).

* Assignments may be reversed.

4.3.4 Aqueous extracts

A total of 46 g of aqueous extract was obtained from the decoction method and 71 g of aqueous extract from soxhlet extraction. Each of these aqueous extracts were then separately dissolved in 70% V/V methanol before being subjected to liquid-liquid partitioning with hexane, followed by dichloromethane and ethyl acetate. Each of the aqueous extracts was partitioned twice with each of the solvents to increase the yield.

Aqueous extract (decoction)

Liquid-liquid partitioning of the aqueous extract from the decoction method gave 21 mg of hexane extract, 1.2 g of dichloromethane extract, 7.6 g of ethyl acetate extract and 33.5 g of aqueous methanol upon evaporation.

Dichloromethane extract (1.1 g) from the partitioning was subjected to reversed-phase flash column chromatography (40 mm column diameter) using a series of decreasing polarity solvents. The sample was pre-absorbed with small quantity of C-18 silica and added it as a dry mixture onto the column then eluted sequentially with 800 mL of each of the following solvent systems:

40% methanol / 60% water
60% methanol / 40% water
80% methanol / 20% water
100% methanol

A total of 64 x 50 mL fractions were collected. After TLC analysis, appropriate fractions were combined to give 10 fractions, Aq(Dct)D01-Aq(Dct)D10.

Ethyl acetate extract (7.5 g) from the partitioning was subjected to reversed-phase column chromatography (40 mm column diameter) using a series of decreasing polarity solvents. The sample was pre-absorbed with small quantity of C-18 silica and added it as a dry mixture onto the column then eluted sequentially with 800 mL of each of the following solvent systems:

30% methanol / 70% water
40% methanol / 60% water
60% methanol / 40% water

80% methanol / 20% water

100% methanol

A total of 80 x 50 mL fractions were collected. After TLC analysis, appropriate fractions were combined to give 11 fractions, Aq(Dct)EA01-Aq(Dct)EA11.

Aqueous methanol residue (33.4 g) from the partitioning was subjected to reversed-phase column chromatography (40 mm column diameter) using a series of decreasing polarity solvents. The sample was pre-absorbed with small quantity of C-18 silica and added it as a dry mixture onto the column then eluted sequentially with 800 mL of each of the following solvent systems:

20% methanol / 80% water

30% methanol / 70% water

40% methanol / 60% water

60% methanol / 40% water

100% methanol

100% acetonitrile

100% tetrahydrofuran

A total of 112 x 50 mL fractions were collected. After TLC analysis, appropriate fractions were combined to give 11 fractions, Aq(Dct)AM01-Aq(Dct)AM11.

Aqueous extract (Soxhlet)

Liquid-liquid partitioning of the aqueous extract from the soxhlet method gave 27 mg of hexane extract, 1.9 g of dichloromethane extract, 6.2 g of ethyl acetate extract and 52 g of aqueous methanol residue upon evaporation.

Dichloromethane extract (1.8 g) from the partitioning was subjected to reversed-phase flash column chromatography (40 mm column diameter) using a series of decreasing polarity solvents. The sample was pre-absorbed with small quantity of C-18 silica and added it as a dry mixture onto the column then eluted sequentially with 800 mL of each of the following solvent systems:

40% methanol / 60% water

60% methanol / 40% water

80% methanol / 20% water

100% methanol

A total of 64 x 50 mL fractions were collected. After TLC analysis, appropriate fractions were combined to give 14 fractions, Aq(Sox)D01-Aq(Sox)D14.

When a solution of fraction Aq(Sox)D02 was left standing, clear solids [59] crystallized out of solution. Only the ^{1}H NMR spectrum was aquired for compound [59]. Compound [59] was not fully characterized.

Ethyl acetate extract (6.1 g) from the partitioning was subjected to reversed-phase flash column chromatography (40 mm column diameter) using a series of decreasing polarity solvents. The sample was pre-absorbed with small quantity of C-18 silica and added it as a dry mixture onto the column then eluted sequentially with 800 mL of each of the following solvent systems:

30% methanol / 70% water

40% methanol / 60% water

60% methanol / 40% water

80% methanol / 20% water

100% methanol

A total of 80 x 50 mL fractions were collected. After TLC analysis, appropriate fractions were combined to give 11 fractions, Aq(Sox)EA01-Aq(Sox)EA11.

When a solution of fraction Aq(Sox)EA02 was left standing, clear solids crystallized out of solution. The clear solids (125 mg) [60] crystallized out of solution Aq(Sox)EA02 was further characterized using NMR, melting point mass spectrometry, FTIR, UV-visible spectroscopy. Compound [60] was identified as 2-*deoxy*-D-chiro-inositol. Details of the data are presented below. Compound [60] was found to have similar ^{1}H NMR and ^{13}C NMR with compound [59].

Aqueous methanol residue (51 g) from the partitioning was subjected to reversed-phase flash column chromatography (40 mm column diameter) using a series of decreasing polarity solvents. The sample was pre-absorbed with small quantity of C-18 silica and added it as a dry

mixture onto the column then eluted sequentially with 800 mL of each of the following solvent systems:

20% methanol / 80% water

30% methanol / 70% water

40% methanol / 60% water

60% methanol / 40% water

100% methanol

100% acetonitrile

100% tetrahydrofuran

A total of 112 x 50 mL fractions were collected. After TLC analysis, appropriate fractions were combined to give 11 fractions, Aq(Sox)AM01-Aq(Sox)AM11.

Compound

2-*deoxy*-D-chiro-inositol [60]

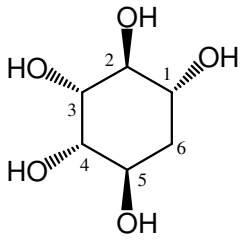

[60]

26 mg of [60] was isolated from Aq(Sox)EA02 as colourless crystals. **MP**: 230 – 233°C. **$[\alpha]_D$:** +23.6° (c 0.22, water). **IR**: ν_{max} (nujol) 3306 cm^{-1} (OH). **^{1}H NMR** (600 MHz, D_2O); δ_H: 1.86 [1H, ddd, $J_{2,6\alpha}$ = 3.6 Hz, $J_{5,6\alpha}$ = 11.5 Hz, $J_{6\beta,6\alpha}$ = 14.4 Hz, H(6α)], 2.04 [1H, dddd, $J_{2,6\beta}$ = 1.2 Hz, $J_{2,6\beta}$ = 3.6 Hz, $J_{5,6\beta}$ = 4.8 Hz, $J_{6\alpha,6\beta}$ = 14.4 Hz, H(6β)], 3.62 [1H, t, $J_{3,4}$ = 9.6 Hz, $J_{4,5}$ = 9.6 Hz, H(4)], 3.76 [1H, ddd, $J_{3,5}$ = 0.6 Hz, $J_{1,3}$ = 3.6 Hz, $J_{3,4}$ = 9.6 Hz, H(3), 3.80 [1H, dddd, $J_{3,5}$ = 0.6 Hz, $J_{5,6\beta}$ = 4.8 Hz, $J_{4,5}$ = 9.6 Hz, $J_{5,6\alpha}$ = 11.5 Hz, H(5)], 3.98 [1H, td, $J_{2,6\beta}$ = 1.2 Hz, $J_{2,6\beta}$ = 3.6 Hz, H(2)], 4.07 [1H, q, $J_{1,3}$ = 3.6 Hz, H(1)]. **^{13}C NMR** (600 MHz, D_2O); δ_C: 35.2 [C(6)], 70.5 [C(1)], 70.8 [C(5)], 72.9 [C(3)], 74.1 [C(2)], 76.4 [C(4)]. **ESI-MS** *m/z*: 166.0751 (calculated for $C_6H_{12}O_5$ + H, 165.0762).

4.4 Bacteria and growth conditions

The bacterial test strains provided by Dr Susan Semple, Sansom Institute, University of South Australia were *Staphylococcus aureus* ATCC 25923, *Streptococcus pyogenes* ATCC 10389, *Pseudomonas aeruginosa* ATCC 27853 and *Escherichia coli* ATCC 25922. These bacterial strains were stored as stocks at -70°C and freshly grown on blood agar for use in the antibacterial assay.

All bacterial test strains were grown on Columbia agar (Oxoid CM331) supplemented with 5% (v/v) horse blood at 37°C. For the broth micro-dilution assay to determine minimum inhibitory and bactericidal concentration, all bacteria except *Streptococcus pyogenes* were grown in Cation adjusted Mueller Hinton II Broth (BBL) at 37°C. *Streptococcus pyogenes* were grown in Brain Heart Infusion Broth (Oxoid CM0225) at 37°C in the presence of 5% CO_2.

4.5 Broth micro-dilution assay for minimum inhibitory and bactericidal concentration (MIC and MBC)

Using sterile round-bottom 96-well plates (Sarstedt), triplicate two-fold serial dilutions of extract (100 µl/well) were prepared in broth containing maximum of 1% (v/v) DMSO to produce a concentration range from 2000 to 62.5 µg/mL (*Staphylococcus aureus*, *Escherichia coli* and *Pseudomonas aeruginosa*) and 8000 to 250 µg/mL (*Streptococcus pyogenes*).

A two-fold serial dilution of ampicilin (Sigma, St. Louis, MO) to produce a final concentration range from 0.4875 to 0.0152 g/mL was used as standard positive control for Gram-positive strains (*Staphylococcus aureus* and *Streptococcus pyogenes*). Gentamicin (Sigma, St. Louis, MO) was used as standard positive control for Gram-negative strains (*Escherichia coli* and *Pseudomonas aeruginosa*). The final concentration of two-fold serial dilution of gentamicin for *Escherichia coli* and *Pseudomonas aeruginosa* varied (based on the acceptable limits for quality control strains) ranging from 1.300 to 0.0406 µg/mL (*Escherichia coli*) and 2.600 to 0.0813 µg/mL (*Pseudomonas aeruginosa*).

All of the wells except controls for extracts, saline and media sterility were added with 100 µL of 0.5 McFarland bacterial cell suspension (1 x 10^8 CFU/mL) which had been diluted in 1:150 ratio (prepared in the appropriate broth) to correspond approximately 1 x 10^6 CFU/mL. The subsequent 1:2 dilution resulted in 5 x 10^5 CFU/mL final inoculum concentration for the assay. The final concentration of extracts was 1000 to 31.25 µg/mL (*Staphylococcus aureus*, *Escherichia coli* and *Pseudomonas aeruginosa*) and 4000 to 125 µg/mL (*Streptococcus pyogenes*).

According to Gibbon (2004), natural products and extracts displaying MIC value over 1000 µg/mL have little relevance in a clinical perspective as there is likely that a number of relatively inert substances may display antibacterial activity at such a high concentration.[69] However, at this low concentration for crude extracts, there is a possibility that the amount of active compounds would be too little to be detected as the crude extracts are a mixture of different components. Therefore, the maximum concentration of crude extracts for antibacterial assay was set at 2-fold dilution higher than 1000 µg/mL to give a maximum concentration of 4000 µg/mL.

Plates were set up according to a previously suggested format (Cos *et al* 2006)[68], as shown in ***Figure 4.1***. Plates with bacteria other than *Streptococcus* species were then incubated at 37°C overnight. The *Streptococcus* species were incubated at 37°C in the presence of 5% CO_2. After incubation, the minimum inhibitory concentration (MIC) of each extract was determined as the lowest concentration at which no growth was observed in the duplicate wells. The observation was done visually before adding the resazurin, an oxidation reduction indicator. A 0.01% (v/v) resazurin solution, 10 µL, was then added into the wells.[73] The resazurin method is based on Mann *et al* 1998 with modification. The plates were then placed on a shaker for 3 min and incubated for 30 minutes at 37°C, with additional 5% CO_2 for *Streptococcus* species. Then the plates were assessed visually for any change in colour from blue to pink indicating reduction of the dye due to bacterial growth.

The minimum bactericidal concentration (MBC) was then determined for the extracts with MIC value of 2000 µg/mL and below using a method published previously (Ndi *et al* 2007)[74]. Ten microlitres of each wells of a duplicate plate (not treated with resazurin) that correspond to the MIC and those concentrations above were taken out. Each 10 µl aliquot was mixed with

190 µl of appropriate broth in a sterile 96-well plate. Duplicates were performed. Ten microlitres from each saline control and media sterility control were also taken out and mixed with 190 µl of appropriate broth. The plate set-up is shown in ***Figure 4.2***. The MBC plates were incubated under the same conditions as in the MIC experiment. The presence or absence of bacterial growth in the MBC experiment was determined visually as well as using the resazurin dye, similar to the MIC experiment.

Figure 4.1: Template for broth micro-dilution assay[68] (adapted from Cos *et al*)

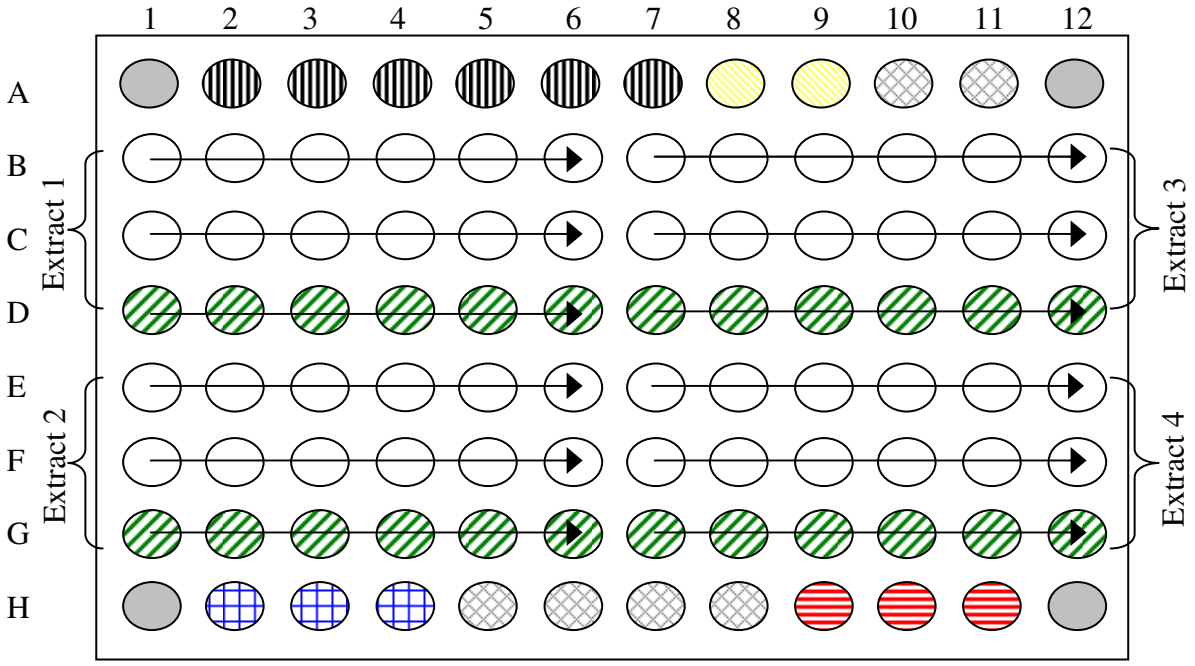

Template for 4 compounds with 6 serial dilutions
(2-fold dilution series for dose range
4000 – 125 µg/mL, 2000 – 62.5 µg/mL and 1000 – 31.25 µg/mL)

Legend:
- Corners of plate not used in assay (to avoid problem of evaporation)
- Non-infected medium control: 0% growth of test organism
- Non-infected medium + extract control (to test for extract sterility)
- Infected control: 100% growth of test organism
- DMSO medium control
- Reference drug control (ampicillin or gentamicin)
- Extract dilutions + test organism
- Empty well

Figure 4.2: Template for duplicate plate (not treated with resazurin) to be tested for MBC[74] (adapted from Ndi *et al*)

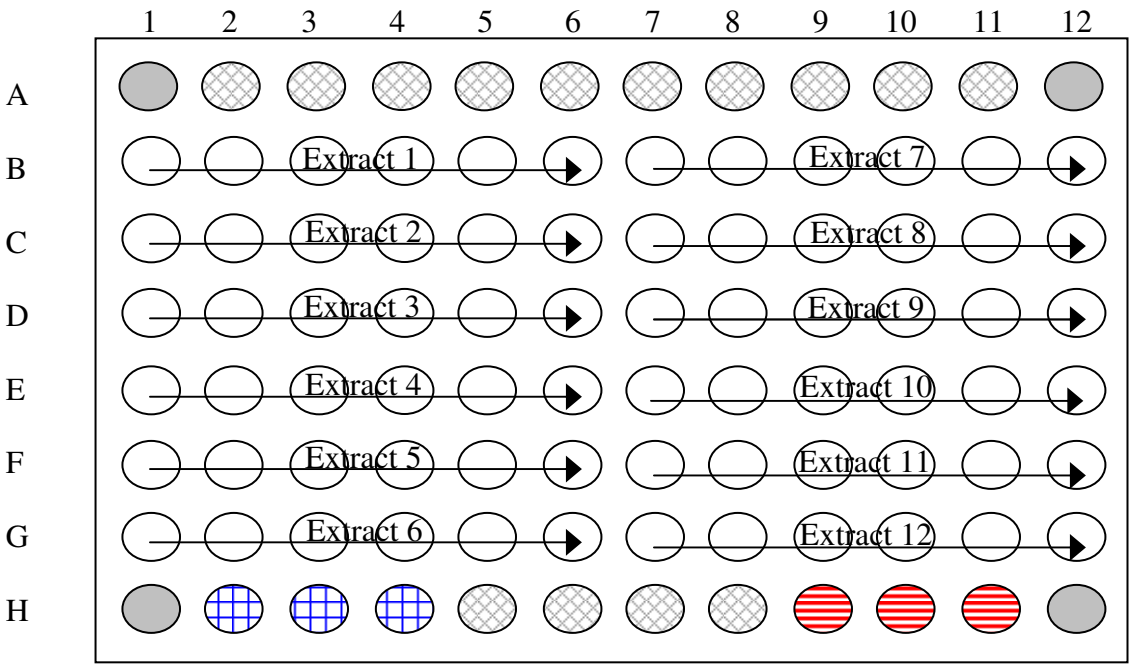

Template for 12 compounds with 6 serial dilutions
(2-fold dilution series for concentration corresponding to the MIC)

Legend:
- Corners of plate not used in assay (to avoid problem of evaporation)
- Non-infected medium control: 0% growth of test organism
- Infected control: 100% growth of test organism
- Empty well
- Extract dilutions + test organism

CHAPTER 5

Conclusion and Future Work

5.1 Conclusion

Based on the literature reports, a total of 27 compounds have been previously isolated from *Scaevola spinescens*. These compounds were isolated from hexane and methanol extracts. Previous work has shown that coumarins, terpenoids, iridoids and flavonoids are the classes of compounds isolated from *Scaevola spinescens*. These classes of compounds have been discussed in **Chapter 1**.

In this study, eleven compounds have been isolated from *Scaevola spinescens*. Six out of the eleven isolated compounds have been identified – 18-*epi*-taraxerol [49], myricadiol [50], 20-*epi*-ursolic acid [51], decursinol [56], luteolin-7-*O*-glucoside [57] and 2-*deoxy*-D-chiro-inositol [60]. The structures of these compounds were determined using 1D and 2D NMR, melting point, UV-Visible spectroscopy, FTIR and high-resolution mass spectrometry. Due to the limitation of time, the structures of the remaining compounds were not able to be determined.

Myricadiol [50], luteolin-7-*O*-glucoside [57] and 2-*deoxy*-D-chiro-inositol [60] have been previously isolated from *Scaevola spinescens*.[5,6] Whereas, 18-*epi*-taraxerol [49], 20-*epi*-ursolic acid [51] and decursinol [56] have not been isolated from *Scaevola spinescens* or any other *Scaevola* species. Therefore, these compounds are new addition to the chemical compounds found in *Scaevola spinescens*. Out of the three newly isolated compounds for *Scaevola spinescens*, two of them are known compound (20-*epi*-ursolic acid [51] and decursinol [56]). Whereas, 18-*epi*-taraxerol [49] is found to be a novel compound. The list of compounds found in *Scaevola spinescens* are shown in ***Table 5.1***.

Overall, the first aim of this study was partly achieved. There are still more compounds in the plant extract that are yet to be identified. Due to limitation of time frame in this study, the complete chemical profiling of hexane, ethyl acetate, methanol and aqueous extracts of *Scaevola spinescens* was not possible. This is because the fractionation and purification of pure compounds from the plant extract as well as structural elucidation were time consuming processes.

Table 5.1: Chemical compounds found in *Scaevola spinescens*

Compounds	Newly found in *Scaevola spinescens*	Previously found in *Scaevola spinescens*
Xanthyletin [2]		[5]
Nodakenetin [3]		[5]
Emmarin [4]		[6]
β-sitosterol [8]		[5]
(3β,22E)-stigmasta-5,22-dien-3-ol [11]		[5]
(3β,24S)-stigmast-5en-3-ol [12]		[5]
Ursolic acid [15]		[6]
Lupenone [17]		[5]
β-amyrin [23]		[5]
Myricadiol [24][50]		[5]
Squalene [25]		[5]
Taraxerol [26]		[5,6]
Taraxerone [27]		[5]
Taraxerol acetate [28]		[5,6]
Judarrylol [29]		[6]
Loganin [31]		[6]
Scaevoloside [34]		[6]
Scaevoloside dimethyl acetal [37]		[6]
Katecateroside [38]		[6]
Luteolin-7-*O*-glucoside [44][57]		[6]
Luteolin-7-*0*-glucuronide methyl ester [45]		[6]
18-*epi*-taraxerol [49]	*	
20-*epi*-ursolic acid [51]	*	
Decursinol [56]	*	
2-*deoxy*-D-chiro-inositol [60]		[6]
2-C-(Hydroxymethyl)-D-ribonic acid-γ-lactone		[6]
Daucesterol		[6]
Hexadecanoic acid, methyl ester		[6]
L-*threo*-Guaiacyl glycerol		[6]
Vanillic acid		[6]

The hexane, ethyl acetate and methanol crude extracts showed antibacterial activity against Gram-positive bacteria, specifically *Streptococcus pyogenes* ATCC 10389 with minimum inhibitory concentration (MIC) ranging from 500 to 4000 µg/ml and minimum bactericidal concentration (MBC) ranging from 500 to 1000 µg/mL. No antibacterial activity was observed against Gram-negative bacteria.

The aqueous crude extracts did not show any antibacterial activity against Gram-positive bacteria at a minimum concentration of 4000 µg/mL. However, significant antibacterial activity against *Staphylococcus aureus* ATCC 25923 was observed in the aqueous fractions with MIC ranging from 31.25 to 4000 µg/mL. The aqueous fractions that had MIC of 31.25 µg/mL are deemed desirable for further fractionation in the future to isolate active compounds that contributes to the antibacterial activity.

The good antibacterial activity found in aqueous fractions with MIC as low as 31.25 µg/mL shows that these active compounds might be a possible source in the healing remedy used by the Aboriginal people. The uses of this plant were discussed in **Chapter 1**. Further investigation into the antibacterial activity of the aqueous extract may be of interest as it might validate the remedy used by the Aboriginal people.

One of the isolated compounds, 20-*epi*-ursolic acid [51] showed good antibacterial activity against *Streptococcus pyogenes* ATCC 10389 with an MIC from 1.9 to 3.7 µg/mL (4.16 – 8.11 µM) and MBC from 3.7 to 7.5 µg/mL (8.11 – 16.4 µM). Compound [51] also showed good antibacterial activity against *Staphylococcus aureus* ATCC 25923 with MIC from 3.7 to 7.5 µg/mL (8.11 – 16.4 µM) and MBC from 7.5 to 15 µg/mL (16.4 – 32.8 µM).

Ursolic acid [15] has been reported to have antibacterial activity against *Staphylococcus aureus* (ATCC 25923 and ATCC 29213) with MIC of 8 mg/mL as well as against *Enterococcus faecalis* (ATCC 29212) with MIC of 4 mg/mL.[75] This suggested that ursolic acid [15] is associated with antibacterial properties. Therefore, it is conceivable that its isomer, 20-*epi*-ursolic acid [51] also shows antibacterial activity. Based on the MIC values, 20-*epi*-ursolic acid has better antibacterial activity compared to ursolic acid. The different stereochemistry at carbon 20 seems to increase the antibacterial activity.

Hexane, ethyl acetate, methanol and aqueous extracts were found to have antibacterial activity. However, not all of the chemical compounds that are responsible for the antibacterial activity were identified in this study.

Furthermore, no investigation on the findings found by Nobbs was done in this study. Another objective of the second aim in this study was to identify any antibacterial activity in the pure

compounds that were previously isolated by Nobbs from three of the crude fractions which were found to have significant antibacterial activity. These pure compounds had not been tested for antibacterial activity (See **Chapter 1**). However, this investigation was not possible as no pure compounds similar to those isolated by Nobbs were identified in this study.

Nevertheless, the overall antibacterial study shows that *Scaevola spinescens* is a potential plant source of antibacterial agents. Active compounds isolated from *Scaevola spinescens* might be potential lead compounds for development of new antibacterial therapeutics.

5.2 Future Work

Initial future work would be determination of the structures of the five remaining isolated compounds ([53], [54], [55], [56], [60]).

For further investigation of the active compounds in *Scaevola spinescens*, a better approach would be bioassay-guided fractionation. This approach can reduce the time needed to isolate active pure compounds. In addition, this also contributes to chemical profiling of the plant. Following up from this study, the bioassay-guided fractionation can be done based on the preliminary screening of the plant extracts for antibacterial assay. Crude fractions that had MIC below 100 µg/mL are deemed desirable for further fractionation and testing on antibacterial assay to identify the active pure compounds. This approach can also help in search of pure compounds to verify the findings found by Nobbs.

20-*epi*-Ursolic acid that has been isolated in this study has good antibacterial activity against *Streptococcus pyogenes* (ATCC 10389) and *Staphylococcus aureus* (ATCC 25923) with MIC ranging from 1.9 to 15 µg/mL. The structure-activity relationship (SAR) study of 20-*epi*-ursolic acid and ursolic acid is important to gain a better understanding of the antibacterial activity.

REFERENCES

(1) Barr, A.; Chapman, J.; Smith, N.; Beveridge, M.; Knight, T.; Alexander, V.; Andrews, M. *Traditional Bush Medicines*; Greenhouse Publication, 1988.

(2) Fabricant, D., S.; Farnsworth, N. R. *Environ. Health Perspect.* **2001**, *109*, 69-75.

(3) Bodkin, F. *The essential reference guide to native and exotic plants in Australia. Encyclopaedia Botanica.*; Angus and Robertson Publisher, 1986.

(4) Lassak, E. V.; McCarthy, T. *Australian medicinal plants*; Methuen Australia, 1983.

(5) Kerr, P. G.; Longmore, R. B.; Betts, T. J. *Planta medica* **1996**, *62*, 519-522.

(6) Nobbs, S. F. PhD Thesis, University of Adelaide, 2001.

(7) ChemistryCentre "Annual Review," Chemistry Centre of Western Australia, 1999-2000.

(8) Kerr, P. G.; Longmore, R. B.; Yench, R. *Biomed. Res.* **1999**, *1*, 3-15.

(9) Carolin, R. C.; Morrison, D. A.; Rajput, T. *Flora of Australia: Brunoniaceae, Goodeniaceae*; Australian Government Publishing Service: Australian Capital Territory, Canberra, 1992.

(10) Jessop, J. P.; Toelken, H. R. *Flora of South Australia.Part III*; 4th ed.; South Australian Government, Adelaide, 1986.

(11) Black, J. M. *Flora of South Australia.Part I*; 2nd ed.; South Australian Government,Adelaide, 1943.

(12) Wee, Y. C. *A guide to medicinal plants*; Singapore Science Centre, 1992.

(13) Cambie, R. C.; Brewis, A. A. *Anti-fertility plants of the Pacific*; CSIRO, Australia, 1997.

(14) Barr, A.; Chapman, J.; Smith, N.; Wightman, G.; Knight, T.; Mills, L.; Andrews, M.; Alexander, V. *Traditional Aboriginal Medicines in the Northern Territory of Australia*; Darwin, 1993.

(15) Moerman, D. E. *Native American Ethnobotany*; Timber Press: Portland, 1998.

(16) Cribbs, A. B.; Cribbs, J. W. *Wild medicine in Australia*; Sydney, 1981.

(17) Khan, A. J.; Kunesch, G.; Chuilon, S.; Ravise, A. *Fruits* **1985**, *40*, 807-811.

(18) Kayser, O.; Kolodziej, H. *Naturforsch., C: Biosci.* **1999**, *54c*, 169-174.

(19) Wohlrabe, K.; Hansel, R. *Arch. Pharm. (Weinheim)* **1977**, *310*, 972-974.

(20) Bruneton, J. *Pharmacognosy, Phytochemistry, Medicinal Plants*; Lavoisier Publishing, 1993.

(21) Cowan, M. M. *Clin. Microbiol. Rev.* **1999**, *12*, 564-582.

(22) Dzubak, P.; Hajduch, M.; Vydra, D.; Hustova, A.; Kvasnica, M.; Biedermann, D.; Markova, L.; Urban, M.; Sarek, J. *Nat. Prod. Rep.* **2005**, *22*, 394-411.

(23) Tolstikova, T. G.; Sorokina, I. V.; Tolstikov, G. A.; Tolstikov, A. G.; Elekhter, O. B. *Russ. J. Bioorg. Chem.* **2006**, *32*, 37-49.

(24) Cambie, R. C.; Rutledge, P. S.; Wellington, K. D. *J. Nat. Prod.* **1997**, *60*, 1303-1306.

(25) Gideon, P. *Biochemical targets of plant bioactive compounds*; Taylor & Francis: London and New York, 2003.

(26) Graikou, K.; Aligiannis, N.; Chinou, I. B.; Harvala, C. *Z. Naturforsch* **2002**, *57c*, 95-99.

(27) Skaltsounis, A. L.; Tillequin, F.; Koch, M.; Pusset, J.; Chauviere, G. *Planta medica* **1989**, *55*, 191-192.

(28) Skaltsounis, A. L.; Tillequin, F.; Koch, M. *Heterocycles* **1987**, *26*, 599-605.

(29) Collins, D. J.; Culvenor, C. C. J.; Lamberton, J. A.; Loder, J. W.; Price, J. R. *Plants for Medicines: a chemical and pharmacological survey of plants in the Australian region*; CSIRO Publication: Victoria, 1990. (42-43)

(30) Rice-Evans, C. A.; Miller, N. J.; Paganga, G. *Trends Plant Sci. Rev.* **1997**, *2*, 152-159.

(31) Cho, S.-Y.; Park, S.-J.; Kwon, M.-J.; Jeong, T.-S.; Bok, S.-H.; Choi, W.-Y.; Jeong, W.-I.; Ryu, S.-Y.; Do, S.-H.; Lee, C.-S.; Song, J.-C.; Jeong, K.-S. *Mol. Cell. Biochem.* **2003**, *243*, 153-160.

(32) Bouaziz, M.; Sayadi, S. *European J. Lipid Sci. Technol.* **2005**, *107*, 497-504.

(33) Chiruvella, K. K.; Mohammed, A.; Dampuri, G.; Ghanta, R. G.; Raghavan, S. C. *Int. J. Biomed. Sci.* **2007**, *3*, 269-278.

(34) Heijnen, C. G. M.; Haenen, G. R. M. M.; Van Acker, F. A. A.; Van der Vijgh, W. J. F.; Bast, A. *Toxicol. In Vitro* **2001**, *15*, 3-6.

(35) Sadeghi-Hashjin, G.; Folkerts, G.; Henricks, P. A. J.; Muijsers, R. B. R.; Nijkamp, F. P. *Clin. Exp. Allergy* **1998**, *28*, 1464-1473.

(36) Digerness, S. B.; Harris, K. D.; Kirklin, J. W.; Urthaler, F.; Viera, L.; Beckman, J. S.; Darley-Usmar, V. *Free Radic. Biol. Med.* **1999**, *27*, 1386-1392.

(37) Rice-Evans, C. A.; Packer, L. In *Flavonoids in health and disease*; 2nd Edition ed.; Day, A. J., Williamson, G., Eds.; CRC Press, 2003.

(38) Patterson, R. *Syst. Bot.* **1984**, *9*, 263-265.

(39) Semple, S. J.; Reynolds, G. D.; O'Leary, M. C.; Flower, R. L. P. *J. Ethnopharmacol.* **1998**, *60*, 163-172.

(40) Anderson, D. A.; Sobieski, R. J. *Introduction to microbiology*; 2nd Edition ed.; The C.V. Mosby Company: St.Louis, 1980.

(41) Locher, C. P.; Burch, M. T.; Mower, H. F.; Berestecky, J.; Davis, H.; Van Poel, B.; Lasure, A.; Vanden Berghe, D. A.; Vlietinck, A. J. *J. Ethnopharmacol.* **1995**, *49*, 23-32.

(42) Jones, W. P.; Kinghorn, A. D. In *Methods in Biotechnology: Natural Products Isolation*; Sarker, S. D., Latif, Z., Gray, A. I., Eds.; Humana Press: Totowa, NJ, 2006; Vol. 20.

(43) Sakurai, N.; Yaguchi, Y.; Inque, T. *Phytochemistry* **1987**, *26*, 217-219.

(44) Merfort, I.; Buddrus, J.; Nawwar, M. A. M.; Lambert, J. *Phytochemistry* **1992**, *31*, 4031-4032.

(45) Soo Lee, I.; Yi Jin, W.; Zhang, X.; Manh Hung, T.; Sik Song, K.; Hee Seong, Y.; Bae, K. *Arch. Pharm. Res.* **2006**, *29*, 548-555.

(46) Breton, F.; Jose, J. *An. Quim.* **1969**, *65*, 825-828.

(47) Tundis, R.; Dequin, B.; Menichini, F.; Tillequin, F. *Biochem. Syst. Ecol.* **2002**, *30*, 689-691.

(48) Taketa, T. C., Alexandre; Breitmaier, E.; Schenkel, E., P. *J. Braz. Chem.l Soc.* **2004**, *15*, 205-211.

(49) Kashiwada, Y.; Nagao, T.; Hashimoto, A.; Ikeshiro, Y.; Okabe, H.; Cosentino, L., Mark ; Lee, K.-H. *J. Nat. Prod.* **2000**, *10*, 131-136.

(50) Tokar, M.; Klimek, B. *Acta Pol. Pharm.* **2004**, *61*, 191-197.

(51) Rehman, A. U.; Riaz, N.; Ahmad, H.; Ahmad, Z.; Malik, A. *J. Chem. Soc. Pak.* **2003**, *25*, 257-259.

(52) Parra-Delgado, H.; Toscano, R. A.; Garcia-Argaez, A. N.; Mariano, M.-V. *Naturforsch., B: Chem. Sci.* **2005**, *60*.

(53) Abyshev, A. Z.; Gindin, V. A.; Semenov, E. V.; Agaev, E. M.; Abdulla-zade, A. A.; Guseinov, A. B. *Pharm. Chem. J.* **2006**, *40*, 607-610.

(54) Abyshev, A. Z.; Zmeikov, V. P.; Sidorova, I. P. *Chem. Nat. Compd.* **1982**, *18*, 277-281.

(55) Nissler, L.; Gebhardt, R.; Berger, S. *Anal. Bioanal. Chem.* **2004**, *379*, 1045-1049.

(56) Lu, Y.; Foo, L. Y. *Phytochemistry* **2000**, *55*, 263-267.

(57) *Carbon-13 NMR of flavonoids*; Agrawal, P. K., Ed.; Elsevier science publishers: The Netherlands, 1989.

(58) Feeny, P.; Sachdev, K.; Rosenberry, L.; Carter, M. *Phytochemistry* **1988**, *27*, 3439-3448.

(59) Gultekin, M. S.; Celik, M.; Turkut, E.; Tanyeli, C.; Balci, M. *Tetrahedron* **2004**, *15*, 453-456.

(60) *Dictionary of organic compounds*; 5th ed.; Buckingham, J.; Donaghy, S. M., Eds.; Chapman and Hall: London, 1982; Vol. 5.

(61) Wikler, M. A.; Cockerill, F. R.; Craig, W. A.; Dudley, M. N.; Eliopoulos, G. M.; Hecht, D. W.; Hindler, J. F.; Low, D. E.; Sheehan, D. J.; Tenover, F. C.; Turnidge, J. D.; Weinstein, M. P.; Zimmer, B. L.; Ferraro, M. J.; Swenson, J. M. *Methods for dilution antimicrobial susceptibility tests for bacteria that grow aerobically; Approved standard*; Clinical and Laboratory Standard Institute: Pennsylvania, 2006.

(62) Madigan, M. T.; Martinko, J. M.; Parker, J. *Brock Biology of Microorganisms*; 8th Edition ed.; Prentice Hall: New Jersey, 1997.

(63) Moellering, J. R. C. *J. Am. Med. Assoc.* **2008**, *299*, 79-87.

(64) Currie, B. J.; Brewster, D. R. *J. Paedtr. Child Health* **2001**, *37*, 326-330.

(65) Rosen, D. A.; Hooton, T. M.; Stamm, W. E.; Humphrey, P. A.; Hultgren, S. J. *PLoS Med.* **2007**, *4*, 1949-1958.

(66) Gagliotti, C.; Buttazzi, R.; Sforza, S.; Moro, M. L.; Emilia-Romagna Antibiotic Resistance study group *J. Infect.* **2008**, *57*, 179-184.

(67) *Performance Standard for antimicrobial susceptibility Testing. Sixteeth Infomational Supplement. M100-S16.*; Clinical and Laboratory Standards Institute: Wayne, PA, 2006.

(68) Cos, P.; Vlietinck, A. J.; Berghe, D. V.; Maes, L. *J. Ethnopharmacol.* **2006**, *106*, 290-302.

(69) Gibbons, S. *Nat. Prod. Rep.* **2004**, *21*, 263-277.

(70) Hadacek, F.; Greger, H. *Phytochem. Anal.* **2000**, *11*, 137-147.

(71) Ghisalberti, E. L. In *Bioactive natural products: Detection, isolation and structural determination*; 2nd edition ed.; Colegate, S. M., Molyneux, R. J., Eds.; CRC Press, 2007.

(72) Brooks, G. F.; Butel, J. S.; Morse, S. A.; Melnick, J. L.; Jawetz, E.; Adelberg, E. A. *Jawetz, Melnick & Adelberg's Medical Micorbiology*; 23rd edition ed.; McGraw Hill, 2004.

(73) Mann, C. M.; Markham, J. L. *J. Appl. Microbiol.* **1998**, *84*, 538-544.

(74) Ndi, C. P.; Semple, S. J.; Griesser, H. J.; Barton, M. D. *J. Basic Microbiol.* **2007**, *47*, 158-164.

(75) Fontanay, S.; Grare, M.; Mayer, J.; Finance, C.; Duval, R. E. *J. Ethnopharmacol.* **2008**, *120*, 272-276.

APPENDICES

Appendix A

Lorentzian / Gaussian resolution enhancement using SpinWorks 3